POSSIBLE CLIMATIC CONSEQUENCES OF A MAN-MADE GLOBAL WARMING*

H. Flohn

September 1979
WP-79-86

*Work sponsored jointly by UNEP and IIASA.

INTERNATIONAL INSTITUTE FOR APPLIED SYSTEMS ANALYSIS
A-2361 Laxenburg, Austria

Prof. (em.) Dr. H. Flohn is of the Institute of Meteorology at the University of Bonn, F.R.G.

PREFACE

There is increasing concern about man's impact on climate. Studying this problem one comes to realize that this influence is not so much felt as a variation of the average values of global climate, such as temperature and pressure. Of concern is instead a change in the climatological patterns, with the average values changing very little.

Actually this could be a change in rainfall patterns, for example. Among other effects, increasing levels of carbon dioxide could cause a man-made global warming.

While it is impossible to determine such changes in climate patterns given the present state of the art, we consider it perhaps useful to study the changes that occurred in the climate patterns of the past. Today's highly sophisticated knowledge in paleometeorology allows to undertake such a venture--a research activity that may also be crucial for our understanding of the forthcoming CO_2 problem.

Professor Flohn has studied this question along these lines, making use of information available to him as of May 1978. He wrote this report under the project "Comparison of Energy Options, a Methodological Study", sponsored jointly by the United Nations Environment Programme (UNEP) and IIASA.

Wolf Häfele

Deputy Director,
Program Leader, Energy Systems

EXECUTIVE SUMMARY

Climatic changes and modifications are not restricted to the atmosphere in which they are mainly observed. They occur within the climatic system consisting of atmosphere, oceans, soil and vegetation, snow and ice, and their multiple interactions. The characteristic time-scales of these subsystems vary between a few days (atmosphere) and up to 10^6 years (Antarctic ice dome). External effects--hypothetical variations in solar radiation, volcanic eruptions--add to the nonlinear internal interactions, but are as yet unpredictable. Of special interest are the most sensitive internal interactions, between the atmosphere and the thin drifting sea ice, and between the atmosphere and the oceans in the regions of frequent upwelling along the equator and some coasts. The heavily glaciated Antarctic continent causes a marked hemispheric asymmetry of the atmospheric-oceanic circulation and of the positions of the large climatic belts. A possible partial instability of the West-Antarctic ice sheet and its role in sea-level changes is also discussed.

Man-made impacts on the climate are obvious at a local scale (direct heat output, atmospheric pollution, changes in surface albedo (reflectivity), heat storage, and water budget). More important, however, are the implications of the increase in carbon dioxide and some atmospheric trace gases: their long residence time between 5 and about 50 years, their large-scale turbulent mixing caused by the atmospheric circulation, and, above all, their absorption in the infrared portion of the spectrum produce a *combined greenhouse effect* which tends to warm the troposphere and cool the stratosphere. The best models available indicate a representative warming of the surface layers of about $2^{\circ}C$ with a doubling of CO_2 concentration in low and middle latitudes; this warming increases to $5\text{-}10^{\circ}C$ in polar latitudes, due to the feedback between snow or ice, surface

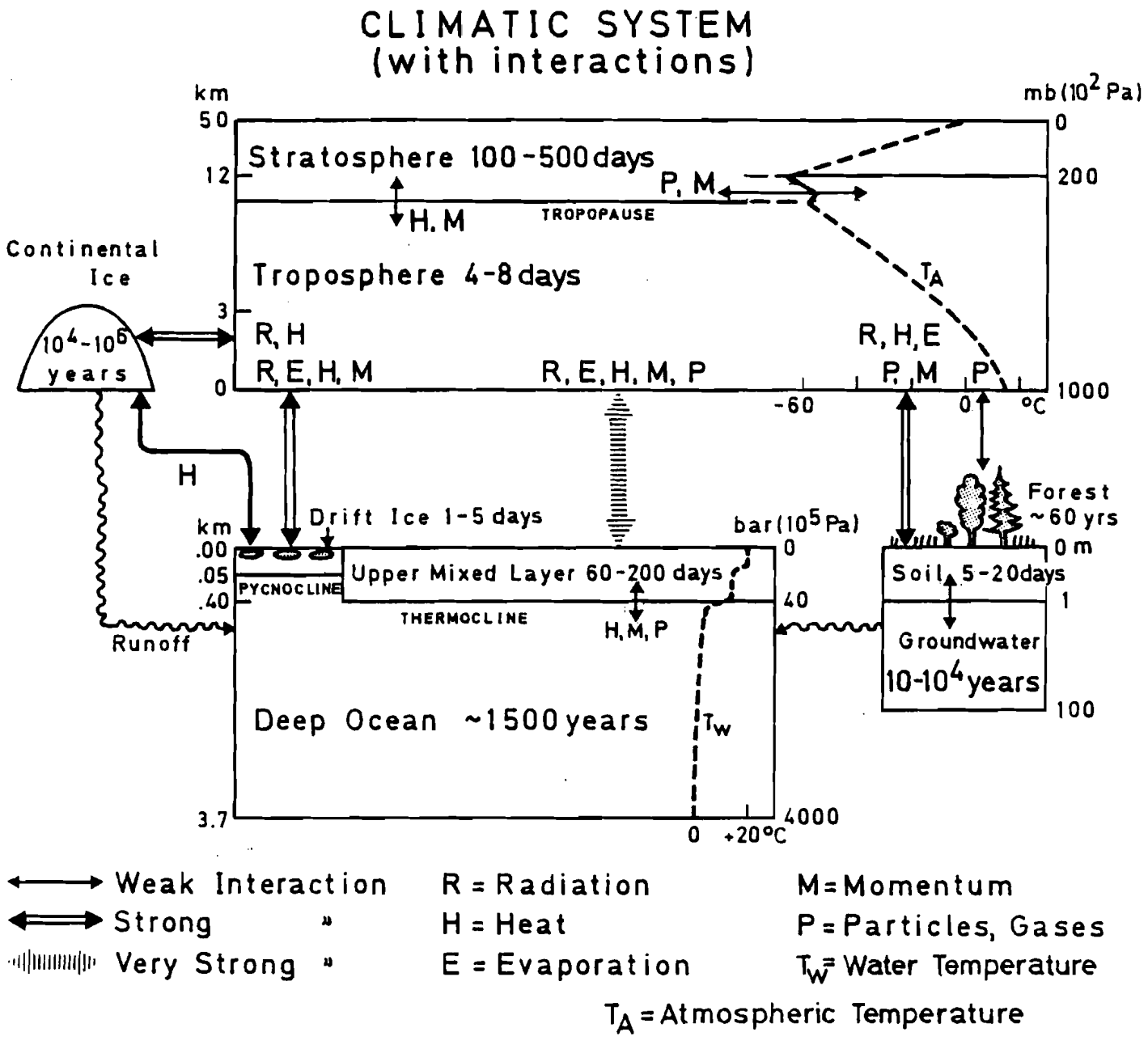

Climatic system, subsystems with characteristic time-scales, and interactions.

albedo and temperature. The effect of other trace gases, especially of nitrogen oxide, one of the final products of nitrogen fertilizers, adds some 50% or more to the CO_2 effect, accelerating the expected global warming.

By using one of the most reliable radiation models for the relation between CO_2 content and representative temperature change (together with a selection of logistic CO_2 growth functions), one obtains an estimate of future temperature evolution that is dependent on the initial growth rate (see figure). Some thresholds of temperature increase can be selected as representing some past warm phases during the long historical evolution of the earth's climate. A global man-made warming of 0.2°C as assumed for the past 80 years cannot be found within the natural fluctuations. An increase of 0.4-0.5°C can unambiguously be evaluated from the existing data sources; this level will probably be reached between 1990 and 2000.

Since really comprehensive models of the climatic system as a whole and its interactions are not yet available and cannot be expected to be forthcoming soon, a *scenario* based on *warm paleoclimatic phases* (see table) is presented in this paper. Such a scenario can be used as a conditional forecast only if the following natural factors remain constant: no change in the solar constant, no major cluster of volcanic eruptions, no disintegration of the West-Antarctic ice sheet, and no changes in cloudiness. Furthermore, the changes in the boundary conditions since the occurrence of past warm phases (changes in vegetation, sea level, mountain building) must also be taken into account.

Table. *Combined greenhouse effect,* CO_2 content (in ppm), and paleoclimatic warm phases.

ΔT	Paleoclimatic warm phases	Virtual CO_2 content	Real CO_2 content[a]
+ 1.0 C	Early Middle Ages (~1000 AD)	420-490	385-430
+ 1.5	Holocene Optimum (~6000 BP[b])	475-580	420-490
+ 2.0	Eem Interglacial (~120,000 BP)	530-670	460-555
+ 2.5		590-760	500-610
+ 4.0	Ice-free Arctic ocean (12-2.5 million years BP)	780-1150	630-880

ΔT = representative warming in low and temperate latitudes.

a The CO_2 greenhouse effect is increased by 50% on account of atmospheric trace gases. The equivalent CO_2 content is based on two extreme versions of the model by Augustsson and Ramanathan (1977); the most likely value lies between the extremes.

b before present.

During the medieval warm phase (~1000 AD), the sea ice around Greenland retreated, causing more northerly cyclone tracks and frequent dry anticyclonic conditions for Europe. Much evidence exists for the Holocene Warm Period (~6000 BP), when it was nearly everywhere more humid than today, especially in the arid belt of the Old World, where the desert was replaced by semiarid grassland densely populated by cattle-raising nomads. Here the role of natural and man-triggered processes (retreat of the North American ice sheet, beginning of desertification) is discussed: under present boundary conditions a return to a similar regional climate is unlikely.

More warming, i.e. +2.0-2.5°C, would be equivalent to the warmest interglacial period 120,000 years ago, undergoing marked shifts of vegetation belts and coastal lines due to a sea-level rise of 5-7 m, which were probably caused by a partial disintegration of the West Antarctic ice sheet. Like in the Holocene Warm Period, the climate was somewhat moister than today in many areas for which data are available. But abrupt coolings of a nearly glacial intensity have also been observed for other interglacials, each lasting for several centuries. If one assumes the contribution of trace gases to the CO_2 greenhouse effect to be 50%, the real CO_2 level equivalent to a 2.5°C warming can be estimated to be 550 ppm ± 10%. A warming in the Arctic would reach about 6-8°C, probably reducing the Arctic sea ice to its central core between Siberia and Canada, and causing at the same time a poleward displacement of climatic belts by several hundred kilometers.

If this level rose to 750 ppm ± 16%, a representative warming of 4°C would be reached. Model studies and paleoclimatic investigations indicate that this value is close to the *critical threshold* of a complete *disappearance* of the drifting *Arctic sea ice*. The sensitivity of this sea ice--now with an average thickness of only 2-3 m--to changes in several climatic factors, such as length of melting period, heat flow from the ocean, and salinity (due to a possible reduction of freshwater inflow), indicates that such a disappearance would probably take no more than a few decades or even less. The thermic conditions mentioned above may be minimum values, but the paleoclimatic evidence collected by the Deep-Sea Drilling Program has revealed that a permanently open Arctic sea existed until 2.3 or 2.5 million years ago, in contrast to the fact that the East Antarctic continent has been glaciated since 12-14 million years ago.

This discovery is quite surprising since such a contrast between a heavily glaciated pole and an ice-free pole must have created a *hemispheric asymmetry* of the atmospheric-oceanic circulation that was much stronger than the asymmetry existing today. Indeed, for the last ten million years before the beginning of the present glacial-interglacial cycle, an Antarctic ice dome of today's height (or higher) coexisted with an open Arctic ocean, with temperate or boreal forests extending to lat 81-83°N, interspersed only with some local mountain glaciers; no evidence of tundra or permafrost in the soil has been found.

Such an asymmetry of the climate would cause the southern arid areas to expand to the vicinity of the equator, displace the meteorological (and thermal) equator near lat 10°N, with an equatorial rain belt only in the northern hemisphere, and shift the northern arid belt to lat 35-45°N, extending it even to southern central Europe. This shift of climatic belts is merely a consequence of fundamental circulation theories: with the temperature difference between the equator and the poles decreasing, the area of the tropical-subtropical circulation belt increases, while the temperate and subpolar belt of westerlies shrinks toward the North Pole. Since no comprehensive climate model of this unexpected pattern has been designed so far, detailed forecasts of the regional climates after such an event are not possible. Simple extrapolation of the climate of the Late Tertiary (12-2.5 million years ago) is not admissible because of the displacement of continental coasts and the building and lifting of most of today's mountains at and since that time. The *stability* of this pattern over a period of as long as ten million years must now be considered a fact. A return to this pattern would most probably lead, after a series of catastrophic weather extremes, to a displacement of the earth's climatic zones by 400-800 km. This would necessarily affect mankind as a whole: beneficially in some areas, but destructively in many others, drastically changing freshwater supply and agricultural productivity.

CONTENTS

POSSIBLE CLIMATIC CONSEQUENCES OF A MAN-MADE GLOBAL WARMING

H. Flohn

NATURAL AND MAN-MADE CLIMATOGENETIC EFFECTS

The recent discussion on the physical background of climatic fluctuations (GARP 1975) aims at one of the basic problems of the geophysical sciences, and not of meteorology alone. Climatogenesis occurs not only within the atmosphere but within a climatic system (Figure 1) that consists of several interacting subsystems with quite different time-scales ("memories" in the usual scientific slang). That this system is apparently fairly well balanced can be concluded from the climatic history of the past 5000 years, when only secondary climatic fluctuations occurred. But even these were effective enough to seriously disturb man's economy and to challenge his bare existence in marginal areas of the polar or arid zones. Many of the physical causes assumed by non-specialists to produce climatic changes are indeed internal effects within the climatic system: for example, an expansion of the Arctic sea ice is, at the same time, cause and effect of climatic fluctuations. Some examples of such feedback responsible for climatic fluctuations will be considered in Chapter II: Internal Climatogenetic Processes.

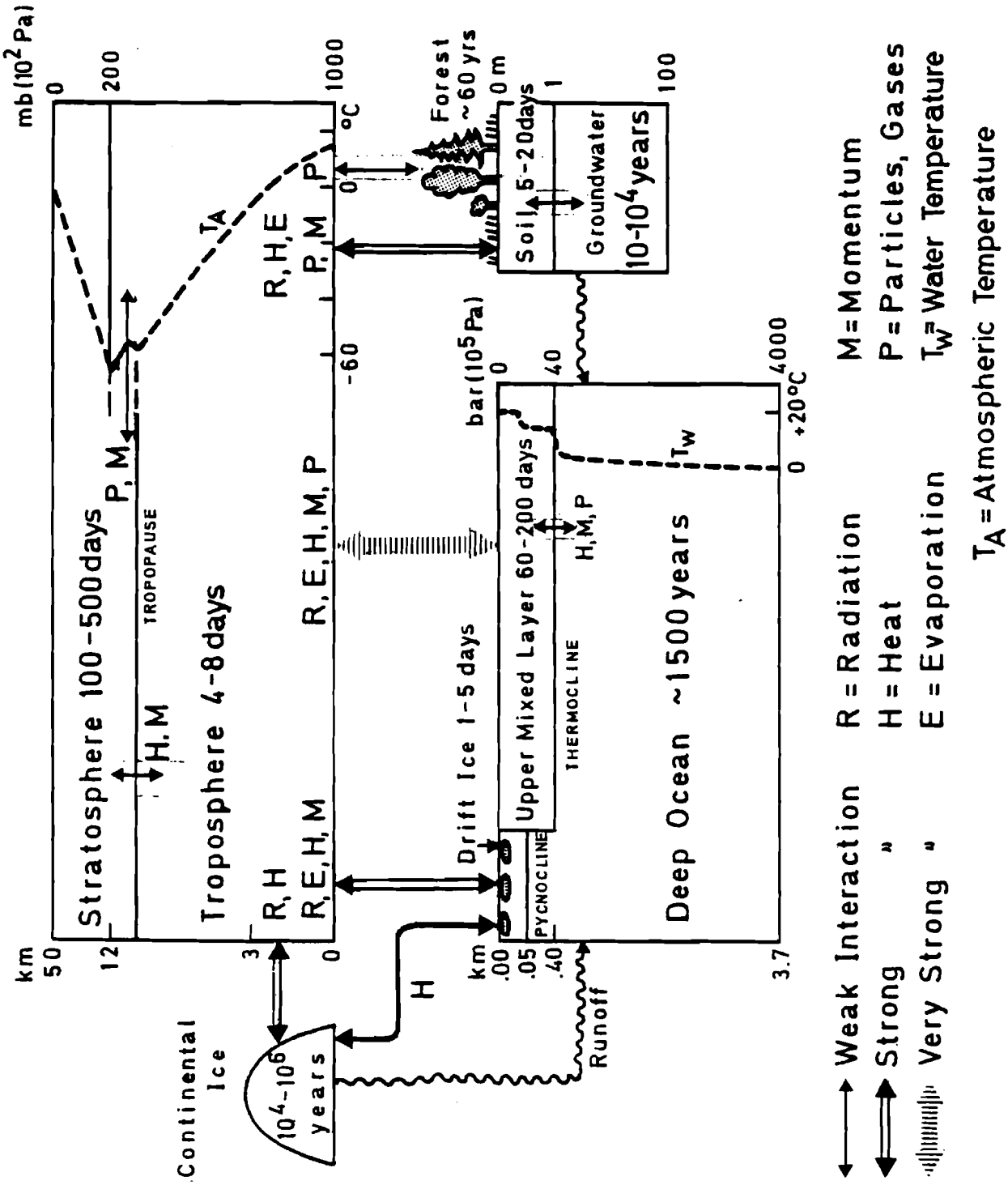

Figure 1. Climatic system, subsystems with characteristic time-scales, and interactions.

External effects operate without, or with only negligible, interaction. The examples given most frequently (and correctly) are heavy volcanic eruptions of the explosive (Plinian) type: they produce large numbers of small particles in the submicron range, floating in the stratosphere (in the Junge layer at about 20-22 km), concentrating in polar regions, and absorbing and scattering parts of solar radiation. This leads (Oliver 1976; Mass, and Schneider 1977; Pollock et al. 1976) to worldwide cooling that increases with the high-latitude feedback between snow, albedo, and temperature. The frequency of these eruptions varies much with time (Lamb 1970; Kennett 1977a, 1977b; Kennett et al. 1975, 1977b); together with earthquakes they are apparently triggered by the slow but discontinuous motion of tectonic plates of the earth's crust. The role of fluctuations of solar radiation in the visible and near-infrared part of the spectrum is still controversial among specialists--continuous high-precision measurement above the level of pollutants in the denser layers of the atmosphere would be needed, preferably from a satellite. There are strong variations in the particle emission of the sun (protons) and its radiation in the far-ultraviolet or roentgen range; their possible role in the climate- and weather-producing troposphere (below 200 mb, or approximately 12 km) is also still controversial and will not be discussed here. Other extraterrestrial effects, if existing, are negligibly small.

It is generally agreed that man-made effects (see e.g. Bach 1976a and b) have up to now only been perceptible at a local and microscale, e.g. in cities or industrial centers. The role of atmospheric dust (in the 1-10 micron range) has sometimes been overrated--at a regional scale it may exist in some deserts or semideserts (notably Central Asia and the Middle East), or in large metropolitan areas. Its effect depends not only on the size and quality of the particles but also on the surface albedo (reflectivity); a warming effect seems to prevail, at least in continental areas. The role of waste heat is restricted to the local scale; even if it were to increase substantially, the short residence time of enthalpy in the atmosphere, which is on the order of hours and days, will most probably inhibit any large

contribution. In contrast to the rather short residence time of tropospheric particles, which is on the order of days or weeks, the residence time of infrared-absorbing gases, such as CO_2, is much longer, i.e. on the order of years and decades. A more detailed treatment will be given in Chapter III: The "Combined Greenhouse Effect" of CO_2 and Atmospheric Trace Gases.

Omitted here are some slow, but certainly effective, man-made changes acting via the biosphere and the soil: destruction of vegetation and its conversion into arable land and/or pastures, including soil erosion, desiccation of swamps, lakes, and marshes, large-scale irrigation (now at about 2.3×10^6 km^2) and reservoirs (now about 0.5×10^6 km^2, not including the multitude of small tanks and ponds), and sealing of the surface by concrete and other building materials. Their climatic effect operates through several physical parameters: surface albedo and roughness, soil moisture and evapotranspiration, terrestrial (infrared) radiation, and absorption by water vapor. All of these processes are at first relevant at a local scale--at a global scale they operate quite slowly. But at least since the Neolithic revolution about 5000 years ago, continental surfaces have been subject to exponentially increasing changes, affecting now at least 30% of the continents, or some 45×10^6 km^2. The effect is probably even much older: Paleolithic man already knew how to use fire for hunting (e.g. in Australia). Destruction of natural vegetation has reached an alarming rate (FAO statistics, reported at the Second International Conference on Environmental Future at Reykjavik, 1977, Polunin, ed., forthcoming) claim the annual rate of destruction of tropical forests, which plays a big part in the CO_2 cycle, now to be 110,000 km^2, and tends to increase the surface albedo everywhere; this is one of the few man-made processes that lead to cooling, at least in cases where the decrease in evapotranspiration does not cause an increase in sensible heating.

Due to the complexity of the climatic system and the lack of models suitable for simulating the essential interactions between its subsystems (Figure 1), any attempt to predict climatic changes in toto is useless at the present time, at least if the forecast should extend beyond one year. Most essential and sobering in this respect is the mere fact that external effects

are yet unpredictable, and will remain so for some time. Instead there is some hope for the feasibility of conditional prediction (also defined rather vaguely as "prediction of the second kind"). Such a prediction may start out from the assumption that external effects, and perhaps also some of the interactions, do not change: what will then be the climatic consequences of one or another man-made process, e.g. of an increase in CO_2? All other factors being held constant, it should be possible to outline, separately or in combination, the possible effects of processes made or triggered off by man with the help of simplified or more sophisticated models. In this way our understanding of climatogenetic processes can at least be systematically improved.

In spite of the fascinating progress we have made by designing physicomathematical models of atmospheric circulation, no model can, at present, adequately describe the climatic system as a whole, including the highly effective positive or negative feedback mechanisms within and between the subsystems. A careful and critical evaluation of the existing limitations to surface climate modeling has been given by Manabe and Holloway (1975), who use Köppen's classification for comparing model results and reality. No model has yet demonstrated, with sufficient accuracy and horizontal resolution, an ability to simulate the present surface climate including its seasonal variation, which is one of the most severe and convincing capability tests. One of the main drawbacks is the lack of effective parameterization of subgrid-scale processes, another the limited capability of even the most powerful computers available. These sober statements must never underrate the achievement of our enthusiastic model designers--climate forecasting is indeed, as John von Neumann put it 25 years ago, in an unforgettable manner, the second most difficult task for a computer, perhaps more difficult than even von Neumann could visualize. There is little doubt that in a foreseeable future more advanced climate models, probably combining deterministic and stochastic approaches, will be able to present satisfactory solutions, at least for the case of conditional prediction.

Realizing this situation, it has been proposed to use, instead of models on a physical and mathematical basis, a scenario that is derived mainly from past climates. This is a scientific tool with a historical (and geological) basis, essentially but not exclusively an empirical approach, and certainly not without specific limitations. Since it is necessary to look back not for only 1000 or 6000 years (Section Va: Medieval Warming, Section Vb: Holocene Warm Period and the Humid Sahara), but for 10^5 (Section Vc: Last Interglacial (Eem Sensu Stricto)) and eventually 10^6-10^7 years (Chapter VI: Ice Free Arctic Versus Glaciated Antarctic?), the boundary conditions of the climatic system vary to such a degree that past experience, just like sensitivity tests for a fairly sophisticated model, can only be used as a first guide into what may happen in a foreseeable future. Nevertheless, in spite of this nearly unimaginable time-scale, our interest has to be restricted just to what could be considered man's time-scale, to what can be expected over the next 50-100 years. Compared with a model, a scenario has one advantage: It describes a situation that has indeed occurred and may therefore arise again. Learning from history means to check how nature has solved the complete set of equations simultaneously and on-line, in all subsystems and at all scales, with a fully four-dimensional, i.e. time-dependent, approach. Since the boundary conditions are varying slowly, but permanently, climatic history can never repeat itself in all details but only in substance.

For these reasons, a scenario for a possible future evolution must be based on the three assumptions:

1. no major change in solar radiation (solar "constant");
2. no unusual clustering of major volcanic eruptions;
3. no unusually large advance ("surge") of the Antarctic ice shelves (see Section IIb: The Role of the Antarctic Continental Ice Sheet).

These assumptions are made because of the unpredictability of such natural effects; effects 1. and 3. are still hypothetical.

A fourth necessary assumption only refers to our present lack of knowledge:

4. no significant variation of average cloudiness.

Indeed, the interaction between radiation (dependent on wavelength) and clouds (dependent on size distribution of droplets and crystals, on cloud type and altitude, on pollution particle content) is not well understood. However, many scientists feel that this concern should not be overemphasized (Cess 1976, 1977). Two reasons are given here (see Figure 8, p.37):

1. The bulk of clouds is formed (dissolved) in ascending (subsiding) motion of different scales: due to the law of conservation of mass all vertical motions are well balanced. Only a few percent of low-level stratus and thin cirrus trails are now manipulated by man.
2. Global warming due to infrared absorption ("Greenhouse effect") decreases with height and reverses its sign in the stratosphere (Figure 6, p.28); in this case the overall thermal stability of the troposphere will decrease and, consequently, also the frequency of stratus clouds, while vertical mixing will increase. With his NCAR model, Roads (1978) demonstrated that fractional cloudiness and relative humidity may even decrease with increasing temperature.

INTERNAL CLIMATOGENETIC PROCESSES

The Role of Polar Sea Ice

Large areas in both polar regions are, permanently or seasonally, covered by a thin blanket of ice floes separated by narrow strips of open water (polynyas, leads). The ice floes, which are covered by snow for most of the year, have an albedo (reflectivity) of almost 80%. This is in contrast to the albedo of open water, which is only 8-12% in polar regions when the sun is low in the sky. During the *melting season* (which in the

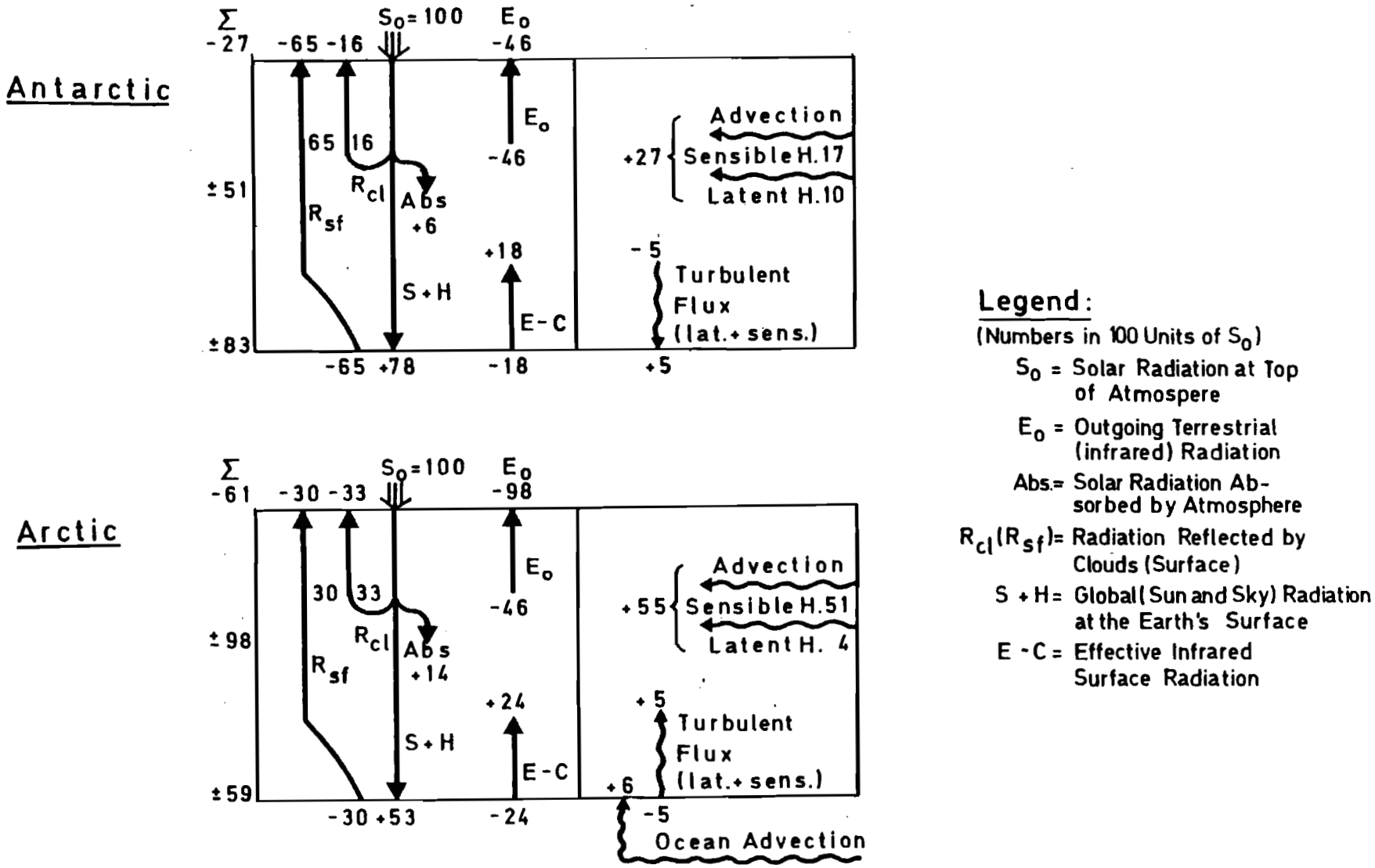

Figure 2. Tentative heat budgets of the atmosphere above the Antarctic (Schwerdtfeger 1976, partly revised) and Arctic (Schwerdtfeger 1970, Vowinckel and Orvig 1970); reproduced from Flohn (1978a).

Central Arctic is restricted to about ten weeks between mid-June and the end of August), the albedo of the ice floes decreases to about 60%, and superficial ponds of meltwater occur, which appear light-blue when seen from an airplane.

The relative area of polynyas varies between 2-3% in winter and up to 12-20% in the melting season (Vowinckel and Orvig 1970; Untersteiner 1975). The average thickness of the Arctic drift ice is quoted to be 2-3 m: this figure, however, is not representative since the thickness of individual floes varies, according to age, between 0.5 m and more than 6 m (Thorndike 1975), as has been verified by submarine expeditions; satellite microwave measurements of surface emissivity have confirmed this irregular mosaic.

Representative data for a heat and radiation budget are very difficult to determine under such conditions; in winter the turbulent fluxes of sensible and latent heat from the polynyas, where the open ocean water ($T_W \approx -2^{\circ}C$) is in direct contact with the cold air below the polar inversion ($T_A \approx -30^{\circ}C$) (where T_A (T_W) = air (water) temperature), are more than 100 times as large as those at the surface of the ice floes, and frequently have an opposite sign (Vowinckel and Orvig 1973). Even during polar summer with permanent daylight, polynyas with a diameter of several kilometers can suddenly freeze over because of cold air advection (as the author observed in late July 1972). Thus the heat budget values given in Figure 2 can only be rough estimates.

In a very careful model study, Maykut and Untersteiner (1971) simulated the physical processes of ice formation and melting, based on observations made in the years 1957-58 and assuming a horizontally homogeneous ice cover. In this one-dimensional model of the ocean-ice-snow-air multiphase system, two processes are particularly effective in reducing the ice thickness: lowered surface albedo (e.g. in relation to the duration of the melting season, but also to pollution by dust or oil wastes), and increased ocean water temperature. During the melting season, about 50 cm of ice melt from above, while for the rest of the year a similar amount freezes from below. Not

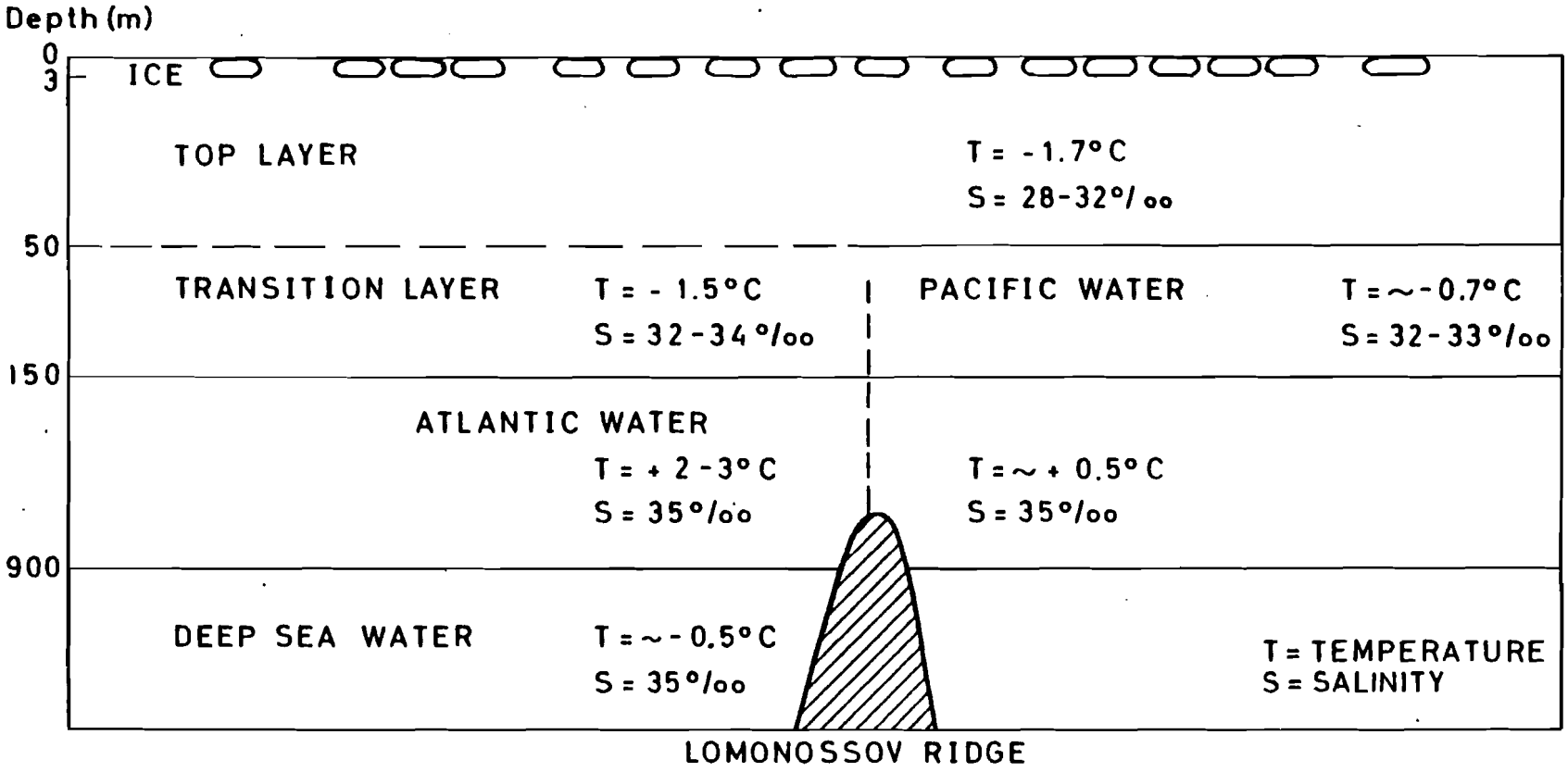

Figure 3. Stratification of the Arctic Ocean (schematic).

included in the model is a possible increase in salinity (and thus density) of the ocean water, e.g. after an artificial deviation for irrigation purposes of part of the freshwater flow from the big rivers in Siberia and Canada (Aagard and Coachman 1975).

At present, the ice-forming processes occur in a shallow (~50 m) but very stable surface layer of the ocean (Figure 3); the excess of this low-saline water together with ice leaves the Arctic basin with the strong and narrow East Greenland Current. If the freshwater inflow is significantly reduced, the salinity and density of the surface layer must increase, which reduces its stability. In a nonstratified ocean with turbulent vertical exchange no permanent icecover would be possible.

The drift ice is driven by winds and the ocean currents; between Greenland, Alaska, and Siberia a large anticyclonic gyre circles clockwise around the central core of the Arctic ice (Rothrock 1975) which has survived for at least 700,000 years, but probably for more than two million years. The total area of the Arctic drift ice varies between 8.2 million km^2 in late summer and 11.8 million km^2 in late spring. Thus only one third of the maximum ice cover is seasonal, with a thickness of nearly 50 cm; the average residence time of an ice crystal in a floe between freezing and melting is on the order of 5-10 years.

In contrast to the high stability of the central core, the marginal parts of the ice in the Atlantic sector between Greenland, Svalbard, and Novaya Zemlya underwent *large fluctuations* already in the historical past (see Chapter V: A Global Warming Scenario Based Upon Past Climates); after a long recession up to Greenland's northern coast (~81°N) the ice advanced around 1320 along the eastern coast, in severe winters blocked Iceland and the Denmark Strait until late summer, and advanced, from the late 17th to the 18th century, several times towards the Faroes and even Norway. Occasionally Eskimos and polar bears stranded with a scattered floe were carried to the coast of Scotland (Lamb, H.H., University of East Anglia, U.K., private communication, 1978). The total area may have varied by more than 20%

during the last millenium, while the southern edge shifted by more than 2000 km.

The strong contrasts of albedo and heat budget along the edges of the ice are of paramount importance for the formation of cold air above the ice and thus for the position of tropospheric frontal zones. The large-scale advance of the ice during the Little Ice Age (1550-1850, with some precursors around 1320 and 1430) is apparently correlated with several phenomena: a rearrangement of cyclone tracks that were displaced far south, a much more frequent occurrence of blocking anticyclones above the then cold surface waters north and west of the British Isles, frequent outbreaks of polar air over western and central Europe across the Alps, and an increase in cyclonic activity and rainfall in the Mediterranean. "Low index" circulation patterns prevailed over most parts of the midlatitude belt of westerlies in the northern hemisphere, and, as happens occasionally today, cold high-tropospheric troughs frequently penetrated into the interior tropics causing anomalous rainfall (Section Vb: Holocene Warm Period and the Humid Sahara).

While such events were rare during the warm period of 1931-60, the recent, rather modest, *readvance* of the ice (Figure 4 for Iceland, 1901-76) coincides with some of the most unexpected *climatic anomalies* of recent years. Among them are the severe winters of 1968/69 in the U.S.S.R. and 1976/77 and 1977/78 in parts of North America, in contrast to an unbroken series of six or seven unusually mild winters in western and northern Europe, and the coincidence of a serious western European drought with abundant rainfall in central Russia during the summer of 1976. Other anomalies were a sequence of the three most severe seasons of Greenland icebergs in the Newfoundland area (1971-73) in this century, or a great frequency of unusually heavy gales in the North Sea area between 1972 and 1976.

The frequency of such quasistationary, apparently "anomalous", weather patterns demonstrates the simultaneous occurrence of large positive and negative anomalies of temperature and rainfall, known e.g. as "north Atlantic see-saw" (van Loon and Rogers, 1978).

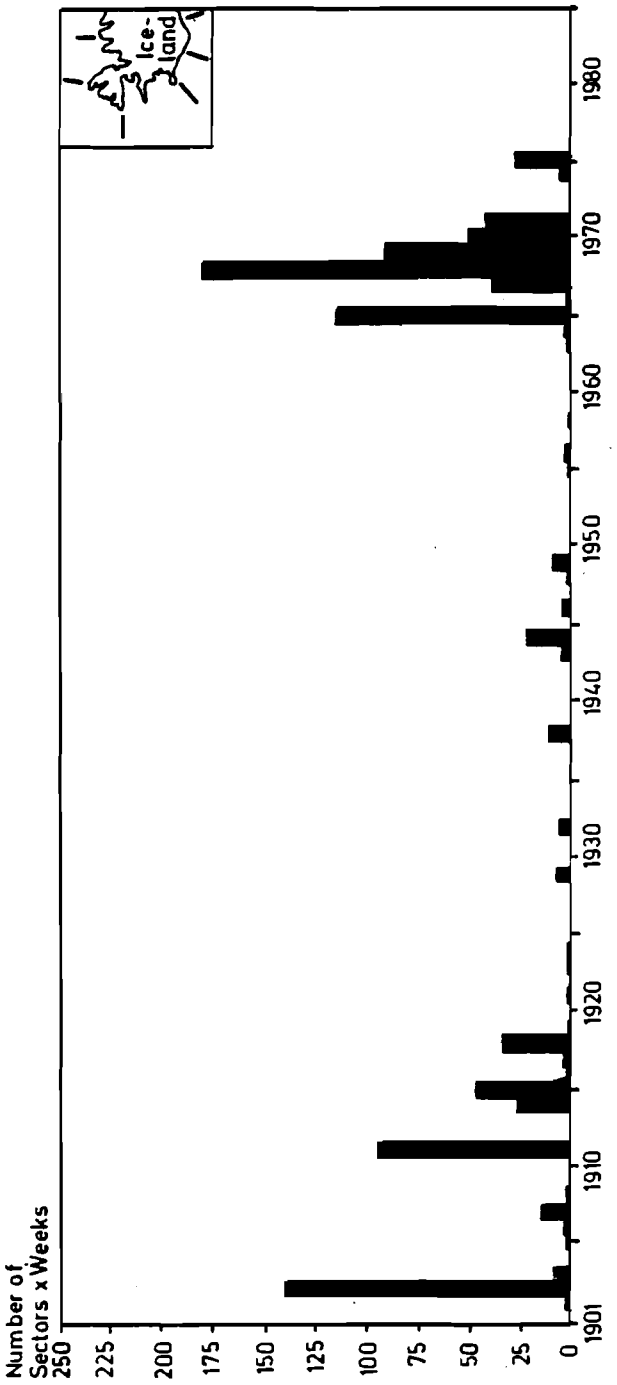

Figure 4. Fluctuations of sea ice at the coasts of Iceland (Courtesy Meteorological Service of Iceland).

This occurrence is correlated with a general *cooling* of the interior Arctic (Figure 9), but masks the small temperature variations averaged along latitude circles.

The physical background of such coolings (or warmings) in the polar zone is far from being understood. One hypothesis (Flohn 1974) is based on the occurrence of one or several volcanic explosions producing great masses of stratospheric particles: due to the stratospheric circulation system, these particles converge and subside above the interior Arctic (north of ~75°N) and Antarctic, forming a *dust layer* there at an altitude of 10-15 km, which is easily visible from an airplane; here it lasts longer than in midlatitudes because of the relative absence of exchange processes between the troposphere and the stratosphere.

By backscattering and absorption, this dust layer reduces solar radiation, surface temperature, and the duration of the melting season. Consequently the average thickness of the ice increases, reducing the heat flow between ocean and atmosphere and leading to cooling and to an extension of the ice: thin seasonal ice grows faster than thick multiyear floes.

In connection with large international research programs (such as POLEX within GARP), more sophisticated three-dimensional, time-dependent models of the multiphase system are now under development, and more complete solutions including all feedback mechanisms may be expected (Washington et al. 1977).

In contrast to the Arctic ice, the *Subantarctic* drift ice is largely seasonal (~85%), it is mainly produced by the extremely cold winds descending and blowing out of the Antarctic continent during the cold season, which is characterized by a strongly negative radiation balance. Its area increases from 3.5 million km^2 in late summer to about 22 million km^2 in spring. The thickness of one-year ice floes varies only between 100 and 150 cm; a low-salinity surface layer of the ocean (like in the Arctic) is *not* developed. The most productive area is the Weddell Sea in the Atlantic sector; from here a large tongue of drift ice frequently extends towards ENE.

In addition to this enormous area of sea ice, the large-scale tabular icebergs should be mentioned, which have an average depth of 200-400 m and an extension of many square kilometers. In extreme cases they are as big as the Netherlands (~30,000 km^2). They break off from the large Antarctic ice shelves, their last debris reaching sometimes as far as lat 35°S in the Atlantic. Climatically they are mainly important because of the large amount of heat they need for the melting process.

The Role of the Antarctic Continental Ice Sheet

One of the basic features of global atmospheric circulation, and consequently also of the wind-driven mixed oceanic layer, is the *asymmetry* with respect to the equator--a fact hardly covered satisfactorily by most textbooks. It is accounted for by one of the fundamental parameters of the circulation, *thermal Rossby number* Ro_T:

$$Ro_T = U_T/r\Omega$$

where $U_T = \frac{\delta u}{\delta z}\Delta z \propto \frac{\delta T}{\delta y}\Delta y$ is the vertical shear of zonal wind u (or the "thermal wind" proportional to the meridional temperature gradient $\delta T/\delta y$) of a layer Δz, r is the earth's radius, y(z) the meridional (vertical) coordinate, and Ω the angular speed of the earth's rotation. This dimensionless number describes the thermal zonal wind, depending on the temperature difference between equator and pole, in units of the rotational speed of a point on the earth's equator (464 ms^{-1}).

In the troposphere it is easy to determine the meridional equator-pole temperature difference, at least for the layers above the surface of the Antarctic ice dome. This is done at Amundsen-Scott station at 90°S, altitude 2800 m. Table 1 gives the result of a survey based on continuous data for a seven-year period. If the results of the South Pole station with an average surface pressure of 681 mb are used to represent the 700 mb level, the error introduced is only about 0.5°C.

Table 1. Average (virtual) temperatures of the midtroposphere between 700 mb (~3 km) and 300 mb (~9 km); I (VII) = January (July).

	Extreme months		Year
Equator (E)	difference	< 0.4°C	- 8.6°C
North Pole (N)	-41.5 (I)	-25.9 (VII)	-35.9°C
South Pole (S)	-52.7 (VII)	-38.3 (I)	-47.7°C
Difference E-N	32.9 (I)	17.3 (VII)	27.3
Difference E-S	29.7 (I)	44.1 (VII)	39.1

These observations demonstrate that, taking into account this systematic error, the Antarctic troposphere is actually about 11°C colder than the Arctic troposphere in the equivalent seasons. This is true in spite of the fact that in summer the Antarctic ice dome enjoys the highest solar (global) radiation of the whole globe: its surface albedo of 84-89% also is the highest.

A meridional equator-pole temperature difference results that is almost symmetric during northern winter/southern summer but *greatly asymmetric* (17°C versus 44°C!) during northern summer/southern winter. This causes a much stronger atmospheric circulation in the southern hemisphere, which crosses the equator and displaces the intertropical convergence zone (ITCZ) towards the north. The zonally averaged position of the *"meteorological equator"*--defined as the latitude of lowest pressure in the tropics and of a change of sign of the average meridional wind component--varies seasonally between 0° and almost 15°N, and reaches, at an annual average, 6°N (Flohn 1967). In July, the thermal Rossby number reaches above the southern hemisphere more than 250% of the value above the northern hemisphere. This point will become important in Chapter VI: Ice-Free Arctic Versus Glaciated Antarctic, where other climatic implications are also considered.

The *physical background* of this *asymmetry* is the quite different heat and radiation budgets of the two polar regions: on the one hand a nearly (85%) landlocked ocean with a thin and perforated cover of drift ice, and an isolated continent with an ice sheet more than 2 km thick on the other hand. Figure 2 from Flohn (1978a) compares the, necessarily preliminary, data that are available on the heat and radiation budgets of Antarctica (Schwerdtfeger 1970, partly revised) and the interior Arctic (Vowinckel and Orvig 1970).

Among the most essential points are the higher albedo (reflectivity R_{sf}) of the Antarctic ice, the region's low cloudiness and atmospheric water vapor content which affect the reflexion from clouds (R_{cl}), and the infrared emission of the atmosphere (E_o). Of minor importance are the turbulent fluxes of sensible and latent heat (evaporation) from the surface, which are directed upward above the Arctic Ocean, but downward above Antarctica.

In both regions, the negative radiation budget at the top of the atmosphere must be maintained by quasihorizontal advection from temperate latitudes: this term is much higher in the Arctic, due to the land-sea distribution dependent on longitudes. Compared with the atmospheric advection the oceanic advection in the Arctic is rather small, since the warm Atlantic water submerges below the shallow cold surface waters (Section IIa: The Role of Polar Sea Ice); the most recent value (see later) is about 30% higher.

In winter, an extremely cold thin surface layer develops above the Antarctic ice dome, with average minimum temperatures below $-70^{\circ}C$, repeatedly reaching $-88^{\circ}C$. This cold layer spreads outward, cools the sea surface, and produces an extended seasonal cover of drift ice, only 100-150 cm thick (see end of Section IIa: The Role of Polar Sea Ice). At the end of the season, the total of Antarctic ice is no less than 36-38 million km^2. Since both the areal extension of the coldest air and the position of the tropospheric baroclinic zone depend on the extension of

drift ice, the southern hemispheric circulation is characterized by a time lag of 2-3 months with respect to the sun's radiation.

The extension of the Subantarctic drift ice and, similarly, of the Antarctic cold surface water, which in two sharp fronts adjoins the warmer water of middle latitudes, strongly depends on longitude: in the Atlantic section it reaches lat 48-50°S, but varies in the vast South Pacific around lat 60°S. Thus the climatic influence of the Antarctic as compared to the Arctic is strongest in the Atlantic section: Bouvet Island (54°S) is almost completely glaciated, whereas Helgoland (54°N) is a summer bathing resort.

About 15 years ago a new unorthodox ice age hypothesis appeared on the scientific scene, proposed by the New Zealand geochemist A.T. Wilson (1964); it was met with much attention from specialists, in spite of the more than 60 hypotheses that existed at the time. His basic assumption was that, at the bottom of a sufficiently thick body of ice, the combined action of pressure from above and geothermal heat flow from below must necessarily lead to melting. In this case the quite stable "cold" ice could be mobilized with the help of regelation processes, which are well-known from "temperate" or "warm" glaciers in midlatitude mountains. In parallel to the rare "surges" of some Arctic or mountain glaciers, he assumed a latent *instability* of the Antarctic ice, which could possibly move forward catastrophically to all sides forming a quasipermanent ice shelf of 20-30 million km^2; the consequence should be a general cooling of the earth and a sudden initiation of a glaciation of the continents in the northern hemisphere. One of the most exciting findings that confirmed one of Wilson's basic assumptions was a discovery by Gow et al.(1968) at Byrd station (80°S, 120°W), where an ice core met with melting water under high pressure at the bottom (2163 m).

The discussion of this hypothesis has led to some important modifications (e.g. Hughes 1973; Flohn 1974b, 1977b), but has left the fascinating basic idea untouched; model computations by

Budd (1975a, b) have demonstrated the interaction of the physical processes involved. The present state of affairs has been outlined by Hughes (1975, 1977): while the bulk of the (eastern) Antarctic ice is stable and rests, with a few small meltwater lakes widely dispersed, on bedrock at a level well *above* sea level, the smaller ice dome of western Antarctica (between South America and long 140°W) rests on a bedrock largely *below* sea level. Here an instability cannot be excluded: the boundary between the floating shelf ice and the slowly moving parts of the continental ice is not fixed, and it has been suggested (see Hughes 1975; Mercer 1978) that the western Antarctic ice sheet disappeared in the geological past. The present situation has apparently (Hughes 1975) not yet reached an equilibrium stage; thus there is some risk--after (possible) removal of the Ronne-Filchner ice shelf--of a catastrophic deglaciation of parts of western Antarctica in a foreseeable future (Mercer 1978). An event of this kind could create a worldwide sea-level rise of 4-6 m (Mercer 1978); its possible time-scale is unknown.

The Antarctic ice sheet with about 26 million km^3 contains by far the largest freshwater reserve of the globe, at an average temperature below -30°C; its mass balance is most probably positive (Schwerdtfeger 1976), about 3 cm water equivalent per year. This figure is somewhat uncertain since some of the outflow components of this vast continent, such as snowdrift, are little known. It should be mentioned that this positive mass balance of the largest storage reservoir is inconsistent with the very slow worldwide rise of the sea level of about 1.1 mm/year. Geophysically, however, sea-level fluctuations are extremely complex and far from being understood.

Equatorial Upwelling, El Niño, and Hydrologic Balance

One of the most surprising features of climatic variability is the irregular fluctuation of sea surface temperatures and of rainfall in a long and narrow belt along the equator across both the Pacific and the Atlantic; no similar feature has been described for the equatorial Indian Ocean. It coincides with

the "equatorial dry belt" of classical climatology; a physical interpretation was first given by J. Bjerknes (1969).

In these two oceans the actual sea surface temperature drops, in a latitudinal belt between about 0° and 4°S, from the average value of tropical oceans ($26\text{-}27^{\circ}$C) to $18\text{-}22^{\circ}$C, and in some cases--especially on the leeward side of islands--to even less than 15°C; the occurrence of penguins at equatorial Galapagos Islands is a striking example of bioclimatic adaptation. Bjerknes' interpretation starts out from the wind-driven Ekman flow in the shallow upper mixed layer of an ocean, reaching only 50-100 m down to the top of the thermocline, which separates, with several strong discontinuities, the cold waters of the deep ocean from the warm mixed layer. By integrating the *Ekman drift* with increasing depth down to the level where the wind-driven component disappears, one obtains a direction perpendicular to the wind, with an (anticyclonic) deviation of the current to the right in the northern hemisphere, and one to the left in the southern hemisphere. Since zonal winds prevail in tropical latitudes, several aspects can be interpreted (see Figure 5) by way of the meridional component of the Ekman drift (ED_y) which can be written as follows:

$$ED_y = -(\rho f)^{-1} \vec{\tau}_x \quad .$$

x and y denote the zonal and meridional components, $\vec{\tau}$ the surface stress vector of wind $\vec{v}$ (proportional to v^2), ρ the density, and f the Coriolis parameter ($f = 2\,\Omega \sin\phi$, with angular velocity Ω and latitude ϕ). Because of $\sin\phi$, the sign of f is reversed at the equator, and in a generally easterly wind, ED_y diverges on both sides of the equator. In the Indian Ocean, where westerlies prevail throughout the year in a narrow band along the equator, the change of the sign of f leads to a convergence of the Ekman drift at $\rho=0$, where $(\rho f)^{-1}$ becomes indefinite.

A more thorough understanding should start from the rotation (vorticity) of the wind stress field: at the lower boundary of the ED layer, the vertical flow component w of the water can be

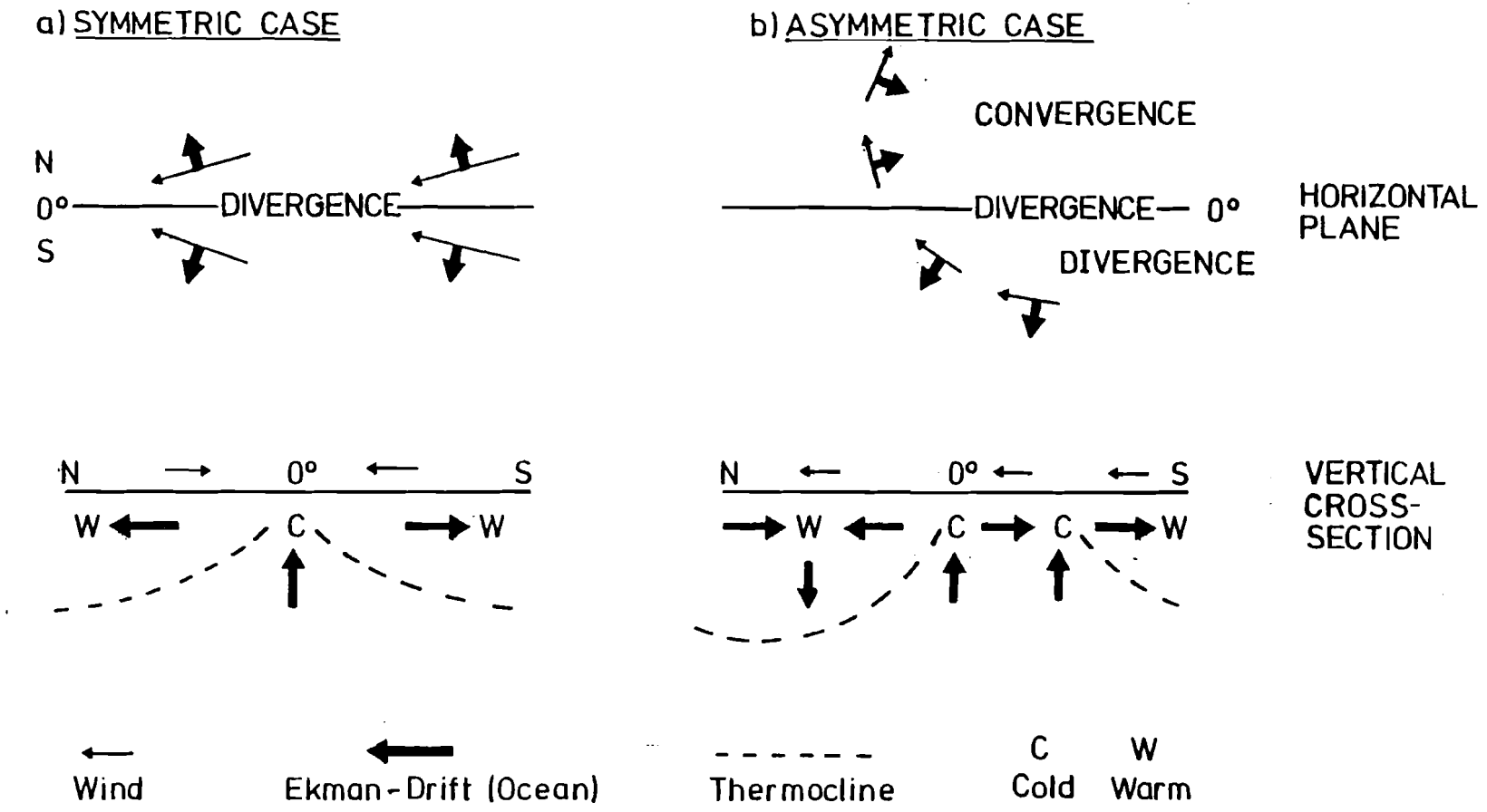

Figure 5. Equatorial flow patterns and upwelling.

expressed as (x,y are the zonal and meridional coordinates, respectively):

$$w = (\rho f)^{-1} \, \mathrm{rot}_z \vec{\tau} \quad ,$$

with the vorticity $\mathrm{rot}_z \vec{\tau} = \frac{\delta \tau_y}{\delta x} - \frac{\delta \tau_x}{\delta y}$.

Due to the asymmetry of the atmospheric (and oceanic) circulation (see Section IIb: The Role of the Antarctic Continential Ice Sheet), the south-east trades cross the equator and penetrate up to about lat 5-8°N with the streamlines usually turned clockwise. This clockwise turn is equivalent to a cyclonic curvature in the southern hemisphere ($\mathrm{rot}_z \vec{v}$ negative); but with the crossing of the equator and the change of the sign of f, the curvature of the flow (by definition) becomes anticyclonic in the northern hemisphere (Figure 5). Since the sign of vorticity is the same on either side of the equator (see Figures 2-6 in Hantel 1972), while f in the denominator disappears at the equator (ϕ=0), being quite small in its immediate vicinity, w must be highly positive (upward) just south of the equator, becomes indefinite at ϕ=0, and is highly negative (downward) just north of the equator. In this case one observes a more or less permanent trend for *upwelling (downwelling)* just *south (north) of the equator*, together with a marked increase in water temperature when crossing the equator towards the north.

The circulation asymmetry reaches its highest peak in northern summer/ southern winter, with a lag of 1-3 months with respect to the sun's position. This is responsible for the seasonal maximum of upwelling in the belt 0-4°S from June to September, i.e. at the time when the symmetry (with respect to the equator) of the wind field reaches its minimum and southerly components of the trades predominate. The upwelling cool water (with an average w of the order of 0.5-1 m/day) stabilizes the atmosphere if T_W (sea surface) < T_A (air). In this case the flux of sensible heat proportional to the temperature difference $T_W - T_A$ is directed downward to the sea, the relative humidity of

the air increases, and evaporation (which is proportional to the vertical gradient of specific humidity $q_w - q_A$) decreases sharply. Recent evaluations of maritime observations (Trempel 1978) in a meridional strip at the Galapagos (long 85-90°W) have revealed that the average evaporation in the belt 0-3°S decreases to 1.0 mm/d in winter (May-October) and to 0.8 mm/d in summer (November-April), compared with 2.8-3.5 mm/d in the adjacent latitudes on both sides; representative values for tropical oceans are somewhat higher (120-150 cm/year). Similar values have been obtained with a larger data set for the equatorial Atlantic (Henning unpublished).

While today equatorial *upwelling* is the prevailing ("normal") mode of the air-sea system, marked changes and reversals occur at irregular intervals, frequently during northern winter/ southern summer, when the southern circulation nearly equals the intensity of the northern circulation; thus the ITCZ representing the boundary between both circulations, which is also called meteorological equator, tends to be close to $\phi=0°$. Along the coasts of Ecuador and Peru, these abnormal periods coincide with the replacement of upwelling cool and nutritious water by a sterile layer of warm water and a drastic reduction of fish catch, for man and seabirds; at the equator itself, the sign of w apparently reverses to downwelling. This anomaly usually starts around Christmas, and has therefore been called *"El Niño"* (the child).

Recent investigations (Wyrtki 1977; Barnett 1977) have demonstrated the large variability of winds and ocean currents, besides that of sea surface temperature and rainfall. The intensity of the large zonal ocean currents, which is here about proportional to the small zonal slope of the sea level, varies (for 12 continuous monthly averages) by ±50%; similarly, the wind stress varies, on an average, between +44% and -25% in similar periods and individual months between +100% and -52% (Wyrtki 1977). Only at the central equatorial Pacific is upwelling or downwelling controlled by the divergence of the Ekman drift; in the Galapagos area and along the Peruvian coast, changes of the

wind field over large distances (~10,000 km) are much more effective than local variations (Barnett 1977). While upwelling coincides with high zonal winds (trades), the downwelling phenomenon occurs during the period of decreasing trades: then an equatorial (Kelvin) wave reverses the vertical circulation in the ocean, causing an "El Niño" event which occurs practically simultaneously (Doberitz 1968) between 80°W and about 160°E, i.e. over a distance of 120° longitude or approximately 13,000 km. It is accompanied by torrential rainfall as in the ITCZ, by thermodynamic instability ($T_W > T_A$), and by lower relative humidity, also causing higher evaporation. Since the correlation between sea surface temperature and rainfall is positive (and well above the 3σ level of significance, see Flohn 1972), rainfall variations are enormous and larger than at any other place in the world: e.g. at Nauru (0.5°S, long 169°E), the rainfall of moving 12 month sequences varies between 95 mm and above 5000 mm (as was observed here between 1916 and 1918!); irregular fluctuations suppress the usual seasonal variation.

Generally speaking, equatorial *upwelling*, with rainfall and evaporation at a minimum, occurs during periods of *strong* atmospheric circulation (which today is mainly controlled from the southern hemisphere), while equatorial *downwelling* (El Niño) with high rainfall and evaporation is synchronous with periods of *weak* circulation. The fact that, in equatorial latitudes, Pacific and Atlantic are practically closed basins leads to some complications. In past epochs with stronger (weaker) zonal circulation--i.e. during some parts of the glacial (strong) and interglacial (weak) epochs--upwelling or downwelling may each have controlled more than 90% or even 100% of the total time (see below).

There is evidence that the fluctuations of T_W and thus also of evaporation were even stronger in those times. With a permanent southerly flow like in glacial times upwelling increases, and the cool water continuously spreads to both sides (Doberitz 1968 or 1969): while thermal stability ($T_W < T_A$) increases, evaporation decreases and may even be reversed to condensation ("dew") at the

cool water surface (with $q_w < q_A$). Conversely, in interglacial periods with distinctly weaker circulation, the tropical warm water with temperatures of 26-27°C may have controlled weather and climate for more than 90% of the total time, with high instability, evaporation, and rainfall. Since the change between contrasting modes depends on τ, which is proportional to v^2, relatively weak variations of the atmospheric circulation can lead to enormous variations of evaporation and rainfall.

The great importance of these processes for oceanic evaporation as well as for the global water balance can be illustrated by a few simplified estimates; extreme examples are the peaks of the last glaciation (about 24-14 ka BP[1]) and of the last interglacial (see Section Vc: Last Interglacial (Eem Sensu Stricto), about 125 ka BP). These two contrasting climates were, at the same time, almost everywhere more arid or more humid than the present climate. Let me tentatively interpret this by giving approximate figures. The area involved may have covered only the equatorial Pacific and Atlantic between lat 10°S and 10°N, extending over 52×10^6 km^2, while for the Indian Ocean little evidence is available. Gardner and Hays (1976) and Prell et al. (1976) have evaluated T_W on the basis of a great number of ocean cores; of particular interest is core A 180-73 at lat 0°, long 23°W. The essential result is that there T_W in August was 7-8° colder 18 ka ago than it is now, while in subtropical latitudes it has remained essentially unchanged. The drop of February temperatures was only 1-3°C; this indicates a much stronger upwelling during southern winter with an extension of the southerly circulation (due to an expansion of the Subantarctic seasonal ice). T_W in August dropped to only 16°C 18 ka ago and even to 14°C at an earlier glacial peak 55 ka ago, in contrast to the present value of 24°C and almost 26°C 125 ka ago. These data, obtained for a sufficient number of cores with different biostatistical techniques and an accuracy of ±1-2°C, indicate that the above-mentioned low value of evaporation E of 0.8-1 mm/d or 30-36 cm/a,

---

[1]ka stands for 1000 years; BP means before present.

with T_W = 18-19°C, is by no means exceptional: E may have been completely reversed with T_W = 14°C.

The present value of E for the areas mentioned above is evaluated to be 132 cm/a or 69 x 10^3 km^3/a (Baumgartner and Reichel 1975). In a *glacial* phase, 36 cm/a may be taken as representative of the large area, which yields only 19 x 10^3 km^3/a, i.e. a regional loss occurs of 50 x 10^3 km^3, or 72%. In a global budget, one has to add the decrease in E by the Arctic sea ice spreading to lat 45°N (Atlantic only): for an area of 14 x 10^6 km^2 this yields a loss ranging from E = 73 cm/a to 15 cm/a or 8 x 10^3 km^3. Furthermore, the drop in sea level by at least 100 m gives a loss of ocean area of 20 x 10^6 km^2 and of E = 12 x 10^3 km^3; an expansion of the subantarctic drift ice 600 km northward in both seasons (Hays et al. 1976) and over an area of about 14 x 10^6 km^2 yields a further loss of evaporation of at least 5 x 10^3 km^3. One obtains a loss of altogether 50 + 12 + 8 + 5 = 75 x 10^3 km^3, which is 15% of the global annual budget of 496 x 10^3 km^3, or 18% of the oceanic evaporation (425 x 10^3 km^3). In a warm *(interglacial)* phase with permanent downwelling, E may have reached 155 cm/a or 81 x 10^3 km^3/a (for the Pacific and the Atlantic together). Here we may add a reduction of the Arctic drift ice area from 10^7 to 7 x 10^6 km^2, which may increase E further by 2 x 10^3 km^3. The total increase is 12 + 2 = 14 x 10^3 km^3/a, i.e. 3% of the global evaporation. But this figure may be too small, because of the neglect of changes on the continents. More essential is the drastic change in the evaporation of equatorial oceans between about 80 (interglacial) and 20 (glacial) x 10^3 km^2/a: this gives the physical background for the nearly complete disappearance of equatorial rain forests during the glacial phases and the replacement by semi-humid grasslands (see also Shackleton 1977).

This *equatorial ocean belt* obviously is a *key area* for large-scale climatic variation--the worldwide effects of changes in T_W in that area on atmospheric flow patterns have been shown empirically by J. Bjerknes (1969) and with a circulation model by Rowntree (1972). This has been even more evident since

Bacastow's (1976) and Newell's (1977) demonstrations, based on records from Mauna Loa, Hawaii, and South Pole stations that, after removal of the seasonal fluctuations, the time variations of the increase in atmospheric CO_2 are also in phase with the irregular change between upwelling and downwelling. Newell (1978) has indicated that this correlation essentially depends on the nutrient content of the upwelling deep water: during a *cool* phase the photosynthesis rate in the upwelling cold water is high and much CO_2 is removed from the atmosphere, which leads to a minimum rate of increase. During a *warm* phase, the uptake of atmospheric CO_2 by the ocean is weak, causing a rate of increase in atmospheric CO_2 that is larger than usual. In this case time variations of the water vapor content and of the CO_2 increase rate are positively correlated. This fact contributes much to a better understanding of the internally coherent processes controlling the climatic variations at the 1000a scale during the last glacial maximum and the Holocene: aridity and drastic reduction of tropical forests 18 ka ago, together with strong cooling of equatorial (but not of subtropical) oceans; precipitation maximum, expansion of tropical forests far into the arid zone (Section Vb: Holocene Warm Period and the Humid Sahara) between 12 and 6 ka BP, together with equatorial warming and weakening of the trade winds (see also Shackleton 1977).

THE "COMBINED GREENHOUSE EFFECT" OF CARBON DIOXIDE AND ATMOSPHERIC TRACE GASES

Any estimate of future climates under the influence of a growing greenhouse effect must take into account that, in addition to CO_2 (Schneider 1975), some other, at least partially man-made, gases also absorb terrestrial radiation, particularly in the window region between 7.5 and 12 μm, just below the region of strong CO_2 absorption (12-18 μm) (Ramanathan 1975, Wang et al. 1976). The strongest absorber of infrared

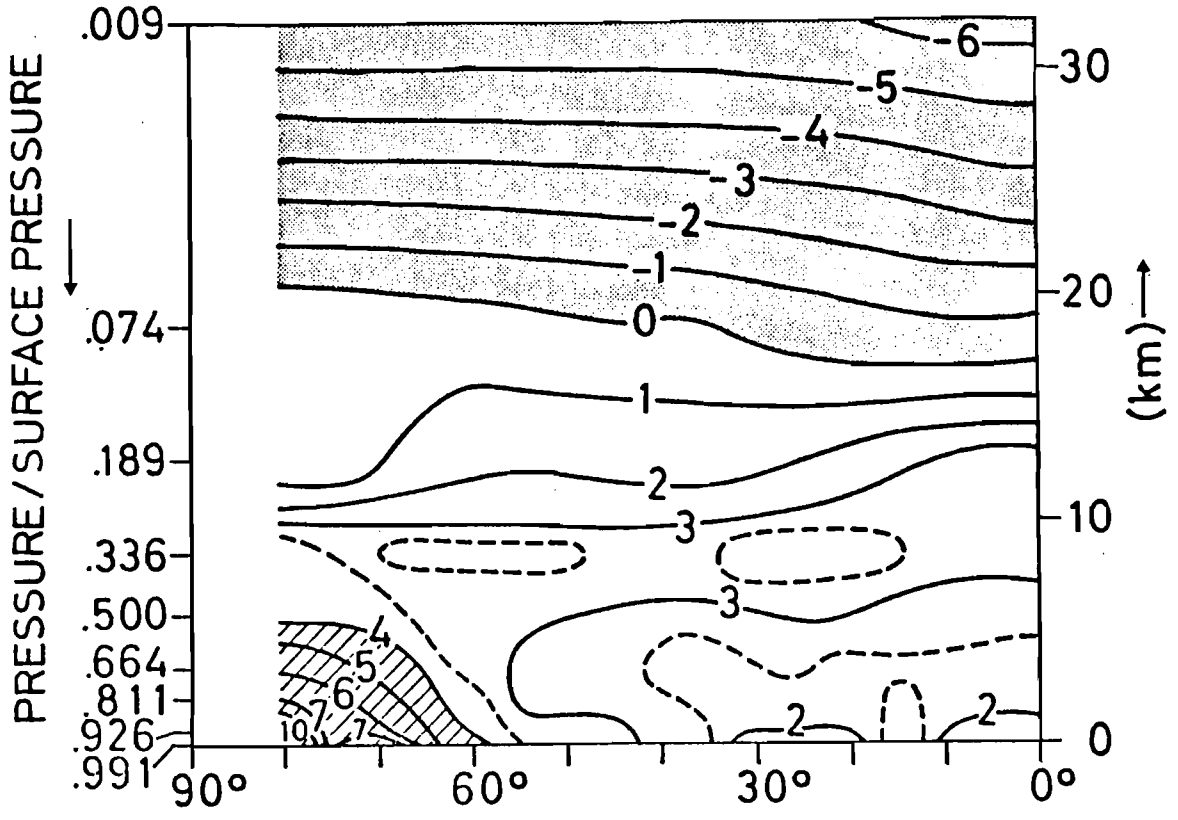

Figure 6. Temperature change (^{o}C) in a vertical-meridional section after a doubling of the CO_2 content, including atmospheric dynamics (Manabe and Wetherald 1975). Note the strong warming of the lower polar atmosphere due to parameterization of the snow-albedo-temperature feedback.

radiation is water vapor: the global amount of evaporation (and precipitation) has recently been estimated to be 496 x 10^3 km^3/a, equivalent to a water column of 973 mm/a (Baumgartner and Reichel 1975). The man-made evaporation over land amounted to 1800 km^3/a (Lvovich 1969) in 1965; this may have probably risen to about 2500 km^3/a (Flohn 1977a) by 1980. The amount is equivalent to only 0.5% of the global value, which is certainly within the limits of error.

With a global warming, the evaporation of the oceans will rise appreciably, as is simulated by some of the most realistic models (Manabe and Wetherald 1975; Wetherald and Manabe 1975) (Figure 6). Because of the importance of equatorial up- or downwelling (Section IIc: Equatorial Upwelling, El Niño, and Hydrologic Balance) for evaporation, significant changes in the atmospheric *water vapor* content are to be expected; a slight increase of "precipitable water", which is at present equivalent to a water column of only 25 mm, also contributes to the greenhouse effect.

While the future increase in CO_2 concentration has been investigated by many authors, the role of trace gases has only recently been recognized. Wang et al. (1976) have taken a one-dimensional radiative-convective model with fixed relative humidity. There the role of clouds is accounted for in two ways, by assuming fixed cloud-top altitude (CTA) and fixed cloud-top temperature (CTT). According to their investigations, the combined effect of man-made trace gases is on the same order of magnitude as the effect of CO_2--any neglect of these processes could mean to greatly underestimate the total greenhouse effect. Table 2 reproduces Wang's table in condensed form as well as the results of an, apparently similar, model for the CO_2-temperature relation presented by Augustsson and Ramanathan (1977) (see also Figure 7). In contrast to the frequently quoted Manabe-Wetherald (1975) model (Figure 6), both models are one-dimensional and neglect atmospheric dynamics and transports. The radiation-cloud interaction is not included, nor any feedback between temperature and snow-ice albedo. Thus the result is only *representative* of *low and middle latitudes*; in subpolar and polar latitudes, the effect on the temperature must be enlarged by a factor of about 3, as indicated also by recent empirical data (Borzenkova et al. 1976). Estimates in the model of Augustsson and Ramanathan (Figure 7) are not much

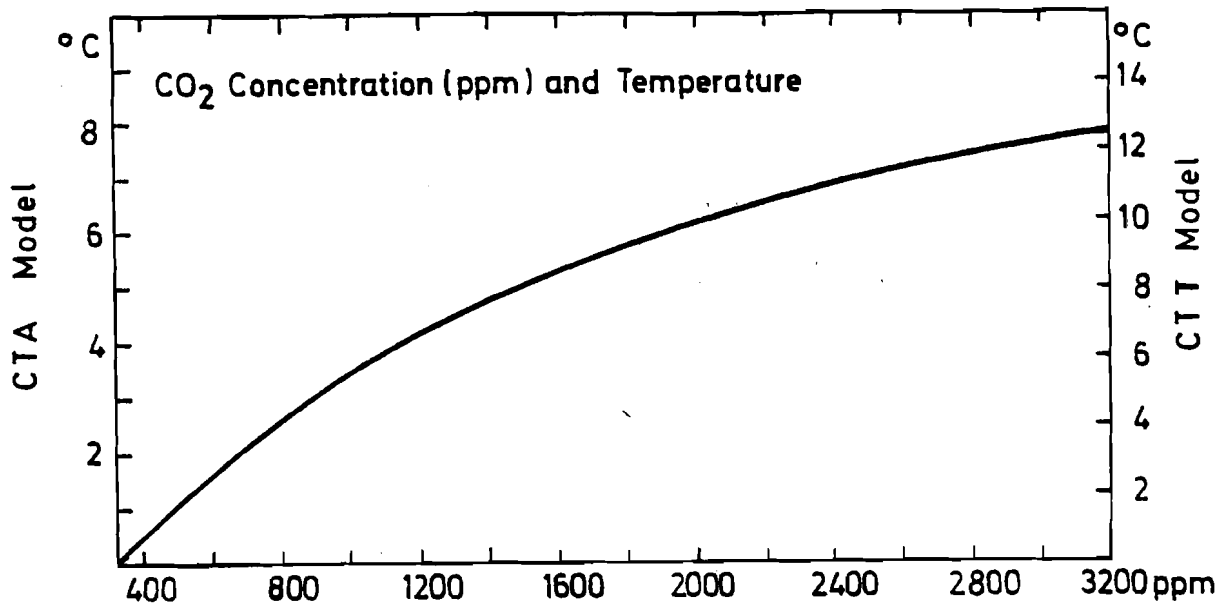

Figure 7. Temperature increase (surface, representative latitudes) and CO_2 concentration, Augustsson-Ramanathan model 1977, CTA and CTT versions (see text) on both sides. The model is one-dimensional and radiative-convective.

different from the results obtained by Manabe and Wetherald (1975): with a doubling of CO_2, the latter model yields a warming of 1.92°C for the latitude belt 0-30° and of 2.20°C for lat 0-50° to be compared with 1.98°C (CTA) and 3.2°C (CTT) in the first model. Some other recent radiation models of the CO_2-temperature relation exist (Schneider 1975; Bach, Rowntree, and Walker, in J. Williams, 1978), which scatter around the models quoted above. A further discussion would go beyond the scope of this contribution.

Table 2. Greenhouse effects arising from changes of atmospheric constituents.

Constituents	Present concentration	Increase (%)[a]	Greenhouse effect (°C) CTA	CTT
CO_2	320 ppm	+100%	1.98	3.2
CO_2	330 ppm	+ 25%	0.53	0.79
O_3	0.34 cm	- 25%	-0.34	-0.47
H_2O (Stratosphere)	3 µg/g	+100%	0.65	1.03
N_2O	0.28 ppm	+100%	0.44	0.68
CH_4	1.6 ppm	+100%	0.20	0.28
$C Cl_2 F_2$+ $C Cl_3 F$	0.2 ppb[b]	factor 20	0.36	0.54
$C Cl_4$+CH_3Cl	0.6 ppb	+100%	0.01	0.02
NH_3	6 ppb	+100%	0.09	0.12
C_2H_4	0.2 ppb	+100%	0.01	0.01
SO_2	2 ppb	+100%	0.02	0.03

Note: The CO_2 data in the first line are after Augustsson and Ramanathan (1977); all others after Wang et al. (1976).

[a]All the growth rates assumed in the Wang model are estimated for 2020 AD; the Augustsson-Ramanathan model is independent of time.

[b]ppb = 10^{-9} volume parts.

The first two lines in Table 2 show that both models coincide well in estimating the CO_2 greenhouse effect, on the assumption that the temperature increase towards the first doubling of CO_2 can be taken as nearly linear (Figure 7). With respect to future changes of the stratospheric constituents due to increasing supersonic traffic, the changes in O_3 and H_2O content are probably too high, since it is doubtful that this traffic will reach the levels Wang used in his calculations. While the sum of infrared absorption, influenced by a decrease in O_3 and an increase in stratospheric H_2O, may yield additional warming (Table 2), it is here assumed that both effects tend to cancel.

One of the most important trace constituents is nitrous oxide (N_2O), produced by denitrification of fertilizers in the soil. Here a strong increase seems unavoidable, considering all the uncertainties of the complex nitrogen cycle in the environment, including the atmospheric residence time of nearly 70 years (Söderlund and Svensson 1976, Hahn and Junge 1977). During the period of 1962-74, the annual average increase in nitrogen fertilizers was as high as 10.7% (Pratt et al. 1977). Even with an only linear growth rate on this order, one could expect an increase of 170% by the year 2000, instead of 100%, as was assumed by Wang for 2020. Pratt estimates the increase from the 1974 level to be between 200 and 450%, while Hahn and Junge more cautiously estimate a rise between 100 and 160%. Under conservative assumptions, Hahn (1979) estimates the greenhouse effect of N_2O alone to be about 25% of that of CO_2, but to amount to about 37% together with NH_3 and HNO_3.

CH_4, which considered a conversion product of CO, is strongly correlated with the burning of fossil fuel. The high contribution of chlorofluoromethanes (CFMs) is derived from their chemical inertness and thus from their estimated atmospheric residence time of 30-50 years. Since strong efforts are being made to prohibit the use of these substances in refrigerators, aerosol spray cans etc., we may reduce their increase drastically (from x20 to x3), assuming a linear reduction of the corresponding greenhouse effect. The greenhouse effect of all other gases is small compared to that discussed above.

One point for further discussion is the selection of an appropriate cloud-top-temperature (CTT) model since, due to our ignorance of some important parameters, we still cannot handle adequately the important cloud-radiation feedback. While Augustsson and Ramanathan prefer to hold the cloud-top altitude (CTA) constant, Wang et al. consider the assumption of a constant temperature of cloud-tops more plausible. The CTA model appears to be more consistent with the assumption of constant relative humidity. Table 2 shows that the CTA model is less sensitive than the CTT model. The author of the present paper conservatively favors the CTA model, but also gives results from the CTT model. He feels that the possible role of clouds should not be overestimated (see Chapter I).

Taking the results from Wang's model, and assuming his estimated growth rates as a first order assumption (except for O_3, stratospheric H_2O, and CFMs, see above), one may start from an increase in CO_2 from 330 to 412 ppm, equivalent to a warming of 0.53°C (CTA) or 0.79°C (CTT). In addition one should at the same time expect a warming of 0.81°C (CTA) or 1.19°C (CTT), respectively, from N_2O, CH_4, CFM (x3) and other gases, i.e. 150% more warming in both cases then would be obtained by CO_2 alone. Including the full effects of supersonic transport (O_3 and H_2O) as indicated by Wang et al., this would add a further warming of 0.31°C (CTA) or 0.56°C (CTT), respectively: in other words, an addition to the CO_2 greenhouse effect by 212 or 228%. As mentioned above, the author prefers to disregard this possibility; he believes that his conservative estimates are *more probably too low* than *too high*. This is especially true in view of the possible increase in water vapor (Chapter Vb: Holocene Warm Period and the Humid Sahara, and Chapter Vc: Last Interglacial (Eem Sensu Stricto). All these constituents have narrow absorption bands in the infrared window between the strong absorption bands of H_2O and CO_2, similar to the well-known 9.6 μm band of ozone. It should be realized, however, that two of the N_2O absorption bands (at 7.78 and 17.0 μm) are situated on the flanks of the much stronger bands of H_2O and CO_2, respectively

(Wang 1976, Figure 1). Thus in view of the enormous differences in concentration the question of overlapping needs further investigation; according to Wang et al., an additive effect can be safely assumed. The physical processes of trace gases in the window region (7.5-12 μm) are similar to those of H_2O and CO_2 on both flanks of the window; together these gases act as venetian blinds attached to the atmospheric window.

To remain on the conservative side, the author proposes to add 50% to the *increase* in CO_2 content (to the 320 ppm base used by Wang), and to express this *Combined Greenhouse Effect* (CGE) in units of *virtual* CO_2 concentration given in ppm. This would be equivalent to a contribution of 67% of real CO_2 to the virtual CO_2 level at any selected time. A less conservative suggestion would be to add 100% to the increase in CO_2 content, equivalent to a contribution of only 50% of real CO_2 to the virtual CO_2 level. In other words: if we use the relation between CGE expressed in ppm and temperature according to Figure 7, the real CO_2 value at this level is given in the right-hand columns of Table 3. The most conservative assumption of a 50% addition to CO_2 is preferred.

The expected increase in atmospheric CO_2 strongly depends on the future evolution of the global CO_2 budget. In this respect, the most controversial question is the role of land vegetation, especially of forests: the alarming destruction of the existing virgin forests (110,000 km^2/a according to FAO statistics, reported at the Second International Conference on Environmental Future at Reykjavik, 1977, Polunin, ed., forthcoming) is another source (not a sink!) of atmospheric CO_2. A report of a working group of specialists at the Dahlem Conference (Stumm 1976), based on various models with logistic growth curves, estimated maxima of atmospheric CO_2 concentration between 1100 and 1600 ppm. At a more recent IIASA workshop (Williams 1978), all the participating specialists (e.g. Bolin, Oeschger and Siegenthaler, Zimen) tentatively concluded that there would be a "manifold increase" in CO_2 if all economically exploitable fossil fuel were burned, and if the (initial) CO_2 growth

rate could not be reduced to less than 3%. In a quite recent critical survey, Junge (1978) estimated an increase in atmospheric CO_2 by a factor of nearly 3 until the year 2050, with a further increase after this date. A rather realistic model of the global carbon cycle and the biosphere (Olson 1978) yielded a doubling of atmospheric CO_2 around 2040, and a further increase to a factor of 4-6 (or even higher) in the 22nd century.

Under these circumstances, a scenario of future climatic evolution in the case of man-made global warming should be based on the role of CGE with respect to temperature (Table 3). The CO_2 model of Augustsson and Ramanathan (Figure 7) can be used to outline typical paleoclimatic stages characterized by representative temperature increases.

Table 3 distinguishes the CTA version of the model as well as the more sensitive CTT version. The first threshold that may be selected is the level of warming that can unambiguously be derived from current data sources (see Chapter IV: Recent Climatic History and Perception of Global Warming). This "level of perception" of a quasiglobal warming can be estimated to be 0.4-0.5°C. Using the CTA model version and the last two columns in Table 3, one finds a corresponding real CO_2 level of 360-375 ppm. Figure 8 gives a time-scale for the expected temperature levels, such as are derived from the Augustsson-Ramanathan model (Figure 7), CTA version, and uses CGE together with the logistic CO_2 growth rate model given by Zimen (1976). In view of the most recent developments in the global CO_2 budget, a slight revision on the basis of more realistic models (e.g. Zimen 1977) seems advisable. Assuming the more recent growth rates of 3.5-4% per year to continue, one can conclude that this level will be reached between 1990 and 2000. Under the same assumption the CTT model would yield a date between 1985 and 1990.

Other threshold values (Table 3) are estimates of representative temperature changes over land areas during some characteristic paleoclimatic stages (Chapter V: A Global Warming Scenario Based Upon Past Climates), such as the Early Middle

Table 3. Combined greenhouse effect, CO_2 content, and paleoclimatic phases.

ΔT (°C)	Paleoclimatic phase	Virtual CO_2 (ppm)		Approximate real CO_2 content			
		CTT	CTA	CTT +100%	CTT +50%	CTA +100%	CTA +50%[a]
+ 0.5[b]	Perception of warming	365	395	342	350	360	375
+ 1.0	Medieval warm phase	420	490	370	386	405	432
+ 1.5	Holocene warm phase	475	580	398	422	450	492
+ 2.0	Eem Interglacial	530	670	426	460	495	555
+ 2.5	Eem Interglacial	590	760	455	500	540	610
+ 4.0	Ice-free Arctic ocean	780	1150	555	630	740	880

a = i.e. with a 50% (100%) contribution of trace gases to the increase in virtual CO_2
b = based on present CO_2 of 330 ppm
ΔT = expected temperature increase (°C)
CTA, CTT = versions of the Augustsson-Ramanathan model (1977)

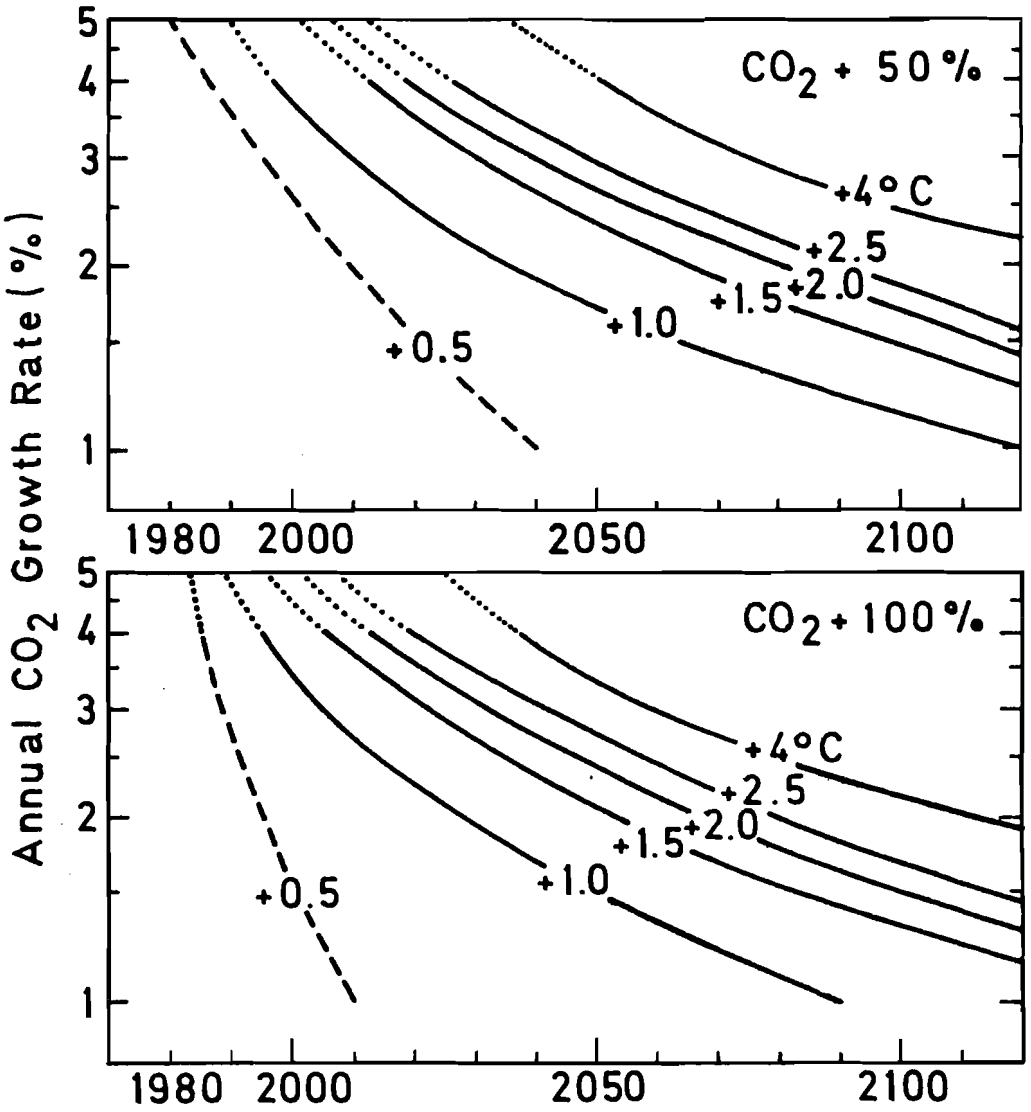

Figure 8. Combined greenhouse effect extrapolated using logistic CO_2 growth rates (Zimen 1977a). The curves labeled temperature are, in fact, curves of virtual CO_2 content; temperature after Figure 7, CTA version.

Ages (about 900-1100 AD), the postglacial (Holocene) Optimum (about 6500-5500 BP), and the Eem stage of the last interglacial.

Considering possible consequences, one of the most important questions is the following: when are these CGE thresholds to be expected? The answer depends on developments and decisions in the fields of economics and politics in a pluralistic society. The author feels incompetent to deal with this problem. Only a first order estimate, based on a logistic growth rate between 3% and 4%, could be tentatively given. In this case, the 1.5°C threshold (equivalent to the Holocene warm period, Section Vb:

Holocene Warm Period and the Humid Sahara) could be reached between 2005 and 2030, and the 2.5°C threshold (equivalent to the Eem period, Section Vc: Last Interglacial (Eem Sensu Stricto)) between 2020 and 2050. Figure 8 also contains estimates based on the, apparently unrealistic, growth rates of 1-2% on the basis of which any immediate climatic risk could be avoided. For the present purposes, it seems more appropriate to label the stages of a warming scenario using approximately equivalent levels of virtual CO_2 instead of fixed calendar years.

RECENT CLIMATIC HISTORY AND PERCEPTION OF GLOBAL WARMING

At the present time, global or hemispheric variations of surface temperature (T_a) can be detected only with the help of an existing network of "Climate" stations situated almost exclusively on the continents and a number of islands. This network suffers from many gaps, especially in oceanic regions, where the small number of stationary weather ships has been reduced drastically since 1973. This uneven distribution of stations is not sufficiently representative to smooth the large irregular anomalies occurring over months, seasons, and years--a lot of noise is due only to the inadequacy of the station network available. Thus interannual hemispheric temperature variations on the order of 0.2-0.3°C can be hardly distinguished from noise.

Several recent papers give an overview of the most recent fluctuations. R. Yamamoto et al. (1975) has presented monthly data of T_a from 343 stations of the northern hemisphere for 1951-73, which he objectively analyzed with a cubic spline technique using moving three-month averages. Typically, the most striking variations occurred in the latitude belt 60-85°N; a significant reduction in temperature occurred after a volcanic eruption, with time delays on the order of 3 to 12 months. This effect of stratospheric dust of volcanic origin has also been analyzed with much longer data series by Oliver (1976) and Mass and Schneider (1977). R. Yamamoto et al. (1977) extended their analysis to the period of 1957-72 (with 431 stations), and included the southern hemisphere. Still longer series of

annual averages have been analyzed by Borzenkova et al. (1976) for several latitudinal bands between 82.5°N and 17.5°N, including the meridional gradient in the belt of 75-25°N. The interannual fluctuations are large, specially in Subarctic and Arctic latitudes; for example, in the belt of 57.5-72.5°N, this parameter amounts to 0.5°C and in the polar belt of 72.5-87.5°N to 0.63°C, both from 1940 to 1975. The hemispheric average reached a maximum around 1938, dropped by about 0.5°C until about 1963, and has been slightly rising since, especially in the polar cap.

In high southern latitudes, the period since 1943 has been characterized by a weak warming (Damon and Kunen; Yamamoto et al. 1977); this is also true for long records in the Subantarctic (Limbert 1974) and New Zealand (Salinger and Gunn 1975). The equatorial belt has undergone only short-lived fluctuations. According to a quite recent synthesis presented by nine authors (Kukla et al. 1977) from the U.S.A., Japan, and the F.R.G., interannual fluctuations contribute most of the variance observed, and are in phase over most of the northern hemisphere and over parts of the southern hemisphere. The long-term trends are significantly smaller--i.e. on the order of 0.01 to 0.02°C per year, see also Walsh (1977)--than the interannual fluctuations. This noise apparently demonstrates the role of internal feedback mechanisms within the climatic system and of external short-lived effects, such as volcanic events. These data do *not* show a reversal in the cooling trend of the last decades, especially not in the upper air temperatures; only the Arctic and Subarctic $T_{surface}$ data increase or remain more or less constant.

A comparison of these results indicates the great difficulties in obtaining representative data of actual temperature changes. This is especially true for the Arctic region, where the trends at the Asiatic and American sectors can be quite the opposite (Walsh 1977), indicating (as is demonstrated by averages for tropospheric layers, e.g. 500/1000 mb) a longitudinal displacement of the center of the polar cold vortex.

Since all climatic variations are subject to large longitudinal variations, which can frequently mask the latitudinal changes, it is preferable to use maps (van Loon and Williams, 1976 and 1977) and/or empirical orthogonal functions (Walsh 1977) for an adequate description of climatic change, at least for parameters such as pressure, geopotential, or temperature. A good example of climatic variability dependent on longitude is the Greenland/NW Europe see-saw (van Loon and Rogers 1978), which has been known for more than two centuries; similar cases should also occur in other areas because of the quasistationary behavior of the long waves of the atmospheric westerlies.

Unfortunately most investigations so far have concentrated on temperature changes, and little is known about large-scale rainfall patterns, which have perhaps the greatest impact on economy and society. Here records from single stations often are not representative and inhomogeneous; the use of areal averages is meaningful only (!) if the data used are internally coherent, which is often not the case because of the rather rapidly declining spatial correlations, such as in the Mediterranean. Recent evaluations (Doberitz 1969, Flohn and Fleer 1975, Hastenrath 1976, 1977) have demonstrated the role of the longitudinally oriented Walker circulation (J. Bjerknes 1969) in the tropics. (It was originally named Southern Oscillation by Sir Gilbert Walker in the 1920s, an index has been given by Wright (1975).) This circulation today controls a see-saw correlation between equatorial upwelling and downwelling (Section IIc: Equatorial Upwelling, El Niño, and Hydrologic Balance) in the Atlantic and in the Pacific (Doberitz 1969), which is similar to the see-saw between the Pacific and Indonesia with the Indian Ocean, as was outlined by Walker and his successors (Berlage 1957, 1966). Since it is impossible to review the numerous investigations in this context, see Wright (1977).

The recent *cooling* of the northern hemisphere, existing since about 1940, has been -0.3 or -0.4°C: this is apparently contradictory to the hypothesis of man-made *warming*. But

note that the temperature trend of middle and high southern latitudes is reversed at the same time. One interpretation is by Damon and Kunen (1976), who consider the development in the southern hemisphere to represent the true CO_2 warming trend that is masked in the northern hemisphere by cooling, due to man-made particles and volcanic eruptions. Both arguments are not very convincing; in particular the latter is not confirmed by the recent occurrence of volcanic eruptions in the tropics south of the meteorological equator (Bali 1963, Galapagos 1968). Another possible interpretation is that, without the assumed warming that is due to CO_2 and equivalent to about $+0.2^{\circ}C$, the natural cooling of the northern hemisphere (which is probably partly due to volcanic activity, which had a minimum between 1912 and 1948) would have reached $-0.6^{\circ}C$. Because of the high interannual variability, this argument cannot be verified. A look at past climatic data indicates a variation of ± 0.5-$0.6^{\circ}C$ around a moving 100a average for the last centuries: this is a reasonable limit for natural fluctuations. In the northern hemisphere, such a warming could be observed on the basis of 5- or 10-year averages; this would have been above the noise level produced by interannual variability.

There are some signs (see Kukla et al. 1977) that the cooling after 1945 has already passed its climax: since about 1974, the polar region has not been as extremely cold as it was between 1964 and 1972, when the Arctic ice was progressing toward Iceland and Newfoundland (Figure 9). Evidence can be found in the monthly surface temperature maps of "Großwetterlagen Europas" issued by the FRG Weather Service (see also Walsh 1977). The opposite temperature trend in high latitudes of both hemispheres and the small changes observed for low latitudes indicate that the *cooling* of the Arctic between 1940 and 1970 was *not* a global phenomenon. If future man-made warming is superimposed on the natural fluctuations occurring in irregular intervals of several decades, it should intensify the natural warming episodes and weaken (or even reverse) the natural cooling episodes. A warming of about $0.5^{\circ}C$ above the noise level, main-

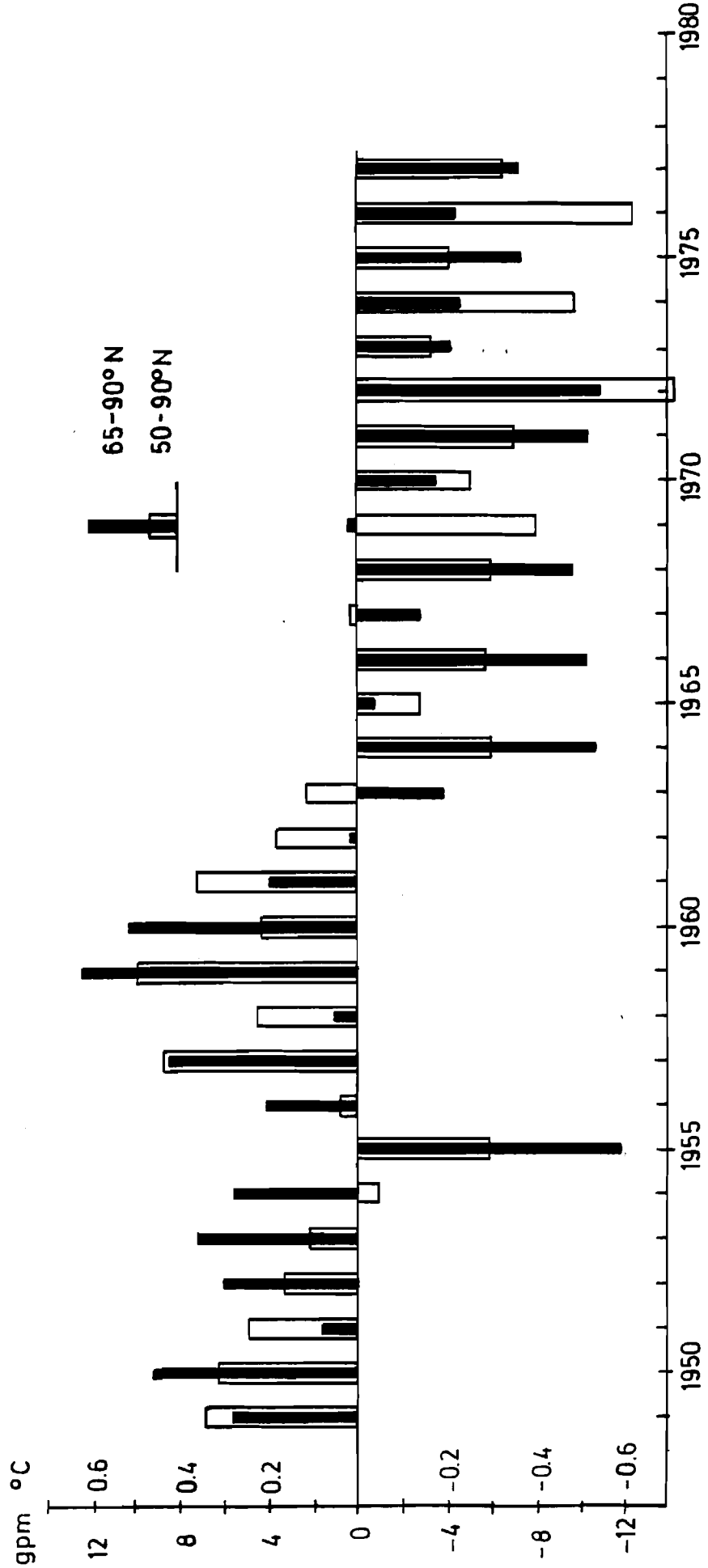

Figure 9. Average annual temperature of the 500/1000 mb layer above the polar caps 65-90°N and 50-90°N, deviations from 1949-73 average (courtesy Dronia 1974).

tained for a period of about ten years, would coincide with the expected tendency: only this might be a sufficiently convincing argument against scientific scepticism.

Thus a *global warming of 0.5°C* can be assumed as a reasonable threshold for a general perception of warming--even if it may be still impossible to distinguish quantitatively between the contributions by natural and anthropogenic processes. For that period, a repetition of some climatic patterns in the reference period (to avoid the misleading term "normal") of 1931-60 can be expected, which has been one of the warmest periods over the last 500 years. This period was also characterized by a relatively low interannual variability in *some* regions (e.g. India), except for western and central Europe, where severe winters and exceptional wet or dry summers were observed in the 1940s (see, e.g. Ratcliffe et al. 1978).

A more general notion of the recent short-lived climatic fluctuations can be obtained from the monthly maps of the 500/1000 mb layer for large areas of the northern hemisphere, published in "GroßwetterlagenEuropas" since 1949 (see above): the thickness of this layer is proportional to the temperature, and represents the average temperature of the lower half of the atmospheric mass (~0-5 km).

Figure 9 (Dronia 1974) gives the deviation of area averages for the polar cap 65-90°N and for lat 50-90°N from a 25-year average (1949-73) for each calendar year. This procedure suppresses all latitude-dependent variations. In this layer, the systematic deviations of the individual radiosondes are generally below 0.5°C and can be neglected. The year-to-year variations are still relatively large--a good example is the year of 1955, when a great anomaly centered in the Pacific. The marked cooling during 1962-64 cannot be interpreted as having been caused by the Agung eruption (Bali) in early March 1963, although this event probably contributed to it. But since then the average temperature of the lower troposphere in polar latitudes has remained a few tenths of a degree cooler

than it was before. A worldwide comparison, based on 63 evenly spaced radiosonde stations in 1958-76 (Angell and Korshover 1978), has verified the warming trend in high southern latitudes, indicating a cooling in northern and southern temperature latitudes, as well as an increasing temporal variability in the tropics; in all latitude belts, 1976 was one of the coldest years on record.

In addition to such temperature data it is necessary to obtain, in the near future, continuous records of some integrating parameters, such as the extension of sea ice at the end of the melting season (in August or late February, respectively), especially for the North Atlantic sector where the greatest fluctuations are to be expected. The Commission on Snow and Ice of the International Union of Geophysics and Geodesy (IUGG) collects data of the glacier variations of many mountains; for our purpose the extended permanent ice fields and snowbeds in high latitudes are of paramount interest, more than valley glaciers in alpine mountains that, in quite a number of cases, only respond to local conditions. Their variations in size at the end of the melting period should be monitored, including e.g. the relative area of snowbeds in the, partly unglaciated, Queen Elizabeth Islands (Canadian Archipelago) and similar islands in the Siberian sector of the Arctic. Special mention should be made of the following ice fields (Hattersley-Smith 1974):

Iceland:	Vatnajökull, Hofsjökull, Langjökull (partly controlled by volcanic and geothermal activity); Drangajökull (NW)
Baffin Island:	Penny Ice Cap (66-67°N), Barnes Ice Cap (70°N)
Devon Island:	(75°N)
Axel Heiberg Island:	(79-81°N; investigated since 1959)
Norway:	Folgefonn (60°N), Hardangerjökull, Jostedals Breen, Svartisen (67°N)
Svalbard:	Edge Island, Nordaustlandet
Severnaja Zemlja:	(78-81°N)

In the southern hemisphere, the large Patagonian ice field should be mentioned, situated at lat 48-50°S (Schwerdtfeger 1956, 1958). A continuous evaluation of the *snow-covered* land area based on satellite data (Kukla et al. 1977b) is also neces-

sary; according to recent experience (1971-72), the early appearance of a continuous snow cover in *fall* is of great importance for the evolution of cold-season surface temperatures at boreal continents.

A GLOBAL WARMING SCENARIO BASED UPON PAST CLIMATES

Medieval Warming

According to the wealth of evidence collected by Lamb (1977; see there also references quoted after Chapters 13 and 17), the Early Middle Ages was the warmest period of the last millenium. Its temporal peak slightly differs between areas (Dansgaard et al. 1975, Alexandre 1977, Wigley 1977); the most remarkable period was between about 900 and 1050. It was characterized by unusually warm and hospitable conditions in Arctic latitudes (Barry et al. 1977), with a disappearance of sea ice in the East Greenland Current, cereal cultivation in Iceland and Norway up to 65°N (and even experimentally in Greenland), and Eskimo settlements as far north as Ellesmere Land and the New Siberian islands. At this time, forests in Canada advanced up to 100 km north of the present timberline, simultaneously with an upward shift of the tree limits in many European mountains, indicating a temperature increase around + 1°C (Table 4). Frequent droughts occurred all over Europe south of 60°N, including the Caspian Sea, which stood at -32 m, i.e. lower than now, after losing much water for irrigation, and which rose by 12 m until the 14th century. In the Mediterranean region, the Dead Sea was nearly as low as it is now (C. Klein, Jerusalem, personal communication, 1977), but the northern part of the Sahara was definitely wetter: crossing by horse caravan (!) has been reported for that time (Nicholson), as well as the end of earlier cattle rearing around Kufra oasis, now near the center of aridity. China and Japan had warm summers (Chu 1973, Yoshino 1978), but severe winters in China, with freezing of the lakes on the sides of the Yangtsekiang, have also been reported.

Table 4. Climate estimates, England and Wales (Lamb 1977)

Climatic Periods	Temperature (°C)			Rainfall[a]		Evaporation[a]	Runoff[a]
	Year	Jul/ Aug	Dec- Feb	Year	Jul/ Aug	Year[b]	Year
"Atlantic"[c], 6000 BP	10.7	17.8	5.2	110-115	?	108-114	112-116
Little Optimum[d], 1150-1300 AD	10.2	16.3	4.2	103	85	104	102
Little Ice Age, 1550-1700	8.8	15.3	3.2	93	103	94	92
Recent Warm Period, 1916-50	9.4	15.8	4.2	932mm		497mm	435mm

[a]Percent of 1916-50 average.

[b]Turc's formula.

[c]Holocene Warm Period.

[d]Data probably also valid for 900-1050 AD.

In North America, there is evidence of large cultivations in Illinois and Iowa, including a remarkable urban center (Bryson and Murray 1977). Tree ring data from California mountains also indicate higher temperatures but low rainfall, like in SW Colorado. Evidence from the tropics is very scanty, the rains in Ethiopia concentrated (Nicholson 1976) in the southern part of the country (Nile floods were low and Lake Turkana was high), while no data are available for India. Even reports exist of long-lasting warming on the Antarctic coast, together with a period of marked drought and forest fire in New Zealand.

One interpretation of these data (Lamb 1977a) suggests a northward shift of the cyclone track by 3-5° latitude to 60-65°N and high pressure conditions over Europe, similar to the warmest and driest summers of the period of 1931-60. In winter, a similar pattern occurred in the north, which has not infrequently been related to a "blocking" pattern with severe winters and extended droughts, especially in eastern Europe. Such a pattern would be consistent with the marked retreat of ice from the Greenland seas.

Since the speed of the East Greenland Current is higher than the melting time of ice floes, this indicates a retreat of the Atlantic drift ice to latitudes north of 80°N. Cooling in northern Greenland after 1160 (Dansgaard 1975) coincides with a marked advance of glaciers in the Alps and other mountain ranges, a reappearance of Arctic sea ice around 1320, as well as extreme climatic anomalies and severe famines throughout Europe and a long drought period (200 years) in Iowa and Illinois, leading to mass emigration from these areas (Bryson and Murray 1977): this wave announced, after several interruptions, the transition towards the Little Ice Age (1560-1850).

Holocene Warm Period and the Humid Sahara

The history of the retreat of the melting ice domes of North America and northern Europe after the last ice-age maximum 18,000 years ago is fairly well known (see Lamb 1977a, Chapter 16).

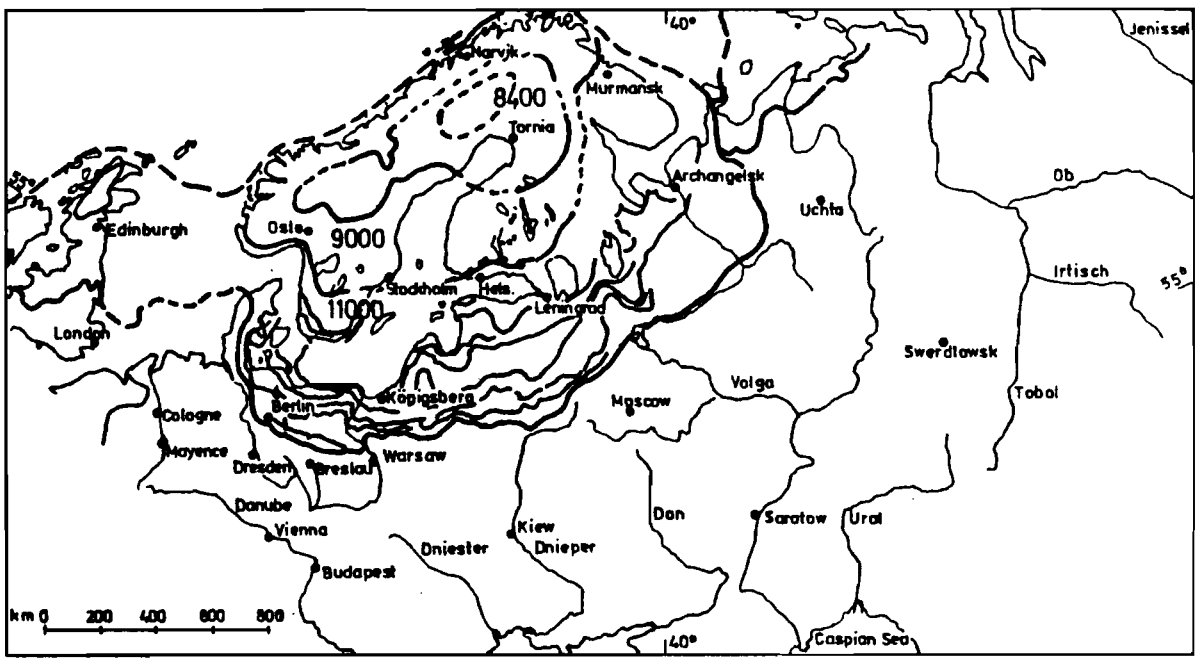

Figure 10. European ice margins of the last glaciation, 18000-8000 BP; after Woldstedt (1969).

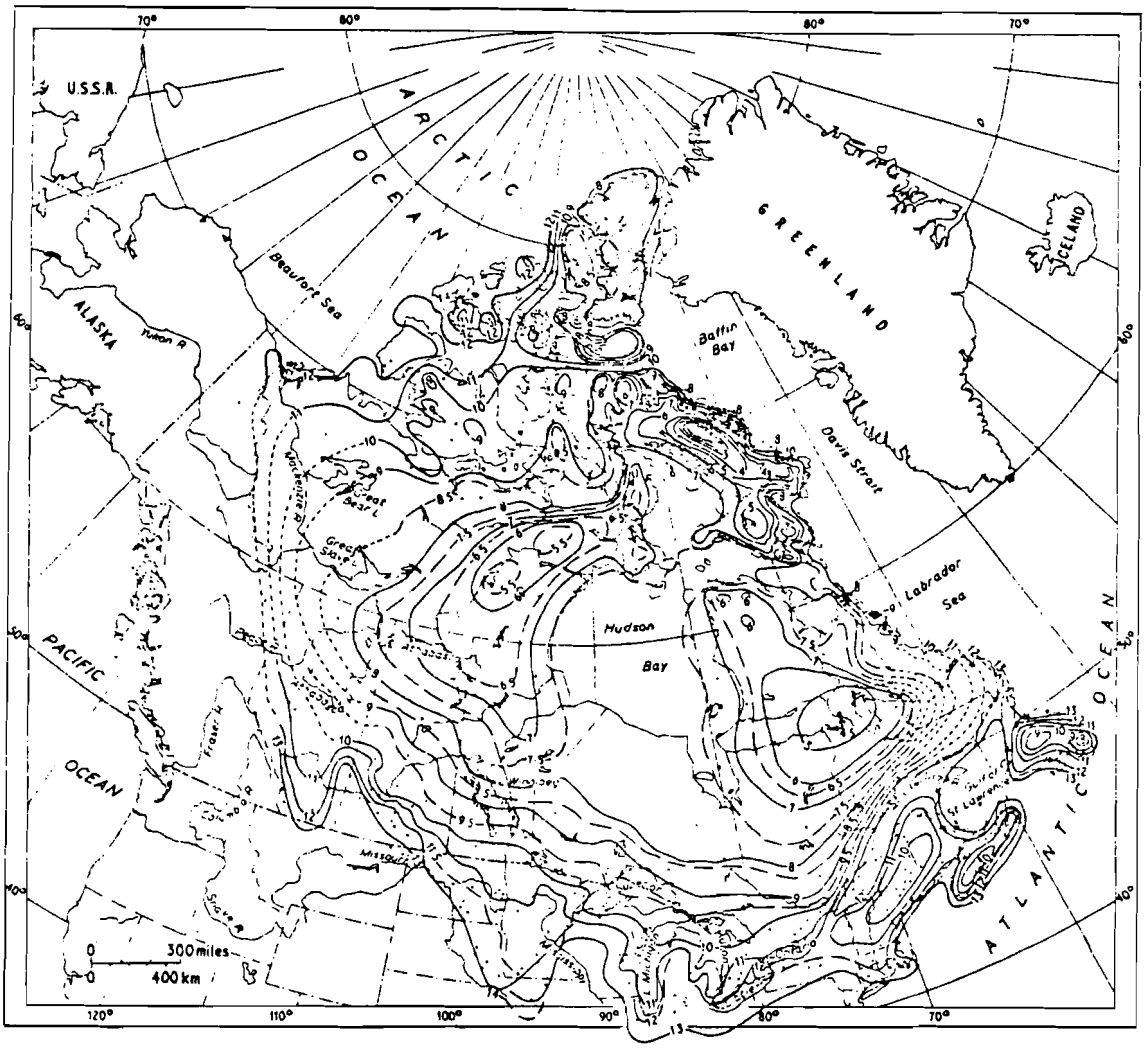

Figure 11. Isochrones of the withdrawal of the North American (Laurentide) ice sheet. All dates before present. Dots show where radiocarbon dates have been established. Moraines, coastlines and all other available field evidence used. Source: Bryson et al. (1969).

While the smaller Scandinavian ice sheet finally disappeared before 8000 BP (Figure 10), the North American ice sheet still covered about 50% of its former area (Figure 11), disintegrating after a catastrophic incursion of the sea into Hudson Bay

(Hughes et al. 1977). Separate ice sheets remained: the Labrador ice did not disappear before about 4500 BP, while some ice fields of about 35,000 km^2 in interior Baffin Land have apparently survived. This created a marked *longitudinal asymmetry* of the atmospheric circulation between 8000 BP and 6500 BP (Lamb 1977a), which faded out by 4500 BP. During this episode, Eurasia and Africa experienced the warmest epoch of the last 75,000 years, but eastern North America remained relatively cool, certainly in summer, with frequent outbreaks of polar air. This caused a predominance of southwesterly winds over the Atlantic, probably producing an intensification of the Gulf Stream and its northward flowing branches. In winter, the frequent occurrence of anticyclonic ridges at long 0-20°W would be consistent with frequent outbreaks of polar air also over central and eastern Europe, extending with copious precipitation into the Mediterranean and northern Africa.

The present description refers mainly to the peak of the epoch, around the year 6000 BP. Data are given here in radiocarbon years; their conversion into calendar years, with a possible difference of up to 12%, is apparently again a matter of controversy. Insufficient time resolution of the data available does not yet allow treatment of the existing fluctuations on a 100a or even 500a scale.

Forests in western Canada and in western Siberia extended 200-300 km farther north than they are today; the summer temperature has been estimated to have been higher by 2-3°. Subarctic forest also covered the northernmost islands of Norway and the whole of Taimyr peninsula. This warm period, however, came to an end around 4800 BP, when, on account of a polar outbreak lasting for no longer than about 200 years, the Canadian timberline moved south by more than 300 km (Nichols 1975). Almost simultaneously with this relatively short event, many important climatic shifts towards a "neoglacial" climate, similar to the Little Ice Age between 1550-1850 AD, occurred in many areas, together with a gradual desiccation of the actual Arid Belt (see later).

The waters of the Kuroshio, between Taiwan and Japan, were up to 6°C warmer than now (Taira 1975). With some delay, the interior Arctic experienced its warmest Holocene period after 4500 BP, with open waters in the fjords and along the northern coasts of Spitzbergen, Greenland, and Ellesmere Land, allowing Siberian driftwood to reach these coasts up to lat 83°N (Vasari et al. 1972; Barry 1977). However, there is no indication that the core of the present Arctic drift ice between Greenland, Alaska, and eastern Siberia has disappeared. As regards the sea level, only conflicting evidence is available for a world-wide rise of a few meters at the time; this question will be considered in Section VIc: Some Implications of a Unipolar Climatic Asymmetry.

In the Subantarctic ocean, the most rapid shrinking of the, mainly seasonal, Antarctic drift ice led to a warming peak as early as 9000 BP (Hays 1977). Similarly, this warm period had already started before 7000 BP (Starkel 1977) in eastern Siberia, where no major ice sheets had formed during the previous glaciation. At Lake Biwa in central Japan, the warm period was initiated before 8000 BP (Fuji). The transition between the glacial and interglacial (Holocene) modes of the atmospheric-oceanic circulation was very complex, superimposed by a series of abrupt changes between cold and warm phases (Bölling, Alleröd) between about 13,500 and 10,800 BP. At the end of this period, the tropical oceans became slightly warmer than they are now, which was most probably accompanied by a substantial weakening of the tropical (Hadley) circulation. Increasing evaporation raised the water vapor content of the tropical air, leading to a rapid expansion of the tropical rainbelt and rain forests (which had been drastically reduced during the previous ice age) towards higher latitudes (Rognon and Williams 1977; Shackleton 1977).

For England and Wales, Lamb has given estimates of the basic climatic parameters, including those representing other climatic stages of interest (Table 4). At the midlatitude oceanic coasts the probable temperature increase was 1.5-2°C. In other continental areas the increase was lower, at least in north-eastern North America. In the area between 85° and 95°W, a tri-

angle with prairie vegetation extended into Wisconsin and Illinois, reaching a maximum at about 7000 BP (Bernabo and Webb 1977). Together with some areas in SW Siberia and in eastern Turkey, this is one of the few areas that was then drier than it is now. The occurrence of thermophilous species in European and Asiatic forests (Frenzel 1967, 1968a, b) indicated somewhat higher temperatures and rainfall. Permafrost in eastern Siberia retreated several hundred kilometers north of its present position: a similar retreat in Canada and Alaska can be expected because of the northward extension of the vegetation lines. In the mountains the upper tree line shifted upwards by 100-150 m, which indicates a warming of nearly $1^{o}C$.

In subtropical latitudes, the present arid areas enjoyed wetter conditions. Since everywhere the temperature was higher or similar to today's temperature, this humid climatic phase (Sarnthein 1978) must have been related to higher precipitation and caused by higher evaporation of the tropical oceans (see Section IIc: Equatorial Upwelling, El Niño, and Hydrologic Balance). This was probably correlated with a weakening of the subtropical anticyclones and of the trade winds.

Perhaps the most surprising feature is the recently established occurrence of a marked *humid* period in the *Sahara*, as well as in the deserts of the Middle East (Nicholson 1976; Faure and Williams 1978). Since parts of this humid phase occurred simultaneously on both flanks of the desert, the model of a parallel shift of climatic zones towards N or S, as the seasonal variations suggest, cannot be considered representative. Evidence based on actual data supports the idea of a tendency towards synchronous shrinking or expansion of the Arid Belt at *both* flanks. This also has been found, on a much shorter time-scale (Nicholson), in the 16th and 19th centuries, together with a prolonged rainy summer season. During the maximum period of this moist period between 8400 and 5900 BP (Figure 12), the remnants of the North American ice and the frequent cold outbreaks within the European or African sectors possibly caused an expansion of the Mediterranean rains towards the south. Marked high-tropospheric troughs extending diagonally across the Sahara trigger off

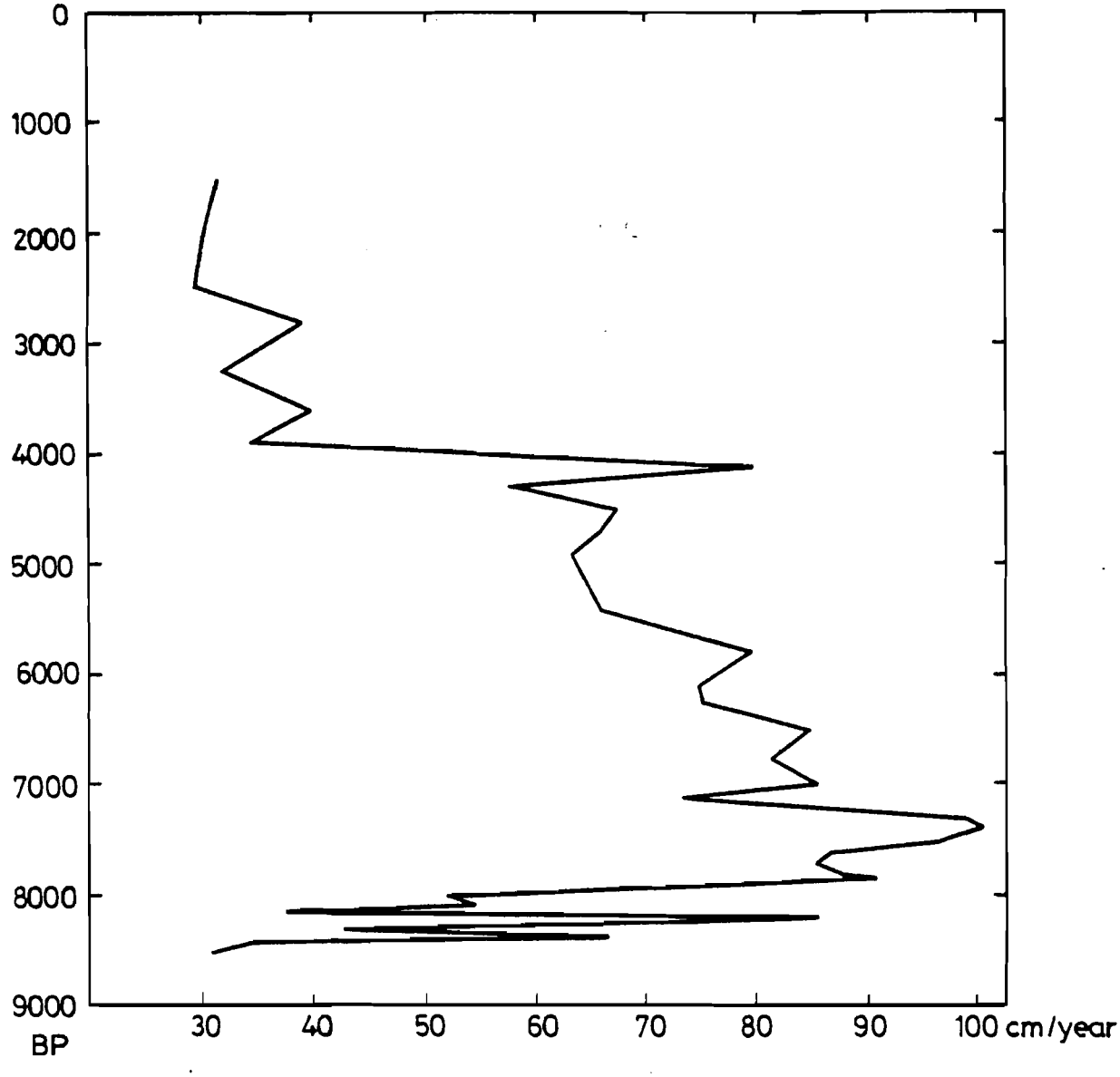

Figure 12. Tentative rainfall estimates for the Lake Chad (Mega-Chad) catchment; pollen data and chronology, derived mainly from local C_{14} data, after Maley (1977a, b). Rainfall estimates for different vegetation types are combined; only during wet phases the pollen assemblage really represents the entire catchment (lat 6-24°N).

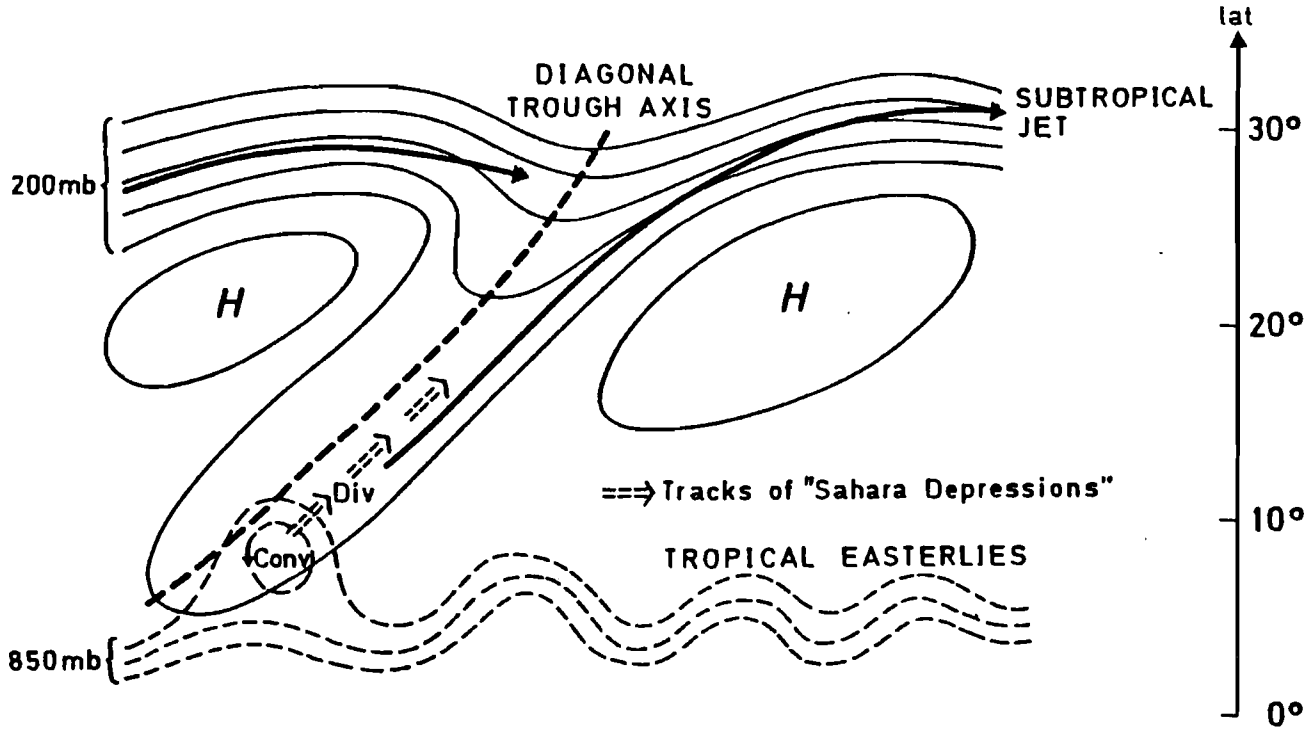

Figure 13. Interaction between "diagonal" upper troughs in the subtropical westerlies (200 mb or ~12 km) and tropical easterlies with traveling vortices (850 mb or ~1.5 km). Coincidence of lower convergent and upper divergent motion produces "Sahara depressions" moving toward NE ahead of the upper trough, which is visible from satellites as an elongated cloud band.

tropical disturbances, which cross the arid zone as "Sahara depressions", initiating more frequent rains even in the central belt between lat 21° and 26°N (Figure 13) (Flohn 1971). In addition to many other, now dry, Sahara lakes, *Lake Mega-Chad* (which stood then at least 40 m higher, with an extension of nearly 320,000 km^2 comparable to the actual Caspian Sea, overflowing at the peak to the Benuë-Niger catchment) represents a quite different hydrologic situation. Similarly, Lake Turkana (formerly Lake Rudolf) discharged into the White Nile catchment (Butzer et al. 1972). Even in the now hyperarid center of the Sahara between Kufra Oasis and Tibesti Mountains--today with less than 5 mm of rain per year--permanent rivers were flowing (Pachur 1975), indicating at least 200 mm, and more probably 300-400 mm, of rainfall. The grasslands were utilized by many groups of cattle-raising nomads (Gabriel 1977).

Similar evidence has been found throughout the Arid Belt of the Old World between Mauretania (long 17°W) and Rajasthan (long 77°E), including the Afar-Danakil depression and interior Arabia. At the margin of Tharr desert (India), with an average recent rainfall of about 250 mm, these rains increased (Figure 14) to values of 500-800 mm during a long moist period between about 10,500 BP and about 3600 BP (Singh 1974; Murray 1977; Bryson in A.B. Pittock et al. 1978; and personal communication). The individual fluctuations may be uncertain, as well as the dates for the beginning and the end of the moist period; the occurrence of a long moist period at this time agrees well with evidence from more than 30 other spots lying more than 8,000 km apart (cf. the summary review by Rognon and Williams 1977). Here again, both monsoonal summer rains and extratropical winter rains increased, occurring at the same spot.

Throughout this area, gradual desiccation set in at about 5500 BP, interrupted by relatively wetter periods. It seems noteworthy, according to most recent data, that the early high civilizations (the Old Empire of Egypt from the first to the fourth dynasties, the Near East urban centers between Jericho and Ur, the Indus culture) started at the end of this relatively wet period, having to fight increasing desiccation. North of about lat 35°N (Butzer 1975), however, the displacement of the winter rains towards the south lead to a dry period in Anatolia and Iran; best evidence has been found by a simultaneous lowering (and salinization) of Lake Van in eastern Anatolia by 300-400 m (Kempe and Degens 1977).

Evidence for the Holocene climatic history of the arid southwest of the U.S.A. is poor, except for the existence of a freshwater lake in central New Mexico in this moist period.

Climatic conditions in Australia during the Holocene warm period were quite similar: increased precipitation occurred at the northern *and* southern margins of the desert together with a slight warming, even at altitudes above 2500 m, in the mountains of New Guinea (Bowler et al. 1976). By contrast, the evidence available for southern Africa (van Zinderen Bakker 1976) indicates warmer, but drier, semidesertic conditions at the interior plateau.

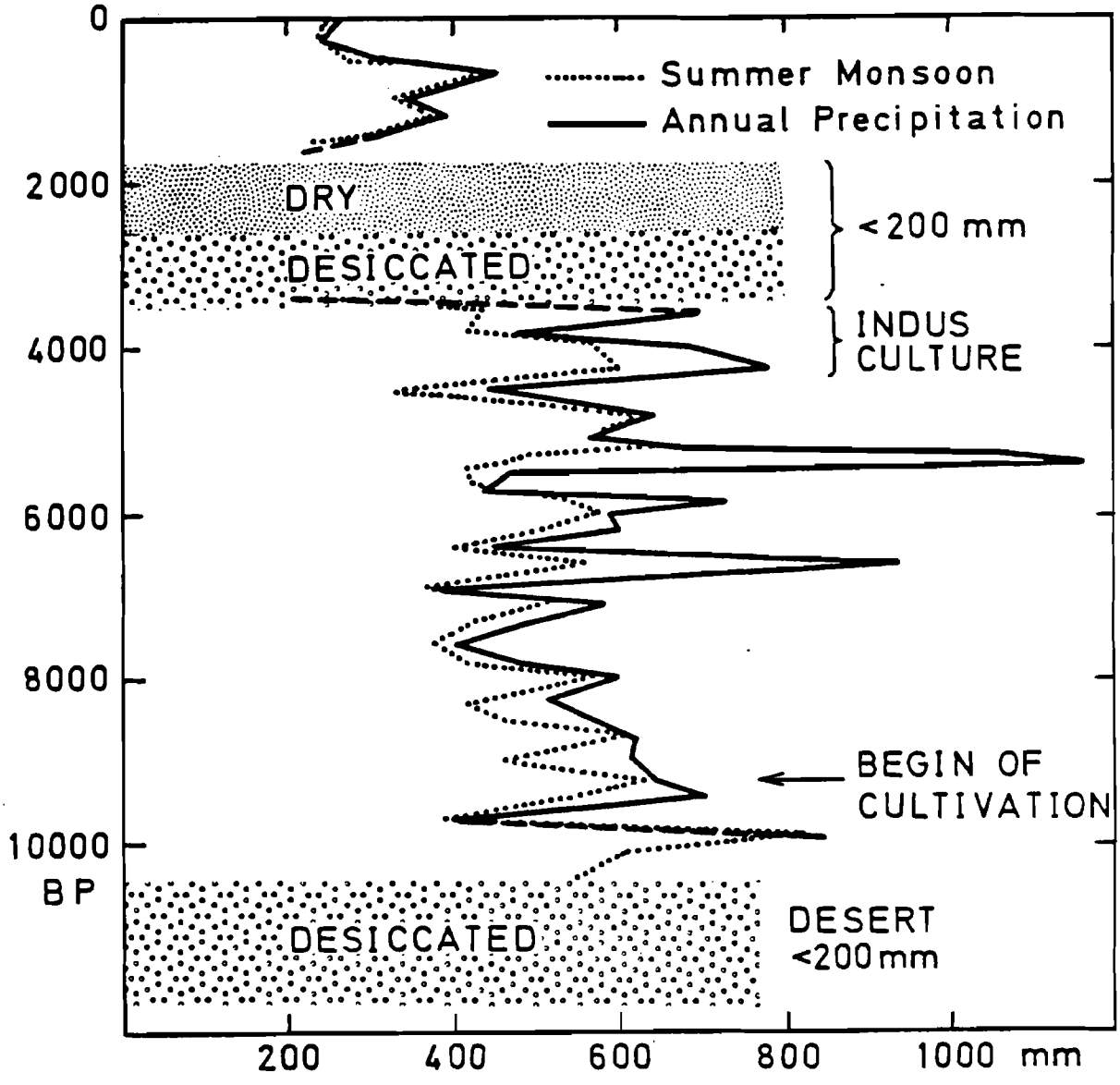

Figure 14. Rainfall estimates in Rajasthan (Bryson 1975; simplified in Bryson and Murray 1977; for pollen data and chronologies see Singh et al. 1974). While the individual fluctuations may be too large, the general tendency is sufficiently reliable and agrees with all evidence available for Arabia and northern Africa.

At this point it is necessary to discuss the question: *to what extent* can *climatic history repeat* itself under varying boundary conditions? There were two such essential conditions during Early Holocene, i.e. until about 5500 BP: the presence of limited and shallow, but not negligible, permanent *ice sheets* only in eastern Canada, and the lack of man-triggered desertification processes.

1. These permanent ice sheets seem to have disappeared eventually, fairly in parallel to the desiccation after 5500 BP. This can be understood if one takes into account the effect a permanent cold source in eastern Canada has on the circulation pattern in the European section, which (similarly as under today's conditions in spring) should favor a great frequency of blocking anticyclones in the region of the British Isles and Scandinavia, with increasing cyclonic activity in the Mediterranean. This should have been effective especially in late spring, summer, and fall, and should have been accompanied by frequent deep troughs over eastern-central Europe extending diagonally into northern Africa (see Figure 13). Similar conditions in the near future could only be expected if a permanent snow cover were to develop in the area of Baffin Island and Labrador; this is unlikely to occur in the next decades, but not absolutely impossible (see Chapter VII: Conclusions).

2. Increasing man-triggered *desertification* (Hare 1976) has probably contributed to the slow and gradual desiccation process. Actual representative rainfall data of many arid regions obtained since 1890 (Rajasthan) or 1904 (southern Tunesia) do *not* reveal a downward trend. Models designed by Charney (1975), Berkofsky (1976, 1977), Elsaesser et al. (1976), and Joseph (1977) describe man-made destruction of vegetation as being the cause of increasing surface albedo and intensification of the actual subsidence processes which should reduce effective rainfall. A reversal of such desertification processes (soil erosion, deflation, destruction of

vegetation, groundwater depletion, and salinization) seems possible only if repeated large-scale rainfall triggers an adequate vegetation cover that can be protected against overgrazing and the ever increasing strain caused by rapid population growth. Only then the weak positive feedback effect "desertification--increasing albedo--increasing subsidence--less rainfall--extended desertification" could be interrupted and (possibly!) reversed. This would necessitate a major concerted effort.

From argument 1. one should conclude to expect no substantial change in rainfall along the northern margins of the Old World Arid Belt. In the southern flank this might be possible if, as is expected, the subtropical anticyclones get slightly less intensive and are displaced towards higher latitudes. This would weaken the trade winds of the northern hemisphere as well as coastal and equatorial upwelling, leading to higher evaporation and a larger water vapor content.

From argument 2. we should conclude that, given our present population growth, reconstruction of the natural vegetation cover is a socioeconomic problem, and that several decades may pass before a reliable long-term increase in rainfall could be achieved in this way. Here much further research of a truly interdisciplinary nature is certainly needed.

The Last Interglacial (Eem Sensu Stricto)

Recent investigations, of ocean cores in low and middle latitudes as well as of continental loess deposits in Austria and Czechoslovakia, have indicated that over the past 2-2.5 million years a sequence of at least 17 large-scale glaciations of northern continents has occurred, interrupted by the same number of interglacials with a climate similar to the present one. Detailed data are available only for more recent events, especially for the last glaciation between about 73,000 and about 14,000 BP; it includes two major glacial peaks at the beginning and end, and at least five shorter periods with a

slightly warmer climate (interstadials). For the controversial subject of chronology, see for example Kukla (1977a).

The last interglacial, here defined as stages 5a-5e (Emiliani and Shackleton, 1974), lasted, with two important interruptions, from about 130,000 BP to 75,000. Its climate in Europe and Asia has been carefully described by Frenzel (1968a), while the information on North America is hardly adequate for a regional description, and evidence for other continents is almost completely lacking. Detailed investigations of the climate at the earliest peak of the last glacial (Eem sensu stricto, or stage 5e Emiliani-Shackleton) at around 125,000 BP are being carried out by the CLIMAP group (Cline and Hays 1976), which evaluates the large number of available ocean cores to obtain a realistic estimate of sea surface temperatures and salinities. Since this subperiod is apparently the warmest of all interglacials, a climatic interpretation is given in the following.

In northern and eastern Europe the climate was much more oceanic than it is at present; this was mainly due to the high sea level of about 5-7 m above today's level, which isolated Scandinavia from the continent by an oceanic channel connecting the Baltic and the White Sea. The sea also penetrated deeply into the continent in western Siberia, along the Ob and Yenisey flood plains up to lat 62°N. Table 5 gives a selection of climatic data from polar and midlatitudes in Eurasia and North America, with temperatures generally 2-3°C higher than today, and still higher in some areas, and slightly more humid (for details see Frenzel, 1967 and 1968). The forests in the actual cool-temperate zone were then thermophilous: deciduous trees like oak, linden, elm, hazel, and hornbeam prevailed. The occurrence of hippopotamus, forest elephants, and lions in southern England is a remarkable feature of this warm climate (Lamb, 1977, p. 188). Thermophilous forest in eastern Siberia indicated a marked retreat of permafrost up to lat 57°N (now around lat 50°N); boreal forests extended up to the coastlines of the time. The high temperature estimates suggest a seasonal retreat of Arctic drift ice far away from the coasts, which, however, were inundated by the high eustatic sea level. While marginal parts of the Arctic drift ice were probably displaced

Table 5. Climatic Differences: Eem-Actual (Frenzel 1967)

Area	Temperatures (°C) January	July	Annual	Rainfall Annual (mm)
Denmark	+2	+1-2	+1.5	0
GDR and northern FRG	+1-2	+3	+2.5	0
Central Poland	+3-4	+3	+3	+50
Northeast Poland	+3-5	+3-5	+5	+50
Byelo-Russia	+5-6	+5	(+6)	0
Central Russia	+9-10	+2	+5	+100
Northwest Ukraina	+2-3	±0	+1	+50
Western Siberia	+4	+3	+3	+100?
Central Siberia	?	?	+6	?
Toronto	+3-4	+2	+2-4	+250
Southeast Alaska	?	+4-5	?	?
Banks Islands (72°N)	?	+4-5	?	?

poleward, its central core in the ocean between Greenland, Alaska, and eastern Siberia has remained unchanged, at least since the beginning of the Brunhes paleomagnetic epoch 700,000 years ago (Herman 1977). Worldwide comparisons of ocean cores indicate that, during this stage, the sea level stood at least 6 m higher than at present, as evidenced at Barbados, Hawaii, New Guinea, Mallorca, and on the lower Thames.

The duration of the Eem sensu stricto was only on the order of 10,000 years; it was terminated by a markedly abrupt and relatively short period of cooling, during which the global ice volume increased and decreased, possibly causing a sea-level change of 60-70 (instead of 100 m or even more like in the last ice age). In the Eem period, Atlantic polar water, with some seasonal ice, retreated north of lat 76°N for about 8000 years, while subtropical waters, which apparently did not extend north of 44°N in the Holocene, reached 52°N (Kellogg 1976).

Two other warm phases followed, but with a less thermophilous forest and a lower sea level. Figure 15 gives a simplified diagram, forest versus tundra, from a peat bog core in NE France (Woillard, 1975 and 1978) illustrating the apparent brevity of the two interrupting cold episodes on the continent. The second cooling (locally called Melisey II) apparently coincides with several marked events in northern Greenland (lat 76°N, Dansgaard et al. 1972), in a deep cave in southern France (Duplessy et al. 1972), in peat bogs in northern Greece (Wijmstra 1978) and California (Adams 1977), and in many ocean cores of the Caribbean (Kenneth and Huddlestone 1972), during cooling stage 5b (Emiliani and Shackleton 1974). The worldwide occurrence of stages 5a-5e (Emiliani-Shackleton) is verified by many complete oceanic and continental cores in all latitudes.

In all well-evidenced interglacials, except for the actual Holocene, such rather abrupt coolings with a Subarctic or Arctic climate have been observed to last only for some centuries or 1000-2000 years ("abortive glaciations"). The physical mechanism of such abrupt, but certainly natural events, recurring about once in 10,000 years, is not yet known; speculations about the possible role of clustering volcanic eruptions or of Antarctic surges (see Section IIb: The Role of the Antarctic Continental Ice Sheet) are still open questions.

There is little evidence for low latitudes; the occurrence of a long humid phase, with a deep lake in the Afar Triangle (west of Djibouti, see Gasse and Delibrias 1976), and also along the western African coast (Diester-Haass 1976), suggests conditions similar to those prevailing during the Early Holocene.

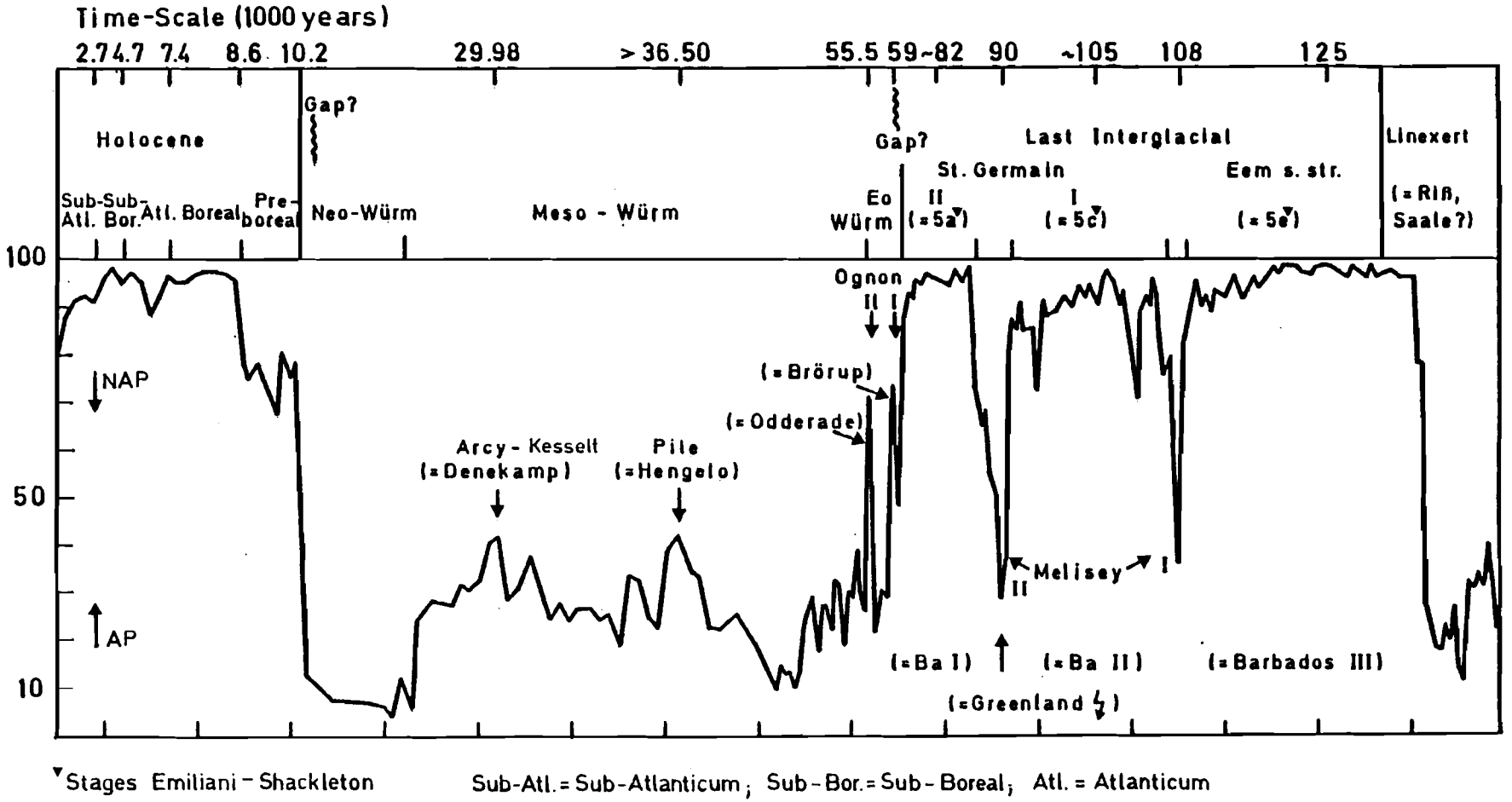

Figure 15. Simplified vegetation history from a fossil bog in southern Vosges (NE France; Woillard 1975). Chronology at the top, percentage of forest pollen (AP upward) versus nonarboreal pollen (NAP downward). Note two abrupt coolings within the interglacial series; the begin of Eem sensu stricto is misplaced slightly to the left and should coincide with the sudden rise of AP.

ICE-FREE ARCTIC VERSUS GLACIATED ANTARCTIC?

Causes and Time-Scale of a Possible Opening of the Arctic Ocean

The most fascinating, and also most controversial, problem of the future evolution of man's climate is the possibility of a complete disappearance of the drift ice of the Arctic ocean (see Section IIa: The Role of Polar Sea Ice). The sensitivity of the multiphase air-snow-ice-ocean system (Figure 1) is demonstrated by the relatively large amount of seasonal melting (from above) and freezing (from below), at an average of about 50 cm/year. Unfortunately no figures for different years are available; recent experience based on ice and weather ship data suggests a high interannual variability. In particular, it is highly sensitive with respect to the heat flow of the ocean below, the albedo of the ice-snow surface during the melting season, and certainly with respect to the length of the melting season ending incidentally with the first snow cover. Having demonstrated the sensitivity of the system, Budyko first (1962) discussed the possibility of artificial removal of the Arctic sea ice, and later on designed simple semiempirical models (1969, 1972) based on the heat balance of the earth-atmosphere system. He noted that small increases in the solar constant or an increase in the atmospheric CO_2 content might lead rather rapidly to an ice-free Arctic ocean, substantially increasing the surface temperature by about 6-8°C in summer, but to more than 20°C in winter.

Since that time arguments for and against such a drastic evolution--which probably goes beyond the imagination of many responsible scientists--have been discussed, in private circles much more than in publications. Since no sufficiently realistic model of the climatic system is available, including the physical and dynamical interaction and the feedback processes between atmosphere, drift ice, and ocean, this problem cannot find a satisfactory solution now. One of the first attempts to simulate atmospheric circulation under such conditions has been made by Fletcher (1973), on the basis of the Mintz-Arakawa model (Figure 16).

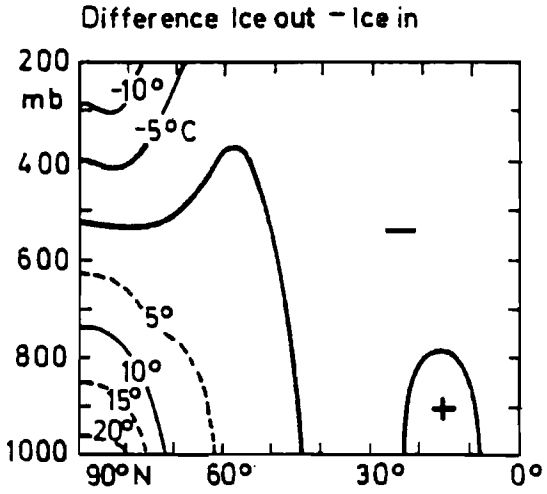

Figure 16.
Temperature change after introduction of an ice-free Arctic ocean into a circulation model (Mintz-Arakawa or RAND model; Fletcher et al. 1973).

Since Budyko's initiative, simple one-dimensional models have frequently been investigated (e.g. Sellers 1969, 1973). One of the most important simplifications was to define the latitude of boundary ϕ_p of the polar zone as equivalent to an average latitudinal temperature of the warm half-year of $-1^{\circ}C$ (Budyko 1977); then the planetary albedo, as seen from space, was taken to be 0.62 (0.77) for the northern (southern) polar cap. This procedure introduces parameterization of the highly effective snow-albedo-temperature feedback. According to Budyko's most recent monograph (1977) the relationship between ϕ_p and solar radiation has the form of a hysteresis loop: ϕ_p is larger (smaller) when the incoming radiation, as determining parameter, increases (decreases) from a value lower (higher) than the actual value (Figure 17) (Budyko 1977; Figure 8). In another diagram (Figure 9, p. 65 of Budyko 1977) he demonstrates the relation between the average planetary air temperature and solar radiation: there the difference between points E (ice-free regime) and 3 (present situation) is equivalent to a temperature change of about $4^{\circ}C$. This is higher than the temperature increase in all warm phases ($1-2.5^{\circ}C$) of the last 2 Ma (1Ma = 10^6 years), but the difference is not very big. If one accepts Budyko's model as a reasonable first guess, the possibility of such a regime cannot be excluded. Furthermore, temperature estimates for the vegetation pattern during relevant past epochs (Section VIb: Coexistence of Open Arctic and Glaciated Antarctic During the Late Tertiary) also suggest a temperature about $4^{\circ}C$ higher

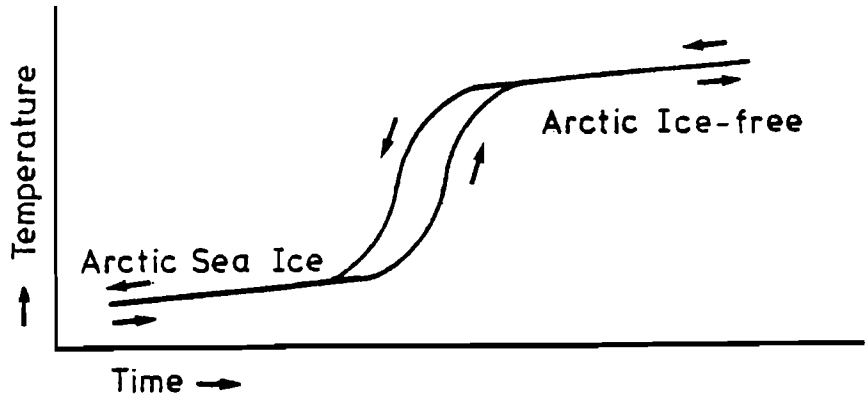

Figure 17. Expected temperature change due to hysteresis in the case of formation or disappearance of Arctic sea ice (arrows), simplified after Budyko (1977).

than today in the northern hemisphere. In this case, however, the hysteresis loop is taken from above and not from below, as must be expected in a possible future evolution.

Looking at seasonal variations in the heat budget of the Arctic sea ice, Maykut and Untersteiner (1971) have stressed the roles of surface albedo and oceanic heat flow; their estimate of the oceanic heat flow (1.5 kcal/cm^{2}a $\approx$2 W/m^2) is, according to more recent data, much too small and should be increased by a factor of 6 to 7 (Aagard and Greisman 1975). The role of the surface albedo during the melting season is effective only in the case of surface pollution, by dust or oil wastes. The role of the flux of sensible heat is on an annual average, slightly less than 10% of net solar radiation as well as of the longwave terrestrial radiation (Figure 2, see also Vowinckel and Orvig 1970); the same is true for the flux of latent heat (evaporation) in the same upward direction. Since the annual net radiation at the surface is quite small at present, the heat flux from the ocean is approximately equal to the two fluxes into the atmosphere.

The melting process of the sea ice takes only 50-60 days (plus an additional 20 days for snowmelt), leading to a phase transition of about 15-20% of the average mass of an ice floe; in the remaining months a similar amount freezes from below.

It is obvious that interannual changes in terms of the heat budget--which should be on the order of ±20% or even higher--may significantly alter these estimates. These are, in substance, verified by only a few 12-month campaigns. If one assumes, for a period of a few years, only a 10% increase in summer melting and a 10% decrease in cold season freezing, the destruction of a 2-3 m ice floe takes a short time. If the melting season started 1-2 weeks earlier, perhaps as a consequence of advective warming, it would most certainly lead to a substantial imbalance of the sensitive mass budget. There is also a negative feedback, however: in winter the accretion rate is negatively correlated with thickness, i.e. thin ice accretes much faster than thick ice (Thorndike et al. 1975), because of the higher value of the upward heat flux. By contrast, a positive correlation exists during melting.

According to the large areal fluctuactions of the ice over the last millenium (Section Va: Medieval Warming) (Lamb 1977a), there is little doubt that at least the marginal sections of the Arctic drift ice can disappear rather rapidly. This argument is not valid for the central core whose maintenance has been verified by several independent lines of evidence at least for the period since the Brunhes-Matuyama boundary 0.7 Ma ago, and has been determined as rather likely for the last 2.3 Ma. However, if the global warming exceeds the amount of fluctuations (up to +2.5°C) of the last 6-8 glacial-interglacial cycles, this argument is not longer true; with a representative warming of 4°C or more like in the Late Tertiary (Section VIb: Coexistence of Open Arctic and Glaciated Antarctic During the Late Tertiary), disappearance of the central core of the drift ice is almost certain. This would be equivalent (Chapter III: The "Combined Greenhouse Effect" of CO_2 and Atmospheric Trace Gases) to an increase in the virtual CO_2 level by a factor of almost 3. The equivalent increase in the real CO_2 level would be by a factor of about 2.5 (Table 3).

The atmospheric heat budget above an ice-free Arctic ocean is completely different from that of the present situation.

Disregarding some earlier attempts, this paper presents some calculations by Vowinckel and Orvig (1970, p.220) as the most complete approach available. The heat budget equation for a column above the Arctic cap (75-90° lat) between the earth's surface (Sfc) and the top of the atmosphere (TA) can be written as follows:

$$R_{Sfc}\downarrow - R_{TA}\uparrow + F_a + F_s \hat{=} 0 \quad ,$$

where R = net radiation flux, F = northward heat transport across 75°N by ocean (s) and atmosphere (a). In equilibrium, the divergence of the downward radiation flux div R $= R_{Sfc} - R_{TA}$ must equal the convergence of the horizontal flux of sensible and latent heat. Table 6 gives estimates for these individual terms, assuming, in the case of an ice-free Arctic ocean, either a cloudless atmosphere or a closed stratus cover. Both assumptions are unrealistic, but the role of clouds of different altitude, thickness, and extension for the radiation fluxes is not yet sufficiently understood. Somewhat more realistic is the assumption of a cloudless sky during summer (from May to August), when the continents favor a thermal circulation with subsidence over the sea; for the rest of the year a closed stratus should prevail (see last line). The data are given in watts/m^2 (1kcal/cm^2a= 1 kilolangley/a = 1.327 W/m^2).

The most interesting result is that of a *positive* annual *net radiation* budget, div R (Table 6, last line); in this case heat would be available for export from the Arctic. The advective oceanic heat flux F_s is, according to the most recent evaluation (Aagard and Greisman 1975), 10.6 W/m^2, much larger than in most earlier investigations (Vowinckel and Orvig, ~7W/m^2). One of the largest terms is the export of ice by the East Greenland Current, which contributes about 50% to the warming of the Arctic ocean, since the ice is melted externally. In an earlier attempt with much greater uncertainties, Donn and Shaw (1966) obtained an imbalance of +26.3 kLy/a ~35 W/m^2. The *heat surplus* coincides with the obvious consideration that, during the *cold* season, heat and water vapor should be *exported* from an ice-free

Table 6. Annual radiation and heat budget (in W/m^2) of the Arctic cap (75-90°N) under different assumptions (Vowinckel and Orvig 1970)

	R_{Sfc}	R_{TA}	div R	F_a+F_s
Present conditions	+ 3.3	+100.8	-97.5	+97.5 W/m^2
Ice-free, no clouds	29.4	59.1	-29.7	+29.7 "
Ice-free, closed stratus	42.7	92.9	-50.2	+50.2 "
Ice-free, seasonally varying[a]	62.1	58.3	+ 3.8	- 3.8 "

[a] see text

ocean towards the continents, which ought to be, in subpolar latitudes, certainly colder than an open ocean. An open Arctic ocean should receive at the surface an annual net radiation of 30 - 60 W/m^2 (Table 6). If one assumes R_{Sfc} = 45 W/m^2, allowing 40% for evaporation in summer (when the small flux of sensible heat is probably downward), then 27 W/m^2 or 20 $kcal/cm^2$ are available for heat storage in the sea. For a 50 m mixed surface layer, this yields an average heat storage of 4 cal/g, which is equivalent to a warming of 4°C in one single summer. If one assumes, under actual conditions, an average area of polynyas to be about 12.5%, the heat gain of the surface layer would have increased by a factor of 8. In winter, infrared emission increases with temperature: if the surface temperature increases from -35°C to 0°C, the blackbody radiation increases only by about 60%. But due to the much higher water vapor content, atmospheric counterradiation will also rise substantially, so that the net infrared radiation of the ocean surface is expected not to change much. These estimates permit the conclusion that a *new equilibrium water temperature* will be reached after a few years, which should be indeed substantially higher than the melting temperature of saltwater; Budyko's estimate of +8°C cannot be so far from reality. This would also be coherent with the air temperatures estimated for Late Tertiary vegetation at highest latitudes.

Coexistence of an Open Arctic Ocean and a Glaciated Antarctic Continent During the Late Tertiary

One of the main arguments against a possibly ice-free Arctic ocean in a foreseeable future has been the existence of the highly glaciated Antarctic continent. Indeed it is not easy to imagine a completely asymmetric planet with one pole ice-free, and the other one covered by an ice sheet more than 2 km thick. It should be mentioned that a similar asymmetry probably existed for several 10^7 years during the Permo-Carboniferous glacial period about 250 Ma ago. At that time, however, several of the earth's continents formed one giant supercontinent (Gondwana) situated at higher latitudes of the southern hemisphere including the pole, while in the northern hemisphere most of our present coal deposits were formed in forest swamps similar to the Everglades in southern Florida. The boundary conditions on the earth's surface are different today, but not *so* much different: actually, one pole is situated on a fairly large and completely isolated ice-covered continent, and the other one in a deep, almost landlocked ocean with a thin skin of floating ice. To some extent, this also causes an asymmetric circulation of atmosphere and ocean (Flohn 1977) (see Section IIb: The Role of the Antarctic Continental Ice Sheet).

As regards the background of a possible evolution of an ice-free Arctic ocean, it is of paramount interest that exactly the same situation *had* existed immediately before the onset of the Pleistocene, with its sequence of glacials and interglacials in the northern hemisphere and a more or less constant glaciation of the Antarctic. As the results of the Deep Sea Drilling Program have shown, the Antarctic ice had developed to its present size about ten million years (i.e. a period five times the duration of the Pleistocene) before the formation of Arctic drift ice. Two recent reviews (Kennett 1977a, Frakes 1978) evaluate the evidence available, arriving at only slightly different results. The end of this period, in the Pliocene (about 2-5 Ma ago), the early hominids, our ancestors, lived in a savanna environment in equatorial East Africa learning how to use pebbles as a weapon and as a tool (Flohn 1978a). (Unfortunately they did not yet know how to

record climate.) To what extent climatic changes may have contributed to the development in the ape-man transition is not yet known.

For the last 50-70 Ma, Antarctica has been situated near the South Pole, but was connected with Australia and other parts of the former Gondwana continent. Both poles were ice-free throughout the Mesozoic and the Early Tertiary (about 200-50 Ma ago) (Schwarzbach 1974). The atmospheric circulation was probably dominated by the tropical Hadley cells reaching, with strong seasonal variations, to lat 50-60^{o} (Flohn 1964b). The meridional extension of Australia and Antarctica caused warm oceanic currents preventing any glaciation until the beginning of the Eocene (55 Ma ago). Soon thereafter, Australia separated from Antarctica and drifted northward at an average speed of 5 cm/a, while Antarctica remained nearly fixed (Kennett et al. 1977a). After a long period of increasing winter snow with possibly local glaciations in West Antarctica and steadily decreasing water temperatures (small surface-bottom difference), the first significant drop in temperature occurred 38 Ma ago, near the Eocene/Oligocene boundary, affecting especially the bottom layers (i.e. a decrease by 5^{o}C within less than 10^{5} years, which is remarkably abrupt for the time, see Figure 18). At this time substantial Antarctic sea ice formed, coinciding with the development of widespread glaciation in parts of the Antarctic continent (Kennett 1977a). Like under present conditions, the cold and dense bottom water spread outward into all oceans, causing a considerable worldwide crisis in the deep-sea fauna. After further climatic fluctuations of more geological importance, including a significant global cooling during the Oligocene (38-22 Ma ago), a *notable Antarctic ice cap* formed during the Middle Miocene (14-12 Ma ago) to become a permanent feature; it probably was still "warm", i.e. with temperatures close to the melting point. This formation occurred roughly at the same time as the volcanic activity sharply increased, as can be noted from many ocean drillings (Figure 19, Kennett et al. 1977c). Soon after that peak, the first mountain glaciers in southern Alaska appeared, as well as a first cold-water fauna in northernmost Japan (Kanno and Masuda 1978), and

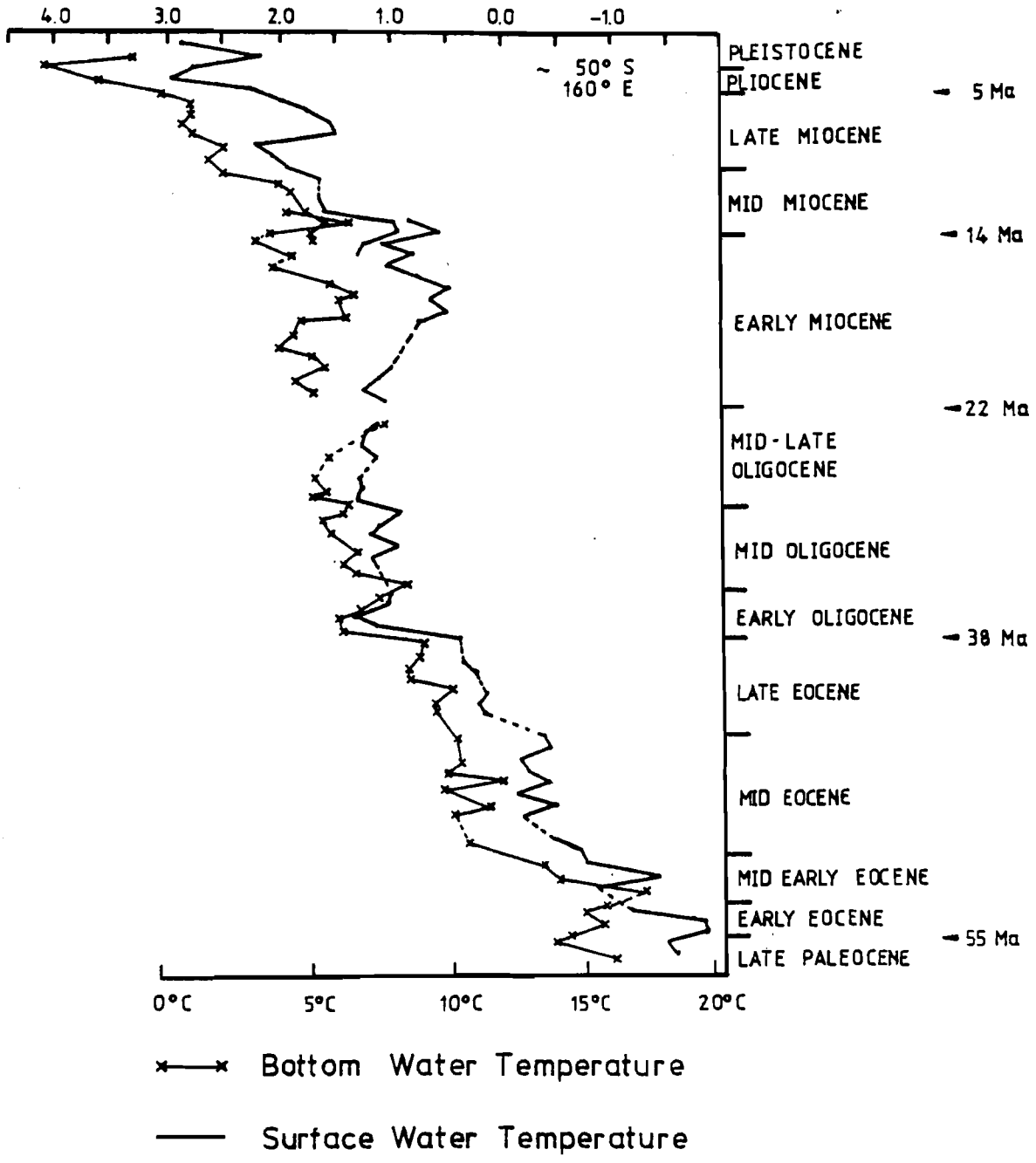

Figure 18. Evolution of surface and bottom (isotopic) temperatures in the Subantarctic (about 50°S, 160°E) since late Paleocene ca. 58 Ma ago (Kennett 1977a). Note the sudden drops about 38 Ma and 13 Ma ago.

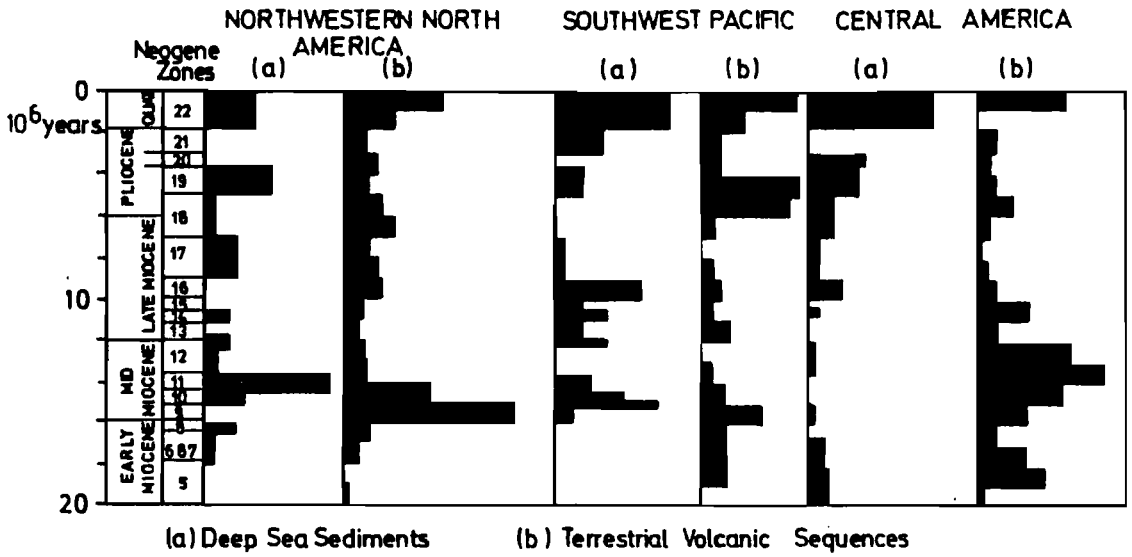

Figure 19. Volcanic ashes in some circum-Pacific provinces during the Late Tertiary and Quaternary (time-scale at left) (Kennett et al. 1977).

a marked drop in the surface temperature in the high latitude Pacific (Savin et al. 1975).

The *highest glacial maximum*, characterized by a "cold" and slowly moving ice dome, was reached at the end of the Late Miocene or Messinian (6.5-5 Ma ago), when the ice volume was 50% larger than it is today. Then the height of the ice dome must have been several hundred meters higher, and the Ross shelf ice reached several 100 km farther north. This peak was accompanied by a remarkable global cooling, by a 300 km northward spread of cold Antarctic surface waters, and a high carbonate sedimentation rate at the equatorial Pacific, indicating strong upwelling of nutritious cool water (Saito et al. 1975). 7-10 cyclic temperature changes were observed, with minima as cold as in the cold phase of the last glaciation; this is not necessarily indicative of a global cooling, but shows the intensity of the equatorial upwelling. One of the most important consequences was a "glacial-eustatic" drop of the sea level of 40-50 m below today's level, due to the storage of water in the Antarctic ice dome. During this drop the Gibraltar Strait, or its predecessor, fell dry isolating the Mediterranean, which evaporated completely 8-10 times to a depth of 3700 m and filled again, leaving a laminated

salt layer of 300-500 m thickness (Hsü et al. 1973,1977). This lamination and the paleoclimatic history of equatorial Pacific sediments indicate a cyclic behavior at a time scale of about 10^5 years, which lasted for about 0.5 Ma, and was probably caused by orbital elements similar to those effective during the Pleistocene.

During and after that time, the *Arctic* enjoyed a cool-temperate climate with boreal forests extending up to the northernmost tip of land; in the Late Miocene and Pliocene the entire shelf north of Asia and Alaska fell dry, and the continents extended 200-600 km farther north, e.g. in Siberia up to 81°N, and in Canada up to 83°N (Hopkins 1967). The vegetation distribution in Siberia shortly before the first appearance of ice on the European continent (Late Pliocene, about 2.5 Ma ago) has been mapped on the base of rich data, published mainly by Russian authors (Frenzel 1968a,b). No evidence of tundra nor widespread permafrost could be found. Summer temperatures have been estimated to have been by about 3°C higher in western Europe, but 4-5°C higher in eastern Europe; there and in Siberia annual and winter temperatures must have been 5-10°C higher than now (Frenzel). Since the relative and absolute heights of many mountains were significantly lower than they are now, as is demonstrated by a flat or rolling topography covering the highest levels, oceanic rainfall could penetrate farther inland; precipitation has been estimated to have been higher by 300-400 mm (Frenzel). Only in a few areas, such as southern California and NW Iceland, local glaciers formed simultaneously with these boreal forests, but produced no significant large-scale climatic effect. A simultaneous glaciation of parts of Greenland can be assumed, but there is no evidence for it, due to the strong, and probably permanent, glacial erosion since that time. Along the coasts of Alaska, well developed boreal mixed forests extended more than 800 km north of some of the present tree limits. The fossil insect fauna at lat 66°N resembled the insect fauna now living in the Vancouver-Seattle area at lat 48-50°N (Hopkins et al. 1971).

——— Quaternary (0-2 Ma)
- - - Late Tertiary (5-15 Ma)
..... Early Tertiary (30-50Ma)

Figure 20. Displacement of northern boundary of the northern hemisphere arid zone (Evaporites are gypsum, salts, etc.) (Lotze 1964).

During Pliocene (5-2 Ma ago) the Ross Ice shelf in *Antarctica* extended beyond its present boundary, and glaciation started (about 3.6 Ma ago (Mercer 1976)) in southern South America. From ice-rafted pebbles one may infer that, simultaneously with a northward shift of the boundary of the cold Antarctica surface water, Antarctic tabular icebergs occurred and spread also northward, reaching north even farther than during the Pleistocene glaciations.

Of special interest is the middle and lower latitude climate. After many careful investigations, Lotze (1964) compiled maps of the position of the *evaporite belt* during past climates, i.e. of the arid zone of playas and sebkhas, where soluble salts were sedimented in dry pans. A combination of the northern limits of the northern arid belt from these maps is presented here (Figure 20), indicating a southward shift from an average latitude of

about 47°N in the Early and Middle Tertiary to 42°N in the Miocene/Pliocene, and to 38°N in the Pleistocene. In the context of this paper, only the latter comparison is important. The multiple desiccation of the Mediterranean that occurred during the Messinian--a short portion of the Miocene/Pliocene from 6.5 Ma to 5 Ma BP--aggravated the arid conditions in southern Europe. A similar southward shift of the vegetation belts of North America has been compiled by Dorf (Figure 21).

During the Messinian, even south-central *Europe* was partly *arid*, with steppe or desert vegetation near Vienna (Schwarzbach 1974; Hsü 1974); SW Germany was also drier than it is now (Schwarzbach in Nairn 1964). While, before these events, tropical marine microfossiles had occurred abundantly in the Atlantic up to lat 58°N, this boundary retreated during the desiccation of the Mediterranean on the eastern side of the Atlantic to about lat 33°N. No such tropical species could enter the Mediterranean after its reopening at the early Pliocene (5 Ma ago), while they still reached farther than lat 50°N in the Gulf Stream region. This indicates a great longitudinal contrast, probably caused by the wind-driven surface currents of the oceans.

Many regional temperature and precipitation estimates are quoted (e.g. Mägdefrau 1968, Schwarzbach 1974). Since in the Late Tertiary many of our present mountains existed only in rudimentary form, these numerical data cannot be taken as being representative of near-future conditions. This is obvious, e.g. in the case of the now arid continental basin of Nevada or the Mojave desert, which enjoyed a rather moist maritime climate near sea level during the Late Miocene. Summer temperatures were then lower by 4°C, and winter temperatures higher than now by 8-10°C (Schwarzbach). During the same time sequences, SW Germany enjoyed a subtropical or, later, warm-temperate climate (Mägdefrau). In the *tropics*, the extension of savanna climates with seasonal rains was much wider than it is today, but the equatorial rainforest with all-year rain was reduced. In the Oligocene and Miocene (Maley 1978), the vegetation patterns of the African

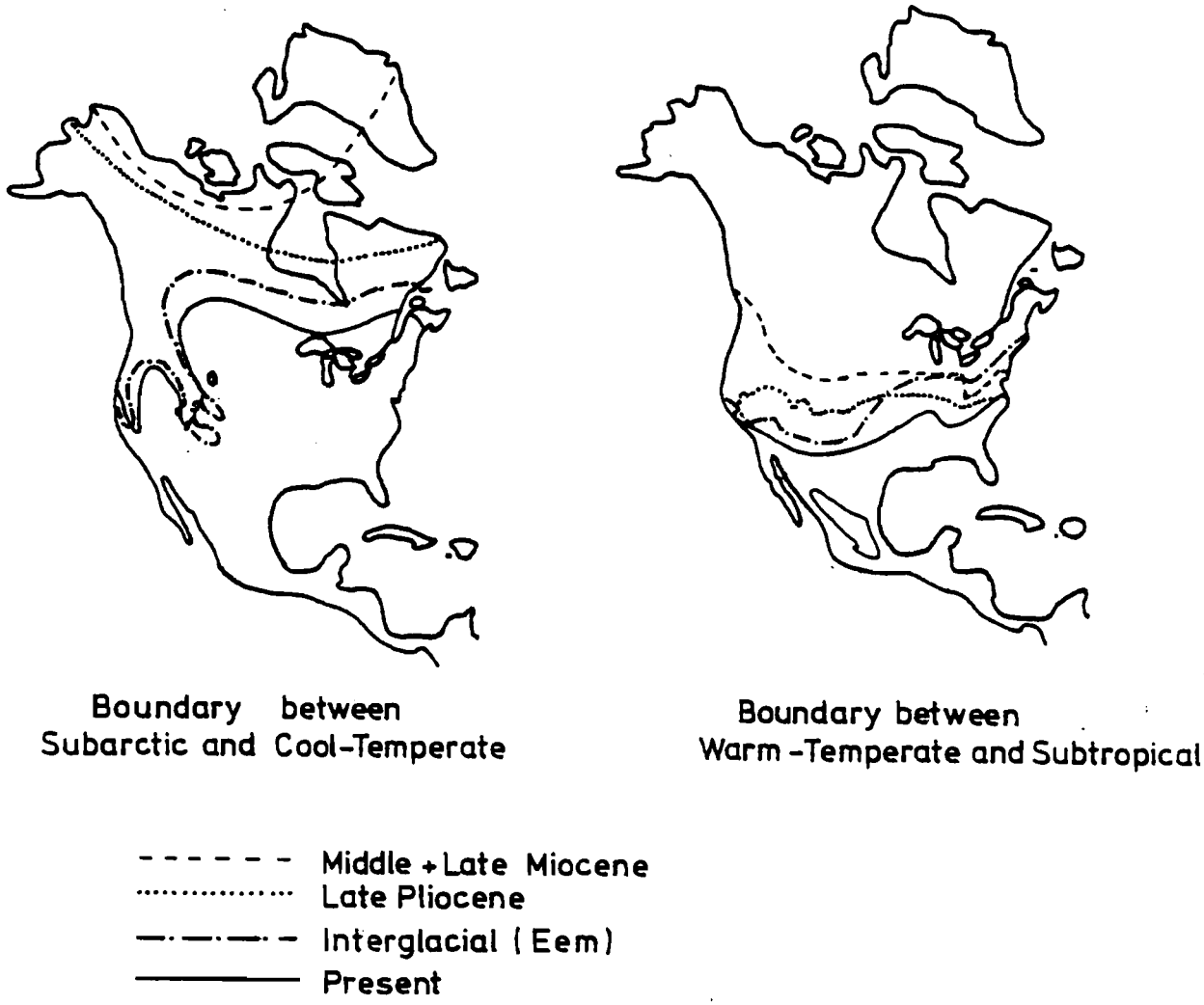

Figure 21. Displacement of vegetation boundaries in North America from Middle and Late Miocene to the present (Dorf 1960).

continent revealed the same marked asymmetry. While the southern Sahara was covered with a tropical humid or at least semi-humid vegetation (which has persisted in southern Nigeria), southern Africa and the Zaire basin were dry and sometimes fully desertic. The same aridity has also been observed in northern Australia especially after the Messinian peak of the Antarctic glaciation (Kemp 1978).

Although certainly still incomplete, this evidence indicates that the *hemispheric asymmetry* of the general circulation was substantially *greater* than it is now (Flohn 1978a). The shape and position of the continents was then by and large similar to the present conditions. Large-scale glaciation of the northern continents did not start until 2.5 Ma ago, the formation of Arctic drift ice only after that date, about 2.3 Ma ago, when the melting waters had produced a shallow, stable low-saline upper layer of the Arctic ocean (Herman 1977). Further evidence for an ice-free Arctic ocean before about 3 Ma ago is formed in the vegetation boundaries described by Frenzel (1968) for Siberia and by Hopkins (1967, 1971) for Arctic North America and the Chukchi peninsula. Thus, the *simultaneous* existence of a continental *ice dome* in the Antarctic and a substantially *ice-free Arctic ocean* is well established for the period between, at least, about 12 Ma until 2.5 Ma ago, characterized by a high degree of stability in spite of second-order climatic fluctuations. This strange situation must have caused marked hemispheric circulation asymmetries of both the atmosphere and the ocean.

It should be added that the worldwide faunal extinction at the end of the Mesozoic (65 Ma ago) in a time span of some 10^5, or "possibly as few as 1-100", years has recently been interpreted (McLean 1978) as having been caused by a sudden "greenhouse effect", i.e. by a positive and rapidly increasing feedback between CO_2 input into the atmosphere and ocean warming. The author interprets the extinction as being due to a severe damage of reproductive cells or of the calcium metabolism on account of increasing temperatures, which is also evidenced by the thinning of dinosaur eggshells. It could have been triggered by a simul-

taneous extinction of marine microfossils, e.g. of planktonic foraminifera in less than 10^4 years (Kent 1978), shortly before the extinction of dinosaurs (Butler et al., 1977; neither one is quoted by McLean). No interpretation of *this* event has been offered as yet. Certainly this is at present no more than an interesting speculative hypothesis. It contains, however, some remarkable parallels to what many scientists expect to happen in a foreseeable future.

Some Implications of a Unipolar Climatic Asymmetry

The coexistence of a fully glaciated Antarctic continent and an open Arctic ocean, for no less than ten million years, immediately before the Pleistocene, is indeed some discovery. It could be made because of the evidence accumulated during the Deep Sea Drilling Project with the "Glomar Challenger". This notion appears so contradictory to the traditional climatological views that hardly more than reluctant adoption can be expected. With no careful and critical survey of the vast geological literature on a global scale being available at present, it is one of the most urgent tasks to pursue. This must be done, however, in cooperation between geologists and meteorologists, with full knowledge of the basic laws of planetary circulation and their consequences.

Attention must be paid, first of all, to the fundamental *circulation theorem* found by V. Bjerknes in 1897 (e.g. Palmén and Newton 1969): in the three-dimensional baroclinic structure of the earth's atmosphere, temperature decreases with height and latitude, while atmospheric density decreases with height but increases with latitude. Not being parallel, isothermal and isopycnic surfaces cut each other at small angles, forming flat tubes (solenoids). According to the circulation theorem, in such a baroclinic field the intensity of a thermal circulation, which is driven by heating differences with latitude and height, depends only on the number of solenoids, i.e. on the temperature change (gradient) along an isopycnic surface. Since the slope of such surface is only 1:300 to 1:2000, the isopycnic temperature gra-

dients nearly equal the horizontal gradients. On a rotating planet, this thermal circulation is distorted by the Coriolis force: in the earth's atmosphere, the zonal (E - W) components of motion, introduced by the earth's fast rotation, are much stronger than the meridional and vertical components.

It cannot be the task of this report to outline the physical concepts of atmospheric circulation (see e.g. Palmén and Newton 1969) nor of oceanic circulation; the latter is driven, near the surface, mainly by the wind, and in greater depth by solenoids between surfaces of constant temperature and density (dependent on salinity). Note, however, that the *intensity* of *atmospheric circulation*, given the earth's rotation and the composition (density) of the atmosphere, depends first of all on the meridional *temperature difference between the equator and the poles*. Section IIb: The Role of the Antarctic Continental Ice Sheet (Table 1), has shown that, even today, the equator-pole temperature difference is about 40% higher in the southern than in the northern hemisphere.

For conservative extrapolation of the temperature/height relation for the case of an ice-free Arctic in winter, one can assume (Figure 22) an average surface temperature of $+4^{\circ}C$ (instead of $-34^{\circ}C$ now!), and a moist adiabatic lapse rate from the cloud base at about 950 mb up to, at least, 500 mb. (This instability probably leads to a cooling of the upper troposphere, e.g. at 300 mb (~9 km) from $-58^{\circ}C$ now to about $-62^{\circ}C$.) This means an average tropospheric warming of $11.5^{\circ}C$. A corresponding tropospheric warming of only $2-3^{\circ}C$ can be expected for summer, when the surface inversion is shallow and unimportant.

For the 300/700 mb layer, assumed as representative for a hemispheric comparison (see Section IIb: The Role of the Antarctic Continental Ice Sheet, and Table 1), the temperature increase in winter is only $+4^{\circ}C$, and the summer increase $+2^{\circ}C$. A conservative annual average increase of $+3^{\circ}C$ results. In this case, the average temperature difference of this layer would decrease to $24^{\circ}C$ between the equator and the North Pole, but still remain $37^{\circ}C$ above the southern hemisphere, where it would be slightly more

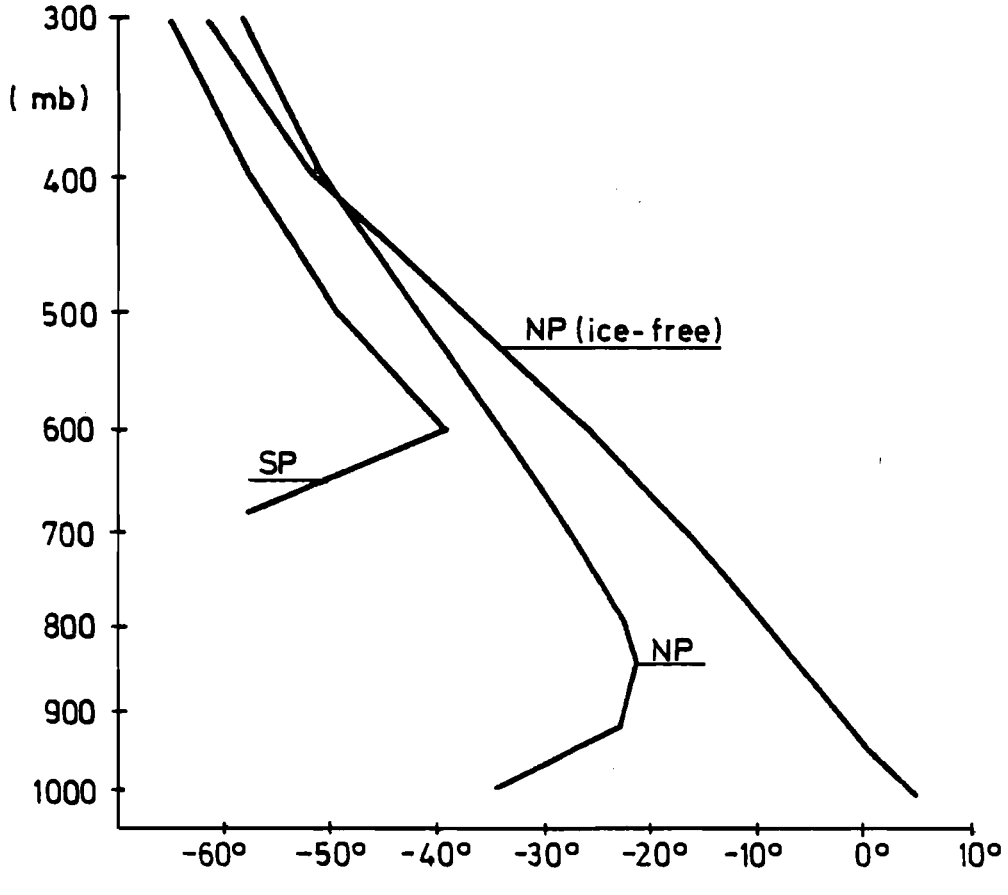

Figure 22. Actual winter temperatures above North Pole (NP) and South Pole (SP); estimated winter temperature above an ice-free North Pole.

than 50% higher than in the northern hemisphere. Here the assumption is made that the greenhouse effect does not significantly alter the meridional temperature gradient: this is certainly not quite realistic and subject to further revision.

In such a unipolar temperature asymmetry, one *fundamental* quantity of the *atmospheric circulation* could be extrapolated. Remember that, in a rotating atmosphere, there are two fundamentally different modes (Palmén and Newton 1969) of meridional exchange of conservative properties, such as angular momentum or enthalpy. The first can be idealized as a helical motion within a latitudinal band, symmetric about the rotational axis, and driven by a thermal circulation in a meridional/vertical plane between the equator and the subtropics: this is the tropical circulation or Hadley cell. The exchange processes of the second mode in higher latitudes are mainly due to traveling and quasistationary eddies, advecting warm (cold) air poleward (equatorward) at both sides of a vortex or long wave, within a belt of westerlies: this belt, identical with the meandering edge of a huge polar vortex, is part of the extratropical or Ferrel circulation. The average boundary between the two modes, which permanently interact in reality, is characterized by the *belt* of *subtropical anticyclones* near the surface and by the maximum of baroclinic westerly winds (i.e. the subtropical jet stream) in the upper troposphere, both in almost coinciding position.

It has been shown (Smagorinsky 1963) that stability or instability of eddies in a baroclinic current depends on a simple criterion related to the circulation theorem, i.e. the ratio between meridional temperature gradient and vertical lapse rate. Since the latter depends mainly on the water vapor content of the atmosphere (see below), the behavior of the eddies is by and large controlled by the meridional temperature gradient: they tend to be unstable in the Ferrel circulation, but stable in the Hadley cell where the meridional temperature differences are weak. Then the latitude-dependent threshold of the so called Z-criterion indicates, at the same time, the seasonally varying position of the subtropical belt (ϕ_{STA}). ϕ_{STA} is given by the

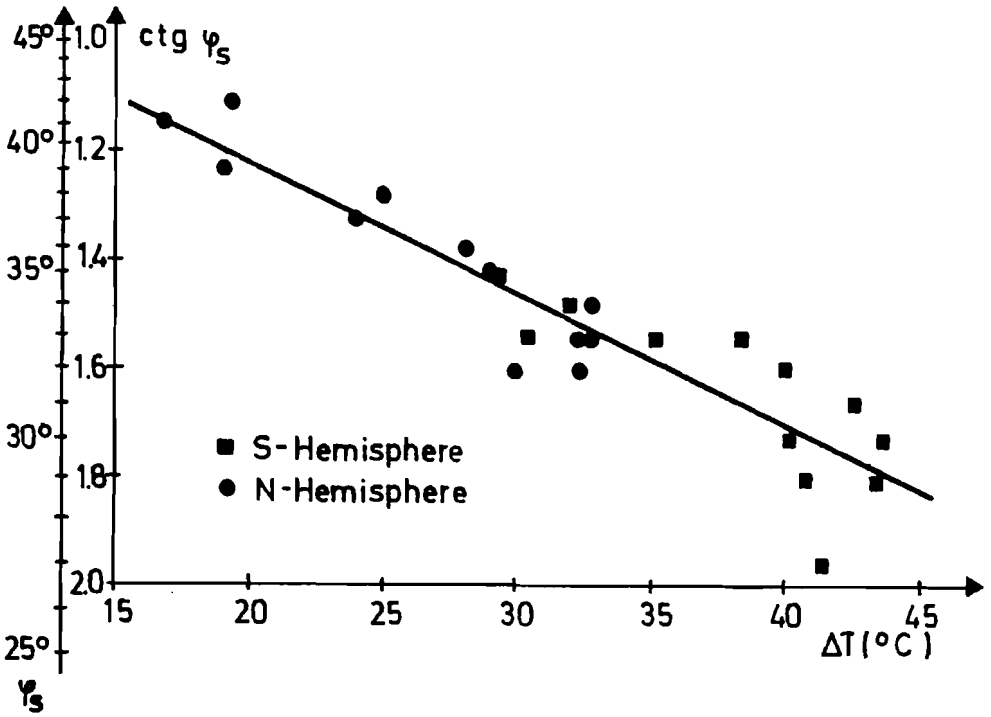

Figure 23. Latitude of the subtropical anticyclonic belt in every month versus actual equator-pole temperature difference; for monthly data for 300/700 mb layer see Flohn (1967); for both subtropical anticyclonic belts see Pflugbeil (1967).

following relation, with r = earth's radius, h = scale height of the atmosphere, Θ = potential temperature, y(z) = meridional (vertical) coordinate, and STA = subtropical anticyclone:

$$\mathrm{ctg}\,\phi_{STA} = \frac{r\delta\Theta/\delta y}{h\delta\Theta/\delta z} \quad .$$

Korff and Flohn (1969) have verified this theoretical concept[2] using monthly averages of many years of both latitude ϕ_{STA} of subtropical anticyclones and the meridional temperature gradient at the 300/700 mb layer, in both hemispheres. With correlation coefficients above 0.85, this relation describes remarkably well the seasonal variation and the actual hemispheric asymmetry of ϕ_{STA} (Figure 23).

[2]The Z-criterion has recently been criticized by Greenhut, who has demonstrated that it leads to incorrect results when applied to tropical latitudes during northern summer, when the average meridional temperature gradient reverses. Here it is only applied to the atmospheric circulation in subtropical and temperate latitudes; the empirical verification given above leaves no doubt about its applicability in this general case.

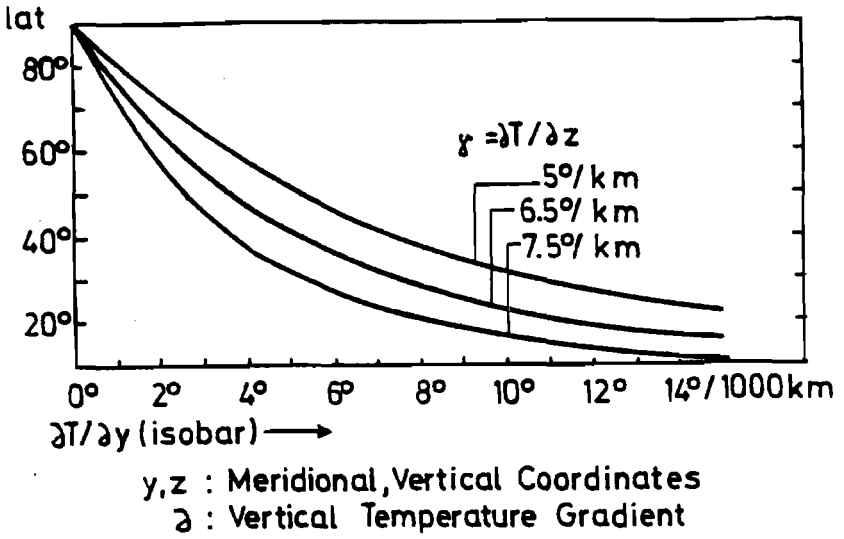

Figure 24. Latitudinal position of the subtropical anticyclonic belt as a function of vertical stability γ and of the meridional temperature gradient $\partial T/\partial y$ (Flohn 1964).

The role of the lapse rate $\delta\Theta/\delta z$ should be taken into account; as early as in 1964 a diagram (Figure 24) was published (Flohn 1964b) demonstrating this effect: an increase in the lapse rate would reduce ϕ_{STA}. A quite similar diagram was published later by Bryson (cf. Williams 1978, p.151). But there are two factors that impede simple quantification by means of Manabe-Wetherald's diagram (1975, see Figure 6):

1. Theoretical considerations leave it open if $\delta T/\delta y$ in Figure 24 can be taken as a linear average between the equator and the pole or as the highest value in the subtropical baroclinic zone (which has been preferred by Flohn, 1964);

2. Simplified introduction of clouds into the Manabe-Wetherald (1975) model yields discontinuities in the tropospheric lapse rate below 300 mb (Figure 6), which make it difficult to use the quantitative estimate in the formula above.

The combined role of meridional and vertical temperature gradients with respect to the Z-criterion merits further investigation.

A simple extrapolation based on the temperature distribution above an ice-free Arctic (Figure 22), with the temperatures above the equator and the South Pole unchanged, would yield only a small northward displacement of the subtropical anticyclonic belt. However, neglecting the 700/1000 mb layer, in which most of the warming (+21°C) occurs, leads to unrealistic results. The Z-criterion is based on the concept of baroclinic instability; the slope of the 300 mb surface, which is representative of tropospheric baroclinicity (or the temperature gradient), depends on the temperature pattern of the troposphere as a whole. Since there is no way of realistically estimating the 700/1000 mb layer at the Antarctic (where it is completely under the surface), one may use more realistic values, valid for the 300/1000 mb layer, to estimate the temperature increase above the Arctic: +11°C in winter, +3°C in summer, and +7°C the year round. This would yield an annual shift of the northern subtropical high-pressure belt (Figure 23) from now lat 37° to lat 43-45°, with the location of the southern subtropical belt remaining unchanged (31°S). In summer, the shift would reach probably not much farther than 100 or 200 km, but in winter the subtropical belt may be displaced by some 800 km or even farther north. This would drastically reduce the extension of the subtropical belt of winter rains, now supplying California, the Mediterranean, the Middle East up to Turkestan (U.S.S.R.), and the Punjab. The belt 45-50°N would probably be frequently affected by summer droughts.

Such an *asymmetric displacement* of the northern STA together with a constant southern STA would also shift the average position of the "meteorological equator" to lat 9-10°N, from its actual position of 6°N. In this case, in northern winter, penetration of the equatorial rain belt across the mathematical equator into the southern hemisphere would occur probably only occasionally; its seasonal displacement would be restricted to the belt between the equator and lat 20°N. As a consequence, tropical summer rains south of the equator would decrease markedly, eventually leading to natural desertification in many countries of the belt at 0-20°S. This would probably be aggravated by more frequent and more intense equatorial upwelling,

causing a drastic reduction of oceanic evaporation in this belt, especially in northern summer/southern winter, when the meteorological equator reaches its northernmost position. In this case, strong equatorial upwelling can be expected to arise permanently (no El Niño situations any more), at least in the Pacific and Atlantic oceans. For the equatorial Indian Ocean, no convincing evidence of past (or present) upwelling is available.

In the big *oceans*, the position of the equatorial upwelling zone is controlled by the disappearance of the Coriolis force at the mathematical equator. Since no meridional climatic shift is possible here, this zone can serve as a marker for latitudinal shifts of tectonic plates (Winterer 1973). A different view expressed by Kozur (1976) results from a misunderstanding of the geophysical background of oceanic upwelling along the equator, which never coincides with the atmospheric intertropical convergence zone (see Section IIc: Equatorial Upwelling, El Niño, and Hydrologic Balance).

In the present *Sudan-Sahel belt*, between about lat 8°N - 18° (or perhaps 20°N), an increase in precipitation *could* be possible. However, this conclusion is based on only one argument: the northward shift of planetary climatic belts. But the actual seasonal advance of the rainfall belt in summer *in Africa* is remarkably small, most probably on account of the tropical easterly jet which, in an area of decreasing speed, forces the air beneath to subside (Flohn 1964a, 1966). This effect should also persist during an ice-free Arctic ocean (see below). Another essential prerequisite, if one follows the convincing model studies by Charney (1975) and many others, would be conservation of vegetation that might reappear because of expanding summer rains, i.e. its protection against overgrazing and other desertification processes triggered by man.

In the *monsoon area* of southern Asia, the planetary circulation patterns are disturbed and largely controlled by the existence of the mountain area north of the Himalayas. Here any rational attempts at predicting the effects of disappearing Arctic sea ice seem to be impossible. Since the late Tertiary, the

altitude of the giant mountain block in this area has increased considerably--vertical motions are still going on, and climatological evidence from a period when the Himalayas did not exist can certainly not be taken as resembling what could be expected under present boundary conditions. Striking evidence for uplifting is the Tibetan plateau, whose weak rolling topography has been raised from near sea level in the Late Tertiary to a present altitude of 4-5 km. Being an elevated heat source, it controls the tropical easterly jet (Flohn 1964, 1968) and the entire monsoon circulation between western Africa and the Philippines. In this wide area, the influence of an ice-free Arctic could be rather weak or even negligible in summer. In winter, a northward displacement of the subtropical jet of lat 5-6° (like in other longitudes, see p. 83) could mean wintertime disturbance across the whole of southern Asia, perhaps with increasing rainfall in areas as remote as Chinese Turkestan, but with decreasing winter rain south of the Himalayas.

After a possible disappearance of the central core of the Arctic drift ice, one of the first consequences in the cold season would be the formation of a baroclinic zone along the *northern coast* of the *continents*, between the cold air continuously formed above the snow-covered land and the relatively warm air above the open Arctic ocean. It must remain an open question as to what extent coastal ice, and perhaps also a thin seasonal mid ocean ice cover, could form.[3] In any case, the rate of snowfall along the northern coasts of the continents and Arctic islands would be enhanced by such a development. In summer, the low-level stratus now above the melting ice could probably disappear, and the thermal circulation arising between the heated continents and the relatively cool water could pro-

---

[3]The development of a thin drift ice cover during winter has recently (April 1979) been suggested in a model investigation by S. Manabe, assuming a four-fold increase in CO_2. As a transitional phase, this seems plausible; some contrasting arguments are the enormous heat storage of an open Arctic ocean during summer and the expected frequency of deep cyclones and gales during the cold season.

duce a distinct predominance of anticyclonic situations above the Arctic ocean, now with subsidence and little cloudiness.

Changes in the *global water budget* (see Section IIc: Equatorial Upwelling, El Niño, and Hydrologic Balance) are difficult to estimate. While a weaker tropical circulation can be assumed for the moderate warm phases considered in Chapter V: A Global Warming Scenario Based Upon Past Climates, evidence from past climates, based on signs of increasing aridity in the Late Tertiary are unambiguous; even more so since the peak of Antarctic glaciation, together with the eustatic drop of the sea level, also reduced the evaporating ocean area. If one assumes strong upwelling for only six months of the southern winter alone, the loss due to this effect is 30×10^3 km^3/a. On the other hand, an ice-free Arctic ocean would evaporate much faster than now, when the evaporation is only in the order of 5-10 cm/a. On the assumption of a rather large increase in evaporation by +100 cm/a, this would yield no more than 10×10^3 km^3/a for an area of 10^7 km^2. The extension of the southern belt to lat 0-20°S, the displacement of the northern STA to lat 35-45°N (or even farther) would--also based on the incomplete evidence from past climates--support a general *increase in aridity*, with a global loss of water on the order of at least 4-5%.

The prospects of a *worldwide rise* of the *sea level* as a possible consequence of global warming must be considered quantitatively. Melting of drifting sea-ice does not change the sea level at all; floating ice is in static equilibrium with water, like an ice cube in a glass of whisky. In the human time scale (of ~100 years), any worldwide sea level rise could only be caused by large-scale *surges* of *continental* ice caps, e.g. on the order of 10^5 km^3 or more, leading (with a density of almost 0.9) to a 25 cm sea level rise per 10^5 km^3 ice melted.

Only one area is prone to such a surge: it is the "western" part of Antarctica (between South America and long 150°W), situated on a rock basement largely below sea level. Surges of this order have been suggested for the 19th century (Lamb 1967) as well as for the postglacial period (Wilson 1978), and the probability of such an event may increase with global warming.

There seems to be a gradual transition between such surges (of unknown time-scale!) and extended calving of existing ice shelves. Possibly more interesting are surges on the order of 2×10^6 km^3, equivalent to a sea-level rise of 5 m; the last event of this kind may have occurred about 110,000 years ago (Hollin) or, with more widespread evidence, about 125,000 years ago (Mercer). The risk of such a large-scale sea-level rise probably produced by a mechanism of calving bays as described by Hughes (1977, p.43), seems to be small, but certainly not zero (see Section IIb); more detailed investigations must again be recommended, as well as a continuous survey of Antarctic ice shelves.[4]

The possiblity of a significant *melting* of continental ice caps (e.g. Greenland, Antarctic) is also rather small. The surface of the Antarctic ice cap, with temperatures between -20°C and -70°C and an albedo of 80-90% can be considered stable; even a very marked warming by a strongly increased transport of warm air would not suffice to cause significant melting (or evaporation). After a possible disappearance of the Arctic sea ice, Greenland (lat 60-83°N) would be affected by some warm-season melting (at least at its southern part), but it would also receive much greater winter snowfall due to increased cyclone activity. It is difficult to estimate the ratio of both processes without model computations. But in the worst and rather unlikely case, an estimated annual net loss of as much as 50 cm water equivalent would cause an additional sea level rise of 2.5 mm/a, as compared with the present value of 1.2 mm/a.

As a result of these considerations, the *probability* of a catastrophic or even only appreciable *rise* of the sea level for the next 100 years seems small (estimated at 1% or less), much smaller than the probability of a large-scale shift of climatic belts due to global warming, but is certainly not negligible.

---

[4]The possible time-scale of such a disintegration can be on the order of 100-200 years, equivalent to an average sea-level rise on the order of 2-5 cm/year. This is suggested by a similar event caused by the catastrophic incursion of the sea into the present Hudson Bay about 7800 BP (Andrews et al. 1972) simultaneous with an observed eustatic sea-level rise of 7-10 m over 200 years at the coasts of NW England (Tooley 1974) and SW Sweden (Mörner 1976).

CONCLUSIONS

Small changes of the global average temperature (Table 3) are utterly misleading for the general reader. A temperature drop of 1°C near the northern boundary of agriculture (affecting, e.g., wheat in northern Canada, or hay in Iceland) may reduce the growing season by several weeks, with detrimental results on harvests. Even more essential are the accompanying changes in the frequency of extremes of the weather in lower and middle latitudes, of long and cold springs, of cool and wet summers, etc. According to the present state of the art, a sudden cooling, similar to those that occurred during the Little Ice Age and its forerunners, cannot be excluded since natural effects (see Chapter II: Internal Climatogenetic Processes) are at present still unpredictable. The most catastrophic years were those of 1316, 1430, and 1570, and in the 1690s and 1780s, the latter apparently affecting Europe[5], North America, as well as Japan. The European revolutions of 1789 and 1848 occurred after sequences of years with bad weather, bad harvests, and high cereal prices; some of the most severe climatic and economic conditions were reported in the years following some of the heaviest volcanic eruptions, e.g. after 1766, 1783, 1815, and finally 1883.

The problem of *natural climatic fluctuations* due to the varying frequency and intensity of volcanic explosions merits some discussion. As far as can be seen, this effect alone could, with a certain degree of probability, counteract the evolution outlined in this admittedly one-eyed scenario (see the basic assumptions given in Chapter I: Natural and Man-Made Climatogenetic Effects, p. 6). Lamb (1970, 1977b) has demonstrated the time variability of volcanic eruptions using an estimated Dust Veil Index (Figure 25). There is little doubt that the peaks of volcanic activity by and large coincide with series of

---

[5] These data have been derived from historical records including a comparison of some 25 long series of cereal prices (1200-1790) in northwest and central Europe. A detailed study is in preparation; cf. also the documented evidence given by Ladurie (1971), Lamb (1977), and many others.

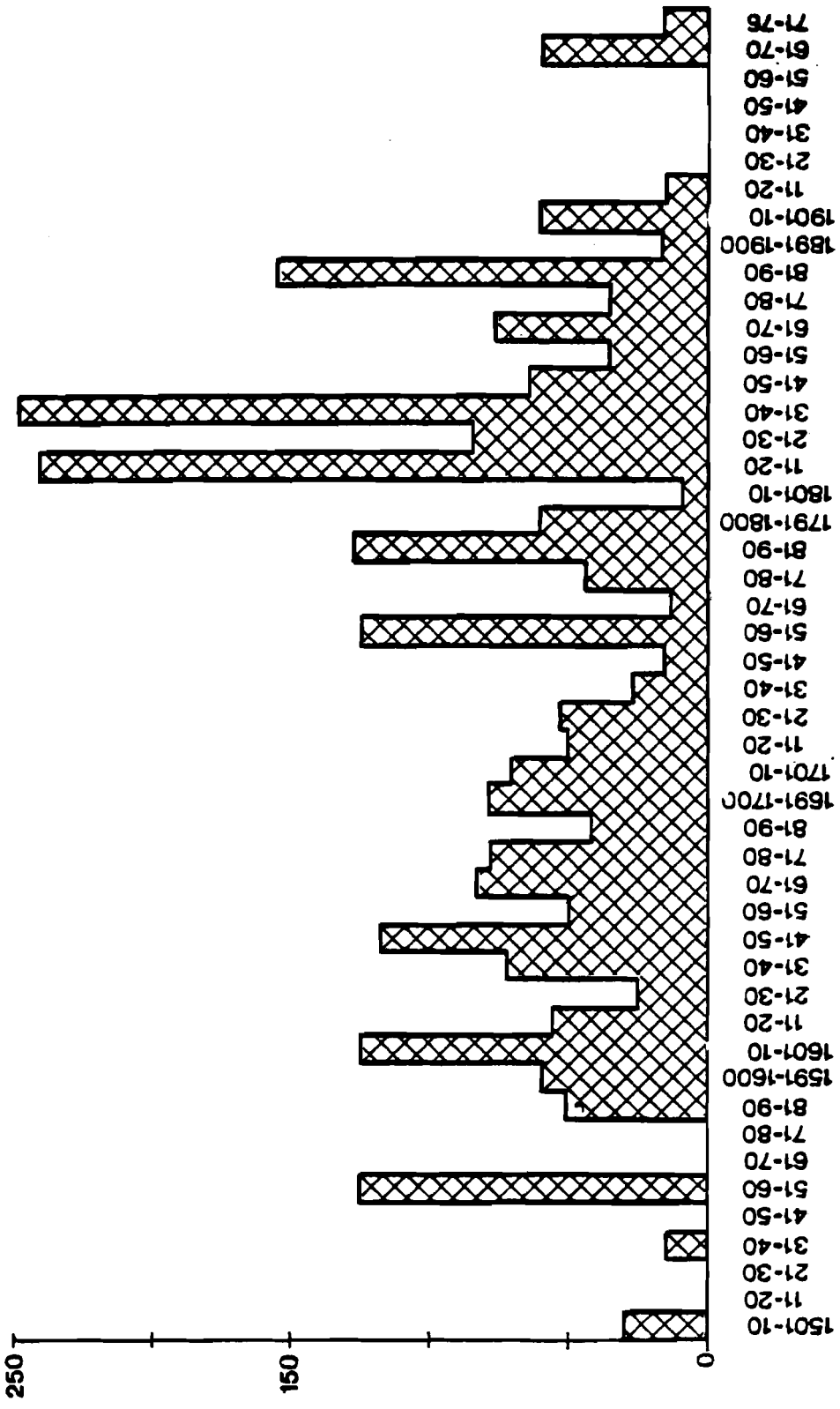

Figure 25. Decadal averages of volcanic activity (Dust Veil Index) since 1500, northern hemisphere only (Lamb 1977b).

particularly cool years (and especially cool summers); their role in climatic history, perhaps at all time-scales (Figure 19), can hardly be overrated. Volcanic eruptions are very difficult to forecast, as has been confirmed by recent examples; such forecasts are virtually impossible beyond the time-scale of weeks or months. At the global scale, the geophysical concept of plate tectonics has contributed much to a better understanding: mid-oceanic rift systems burst, hot material ascends and erupts in individual volcanoes, and plates move horizontally towards the continents where they are subdued by heavy earthquakes. In recent years series of unusually severe earthquakes have occurred, all of them along well-known active tectonic zones, but the volcanic activity has remained moderate. Should we soon expect an increased frequency of really heavy volcanic explosions? There is no answer to this question, but volcanologists would be hardly surprised if this was to happen. An example of the discontinuous manifestations of the slow plate motion--which is probably responsible for the observed clustering of volcanic (and seismic?) events--recently occurred at the mid-Atlantic rift system crossing Iceland. In April 1977 two innocent looking, but steaming, parallel cracks with a diameter of about 1 m each formed in the Myvatn area, and a geothermal power station, just before completion, lost its resources.

Since volcanic activity is unpredictable to date, a statistical technique can be used to estimate the probability of a cooling episode like in the Little Ice Age over the next 100 years. Using Figure A 31 in the excellent report on *Understanding Climatic Change* issued by the U.S. National Academy of Sciences (1974), one can estimate the probability of an event that may occur randomly once every 1000 years over the following 100 years to be about 10-20%. However, this estimate only indicates an order of magnitude, although disregarding such a probability would be irresponsible.

Before this background, our *scenario* leads to the following *conclusions*: if the atmospheric CO_2 content continues to rise, and if other man-made trace gases add another 50% (or more) to

the greenhouse effect of infrared absorption, developments similar to those outlined in Chapter V: A Global Warming Scenario Based Upon Past Climates, must eventually be expected. The Eem period may serve as a first guide to what might happen if the (real) CO_2 content rises to about 500-550 ppm; if the effect of other trace gases were negligible, the relevant threshold of the "virtual" CO_2 content would be about 600-700 ppm. As the Manabe-Wetherald model (Figure 6) indicates, a doubling of the CO_2 content should be accompanied by quite serious regional consequences, some of them benign, but others deleterious.

The *real danger*, however, is related to the possible consequences outlined in Chapter VI: Ice Free Arctic Versus Glaciated Antarctic? Can we stop at a CO_2 content between 550 and 750 ppm? Since the necessary time of transition from one energy system to another is on the order of several decades (Häfele and Sassin 1977a,b), it will soon be too late for any effective countermeasures. The report of a working group of specialists (Williams 1978, p.315) states that "mankind needs and can afford a time window of between 5 and 10 years for vigorous research and planning...to justify a major change in energy politics...". At a first glance, the idea of a planet with one pole heavily glaciated and the other ice-free looks so fantastic and inconceivable that the emotional resistance against it, especially among nonscientists, will be difficult to overcome. There is no doubt that *exactly* this pattern *had existed* and was *stable* for a period of ten million years; this is established as a fact and not as fiction.

It goes beyond the capability of a climatologist, familiar with the historical and geophysical background of his science, to predict the time sequence of future CO_2 increase and temperature rise. This depends on economic and political decisions outside his level of knowledge and experience. As a first guide to different CO_2 growth rates, the reader is referred to Figure 8. Taking into account all uncertainties, especially with respect to the role of the biosphere and the oceans, specialists agree that an increase in atmospheric CO_2 by a factor of 3-6 can be expected over the next 100 years (for references see p. 34).

From a climatological point of view, the *decisive threshold* of the *real* CO_2 *level* should be somewhere between 550 and 750 ppm; that of the *virtual* CO_2 level is somewhat higher, e.g. between 800 and 1000 or 1100 ppm. Above this threshold, the probability of an evolution toward a situation as described in Chapter VI increases rapidly--a development of this kind *could* occur quite *abruptly*, i.e. in a matter of a few decades (or less), and would then be irreversible. Since this situation had been maintained, under purely natural conditions, over a period of no less than ten million years, it would also be stable, after its first reappearance. What *has* happened can happen again: it would, after a series of catastrophic weather extremes, lead to a nearly inconceivable displacement of climatic zones by 400-800 km (or more), definitely affecting mankind as a whole.

The author firmly believes that this risk is *unacceptable* and must be avoided even at very high cost. It is at least as large as but probably much larger than all the risks involved in the (transitional) use of nuclear energy under special precautions. It can be avoided if decisions regarding the future energy policies and all their consequences are carefully planned and can be executed, under an international agreement, without undue delay.

REFERENCES

Monographies

Andersen, N.R., and A. Malakoff, eds. (1977) The Fate of Fossil Fuel CO_2 in the Oceans. Marine Science Vol. 6. New York: Plenum Press.

Baumgartner, A., and E. Reichel (1975) The World Water Balance. Munich: Oldenbourg.

Bryson, R.A., and Th. J. Murray (1977) Climates of Hunger. Madison: University of Wisconsin Press.

Budyko, M.I. (1969) Climatic Changes. Hydrometeoizdat, Leningrad (in Russian). English translation in Am. Geophys. Soc. 1977.

Cline, R.M., and J.D. Hays, eds. (1976) Investigation of Late Quaternary Paleooceanography and Paleoclimatology. Geol. Soc. Am. Mem. 145.

Faure, H., and A.J. Williams, eds. (1979) The Sahara and the Nile. Rotterdam: Balkema.

Frenzel, B. (1967) Die Klimaschwankungen des Eiszeitalters. Braunschweig: Vieweg.

(1968a) Grundzüge der pleistozänen Vegetationsgeschichte Nord-Eurasiens. Wiesbaden: Franz Steiner.

Gabriel, B. (1977) Zum ökologischen Wandel im Neolithikum der Östlichen Zentralsahara. Berliner Geogr. Abh. 27.

GARP, in B. Bolin, ed. (1975) The physical basis of climate and climate modeling. GARP Publication Series 16. Geneva: WMO.

Gribbin, J., ed. (1978) Climatic Change. Cambridge, Mass.: Cambridge University Press.

Hare, F.K. (1977) Climate and desertification. UN Conference on Desertification, Nairobi 1977. A/CONF 74/5. New York: United Nations.

Ives, J.D., and R.G. Barry, eds. (1974) Arctic and Alpine Environments. London: Methuen.

Labeyrie, J., ed. (1974) Variation du Climat au Cours du Pleistocène. Paris: Centre Nationale de Recherches Scientifiques.

Ladurie, E.L. (1971) Times of Feast, Times of Famine. A History of Climate Since the Year 1000. New York: Doubleday.

Lamb, H.H. (1972) Climate: Present, Past and Future, Vol. 1. London: Methuen.

(1977a) Climate: Present, Past and Future, Vol. 2. London: Methuen.

Lvovich, M. (1969) Water Resources for the Future. Moscow: Posveshchenie (in Russian).

Mägdefrau, K. (1968) Paläobiologie der Pflanzen; fourth edition. Stuttgart: Gustav Fischer.

Nairn, A.E.M., ed. (1961) Descriptive Paleoclimatology. London, New York: Interscience.

(1964) Problems in Paleoclimatology. NATO Paleoclimatology Conference at the University of New Castle/Tyne, Jan. 7-12, 1963. London, New York: Interscience.

National Academy of Sciences (1975) Understanding Climatic Change. A Program for Action. Washington, D.C.

Nicholson, S.E. (1976) A Climatic Chronology for Africa: Synthesis of Geological, Historical and Meteorological Information and Data. Ph.D. thesis, Madison: Department of Meteorology, University of Wisconsin.

Olson, J.S., et al. (1978) Changes in the Global Carbon Cycle and the Biosphere. ORNL-1050. Tenn.: Oak Ridge National Laboratory.

Palmén, E., and C.W. Newton (1969) Atmospheric circulation systems. Internat. Geophys. Ser. 13.

Pittock, A.B., et al., eds. (1978) Climatic Changes and Variability. A Southern Perspective. Mass.: Cambridge University Press.

Schwarzbach, M. (1974) Klima der Vorzeit. Eine Einführung in die Paläoklimatologie, third edition. Stuttgart: Enke.

Stumm, W., ed. (1977) Global Chemical Cycles and Their Alteration by Man. Berlin: Abakon.

Takahashi, K. and M.M. Yoshino, eds. (1978) Climatic Change and Food Production. Tokyo: University of Tokyo Press.

van Zinderen Bakker, E.M. ed. (1978) Antarctic Glacial History and World Palaeoenvironments. Rotterdam: Balkema.

Vasari, Y., et al., eds. (1972) Climatic change in Arctic areas during the last ten-thousand years. Acta Univ. Ouluensis A3, Geologica (1).

Williams, J., ed. (1978) Carbon Dioxide, Climate and Society.- IIASA Proceedings Series, Vol. 1. Oxford: Pergamon Press.

Selected References:
Geophysical Background, Models, etc.

Aagard, K., and L.K. Coachman (1975) Eos Trans. Am. Geophys. Union 56: 484-487.

Aagard, K., and P. Greisman (1975) J. Geophys. Res. 80: 3821-3827.

Angell, J.K., and J. Korshover (1978) Mon. Weather Rev. 106: 755-770.

Augustsson, T., and V. Ramanathan (1977) J. Atmos. Sci. 34: 448-451.

Bacastow, R. (1976) Nature 261: 116-118.

(1977) Pages 33-44. The Fate of Fossil Fuel CO_2 in the Oceans, edited by N.R. Andersen and A. Malakoff. Marine Science Vol. 6.

Bach, W. (1976a) Rev. Geophys. Space Phys., 14: 429-474.

(1976b) Borner Meteorol. Abh. 24.

Barnett, T.P. (1977) Phys. Oceanogr. 7:221-236; 633-647.

Berkofsky, L. (1976) Appl. Meteorol. 15: 1139-1144.

(1977) Beitr. Phys. Atmos. 50: 312-320.

Berlage, H.P. (1957) Med. Verh. Kon. Nederl. Meteor. Inst. 69.

(1966) Med. Verh. Kon. Nederl. Meteor. Inst. 88.

Bjerknes, J. (1969) Mon. Weather Rev. 97: 163-172.

Bjornsson, A., et al. (1977) Nature 266: 318-322.

Borzenkova, I.I., et al. (1976) Meteorologia i Gidrologia (7): 27-35.

Bryson, R.A., et al. (1969) Arctic and Alpine Research 1: 1-14.

Budyko, M.J. (1962) Izv. Ak. Nauk USSR, Ser. Geogr. (6): 3-10 (in Russian).

(1969) Tellus 21: 611-619.

(1972) Eos Trans. Am. Geophys. Union 53: 868-874.

Budd, W.F. (1975a) Science (186): 925-927.

(1975b) J. Glaciol. 14: 3-21.

Cess, R.D. (1976) J. Atmos. Sci. 33: 1831-1843.

(1977) J. Atmos. Sci. 34: 1824-1827.

Charney, J.G. (1975) Q. J. R Meteorol. Soc. 101: 193-202.

Damon, P.E., and St. M. Kunen (1976) Science (193): 447-453.

Doberitz, R. (1968) Ber. Dt. Wetterdienst 112.

(1969) Bonner Meteor. Abh. 11.

Donn, W.L., and D.H. Shaw (1966) J. Geophys. Res. 71: 1087-1093.

Dronia, H. (1974) Meteorol. Rundsch. 27: 166-174.

Ellsaesser, H.W., et al. (1976) Q. J. R. Meteorol. Soc. 102: 655-666.

Fletcher, J.O., et al. (1973) WMO Technical Note 129: 181-218.

Flohn, H. (1964a) Bonner Meteorol. Abh. 4.

(1966) Z. Meteorol. 17: 316-320.

(1967) Ann. Meteorol. N.F. 3: 76-80.

(1968) Colorado State University, Department of Atmospheric Science Paper 130.

(1971) Bonner Meteorol. Abh. 15.

(1972) Pages 93-102. Studies in Physical Oceanography, Vol. I, edited by A.L. Gordon.

(1974a) Ann. Meteorol. N.F. 9: 25-31.

(1975) Bonner Meteorol. Abh. 21.

(1977a) Appl. Sci. Dev. 10: 44-58.

Flohn, H., and H. Fleer (1975) Atmosphere 13: 96-109.

Gow, A.J., et al. (1968) Science (161): 1011-1013.

Greenhut, G.K. (1977) J. Appl. Meteorol. 16: 727-734.

Hahn, J., and C. Junge (1977) Z. Naturforsch. 32a: 190-214.

Hahn, J. (1979) Pages 193-213 in Man's Impact on Climate, edited by W. Bach, J. Pankrath and W. Kellogg. New York: Elsevier.

Hantel, M. (1972) Pages 121-136. Studies in Physical Oceanography, Vol. I, edited by A.L. Gordon.

Hastenrath, St. (1976) Riv. Ital. Geofis. 3: 255-256.

(1977) Ann. Meteorol. N.F. 12: 84-86.

Hattersley-Smith, G. (1974) Arctic and Alpine Environments, edited by J.D. Ives, and R.G. Barry, pages 195-223.

Häfele, W., and W. Sassin (1977a) The global energy system. Pages 1-30. Ann. Rev. Energy, Vol. 2, edited by J. Hollander, Palo Alto: Annual Reviews Inc.

(1977b) On energy demand. International Atomic Energy Agency Bulletin 19(6): 21-37.

Henning, D. Colorado State University, Department of Atmospheric Science, unpublished report.

Joseph, J.H. (1977) Pages 487-492. Radiation in the Atmosphere: Proceedings, edited by H.J. Bolle. Princeton: Science Press.

Junge, C. (1978) Promet, Meteorologische Fortbildung (2/3): 21-32.

Korff, H.C., and H. Flohn (1969) Ann. Meteorol. N.F. 4: 163-164.

Kukla, G.J., et al. (1977b) Nature 270: 573-580.

Lamb, H.H. (1967) World Meteorol. Org. Techn. Note 87: 428-453.

(1970) Philos. Trans. R. Soc. London, Ser. A 266: 425-533. For amendments see

(1977b) Climate Monitor 6 (2).

Limbert, D.W.S. (1974) Polar Record 17: 303-306.

Manabe, S., and J.L. Holloway, Jr. (1975) J. Geophys. Res. 80: 1617-1649.

Manabe, S., and R.T. Wetherald (1975) J. Atmos. Sci. 32: 3-15.

Manabe, S. (forthcoming) AAAS-DOE Workshop on Environmental and Societal Consequences of a Possible CO_2-Induced Climatic Change, Annapolis, Md., April 1979.

Maykut, G.A., and N. Untersteiner (1971) J. Geophys. Res. 76: 1550-1575.

Mass, C., and S.H. Schneider (1977) J. Atmos. Sci. 34: 1995-2004.

Newell, R.E., et al. (1978) Pure Appl. Geophys. 116: 351-371.

Oliver, R.C. (1976) J. Appl. Meteorol. 15: 933-970.

Pflugbeil, C. (1967) Ber. Dt. Wetterdienst 104.

Pollock, J.P., et al. (1976) J. Geophys. Res. 8: 1071-1083.

Polunin, N., ed. (forthcoming) Proceedings of the Second International Conference on Environmental Future, Reykjavik, June 1977.

Pratt, R.F., et al. (1977) Climatic Change 1: 109-135.

Ramanathan, V. (1975) Science 190: 50-52.

Ratcliffe, R.A.S., et al. (1978) Q. J. R. Meteorol. Soc. 104: 243-255.

Roads, J.O. (1978) J. Atmos. Sci. (1978) 35: 753-772.

Rothrock, D.A. (1975) J. Geophys. Res. 80: 387-397.

Rowntree, P.R. (1972) Q. J. R. Meteorol. Soc. 98: 290-321.

Salinger, M.J., and J.M. Gunn (1975) Nature 256: 396-398.

Schneider, S.H. (1975) J. Atmos. Sci. 32: 2060-2066.

Schwerdtfeger, W. (1956) Q. Soc. Cient. Argentina 161: 53-82.

(1958) Z. Gletscherkde. Glazialgeol. 4: 73-86.

(1976) Pages 243-355. World Survey of Climatology, Vol. 14, edited by H.E. Landsberg. Amsterdam: Elsevier.

Sellers, W.D. (1969) J. Appl. Meteorol. 8: 392-400.

(1973) J. Appl. Meteorol. 12: 241-254.

Smagorinsky, J. (1963) Mon. Weather Rev. 91: 99-165.

Söderlund, R., and B.H. Svensson (1976) SCOPE Report No. 7: 23-73.

Thorndike, A.S., et al. (1975) J. Geophys. Res. 80: 4501-4513.

Trempel, U. (1978) Diplomarbeit. Bonn University.

Untersteiner, N., in GARP Publication Series 16: 206-224.

van Loon, H., and J. Williams (1976) Mon. Weather Rev. 104: 364-380, 1003-1011, 1591-1596.

(1977) Mon. Weather Rev. 105: 636-647.

van Loon, H., and J.C. Rogers (1978) Mon. Weather Rev. 106: 296-310.

Vowinckel, E., and S. Orvig (1976) Pages 129-252. World Survey of Climatology, Vol. 14, edited by H.E. Landsberg. Amsterdam: Elsevier.

(1973) WMO Technical Note 129: 143-166.

Walsh, J.E. (1977) Mon. Weather Rev. 105: 1527-1535.

Wang, W.C., et al. (1976) Science 194: 685-690.

Washington, W.M., et al. (1977) J. Phys. Oceanogr. 6: 679-685.

Wetherald, R.T., and S. Manabe (1975) J. Atmos. Sci. 32: 2044-2059.

Wright, P.B. (1975) CRU 4. University of East Anglia, Climate Research Unit.

(1977) Report 77-13. Hawaii Institute of Geophysics.

Yamamoto, R., et al. (1975) J. Meteorol. Soc. Japan 53: 482-486.

(1977) Arch. Meteorol., Geophys. Bioklimatol. Ser. B 25: 105-115.

Zimen, K.E. (1977a) Global Chemical Cycles and Their Alteration by Man, edited by W. Stumm.

(1977b) Z. Naturforsch. 32a: 1544-1554.

Selected References: Paleoclimatology

Adam, D.P. (1978) X. INQUA Congress, Birmingham, Abstracts Page 3.

Alexandre, P. (1977) Ann. Econ. Soc. Civil. 32: 183-197.

Andrews, J.T., et al. (1972) Nature 239: 147-149.

Barry, R.G., et al. (1977) Arctic Alp. Res. 9: 193-210.

Bernabo, J.C., and T. Webb III (1977) Quatern. Res. 8: 64-96.

Bowler, J.M., et al. (1976a) Quatern. Res. 6: 359-394.

(1976b) Earth-Sci. Rev. 12: 279-310.

Butler, R.F., et al. (1977) Nature 267: 318-323.

Butzer, K.W., et al. (1972) Science 175: 1069-1076.

Butzer, K.W. (1975) Pages 389-410. Problems in Prehistory: North Africa and the Levant, edited by F. Wendorf and A.E. Marks.

Chu, C.Ch. (1973) Scientia Sinica 16: 226-256.

Cifelli, R. (1976) Nature 264: 431-432.

Dansgaard, W., et al. (1972) Quatern. Res. 2: 396-398.

(1975) Nature 255: 24-28.

(1978) J. Glaciol. 20: 3-30.

Diester-Haas, L. (1976) Quatern Res. 6: 299-314.

Dorf, E. (1960) Am. Sci. 48: 341-364.

Duplessy, J.C., et al. (1970) Nature 226: 631-633.

Emiliani, C., and N.J. Shackleton (1974) Science 183: 511-514.

Flohn, H. (1964b) Geolog. Rundsch. 54: 504-515.

(1974b) Quatern. Res. 4: 385-404.

(1978a) Pages 3-13. Antarctic Glacial History and World Paleoenvironments, edited by van Zinderen Bakker. Rotterdam: Balkema.

(1978b) Pages 124-134. Climatic Changes and Variability: A Southern Perspective, edited by A.B. Pittock, et al. Cambridge University Press.

Frakes, L.A. (1978) Pages 53-69. Climatic Changes and Variability, edited by A.B. Pittock, et al.

Frenzel, B. (1968b) Science 161: 637-649.

Fuji, N. (1976) Pages 316-356. Paleolimnology of Lake Biwa 4.

Gardner, J.V., and J.D. Hays (1976) Pages 221-246. Geol. Soc. Am. Mem. 145, edited by R.M. Cline and J.D. Hays.

Gasse, F., and G. Delibrias (1976) Pages 529-575. Paleolimnology of Lake Biwa 4, edited by S. Horie.

Hays, J.D., et al. (1976) Pages 337-369. Geol. Soc. Am. Mem. 145, edited by R.M. Cline and J.D. Hays.

Hays, J.D. (1978) Pages 57-71. Antarctic Glacial History and World Paleoenvironments, edited by van Zinderen Bakker. Rotterdam: Balkema.

Hollin, J.T. (1977) Boreas 6: 33-52.

Hopkins, D.M., ed. (1967) The Bering Land Bridge. Stanford University Press.

(1971) Palaeogeogr., Palaeoclimatol., Palaeoecol. 9: 211-231.

Hsü, K.J., et al. (1973) Nature 242: 240-244.

(1974) Naturwiss. 61: 137-142.

(1977) Nature 267: 399-403.

Hughes, T. (1973) J. Geophys. Res. 78: 7884-7910.

(1975) Rev. Geophys. Space Phys. 13: 502-526.

(1977) Rev. Geophys. Space Phys. 15: 1-46.

Kanno, S., and F. Masuda (1978) Pages 63-70. Climatic Change and Food Production, edited by K. Takahashi and M. Yoshino. University of Tokyo Press.

Kellogg, T.B. (1976) Pages 77-110. Geol. Soc. Am. Mem. 145, edited by R.M. Cline and J.D. Hays.

Kemp, E.M. (1978) Paleogeogr., Palaeoclimatol., Palaeoecol. 24: 169-208.

Kempe, S., (1977) Mitt. Geol. Paläont. Inst. Univ. Hamburg 47: 125-228.

Kennett, J.P. (1977a) J. Geophys. Res. 82: 3843-3860.

Kennett, J.P., et al. (1975) Science 187: 497-503.

(1977b) Science 196: 1231-1234.

(1977c) J. Volcan. Geotherm. Res. 2: 145-163.

Kennett, J.P., and P. Huddlestun (1972) Quatern. Res. 2: 384-395.

Kent, D.V. (1978) Geology 5: 769-771.

Kozur, H. (1976) Nova Acta Leopoldina N.F. 224: 413-472.

Kukla, G.J. (1977a) Earth-Sci. Rev. 13: 307-374.

Lotze, F. (1964) Pages 491-507. Problems in Paleoclimatology, edited by A.E.M. Nairn. New York, London: Interscience.

Maley, J. (1977a) Nature 269: 573-577.

(1977b) Rech. Franc. sur le Quaternaire. Pages 187-197 INQUA.

(1979) The Sahara and the Nile, edited by H. Faure and A.J. Williams. Rotterdam: Balkema.

McLean, D.M. (1978) Science 201: 401-406.

Mercer, J.H. (1976) Quatern. Res. 6: 125-166.

(1978) Nature 271: 321-325.

Mörner, N.A. (1976) Palaeogeogr., Palaeoclimatol., Palaeoecol. 19: 63-85.

Nichols, H. (1975) University of Colorado, Institute of Arctic Alpine Research, Paper 15.

Nicholson, S.E. (1979) The Sahara and the Nile, edited by H. Faure and M.A.J. Williams. Rotterdam: Balkema.

Pachur, H.J. (1975) Die Erde, Z. Ges. Erdk. Berlin 106: 21-46.

Prell, W.L., et al. (1976) Pages 247-266. Geol. Soc. Am. Mem. 145, edited by R.M. Cline and J.D. Hays.

Rognon, P., and A.J. Williams (1977) Palaeogeogr., Palaeoclimatol., Palaeoecol. 21: 285-327.

Saito, T., et al. (1975) Pages 226-244. Late Neogene Epoch Boundaries, edited by T. Saito and L.H. Burckle. New York: American Museum of National History.

Savin, S.M., et al. (1975) Geol. Soc. Am. Bull. 86: 1499-1510.

Sarnthein, M. (1978) Nature 272: 43-46.

Singh, G., et al. (1974) Philos. Trans. R. Soc. London Ser. B 267: 467-501.

Shackleton, N.J. (1977) Pages 401-427. The fate of fossile fuel CO_2 in the oceans, Marine Science 6, edited by N.R. Andersen and A. Malakoff.

Starkel, L. (1977) Page 433. X. INQUA Congress Birmingham, Abstr.

Taira, K. (1975) Palaeogeogr., Palaeoclimatol., Palaeoecol. 17: 333-338.

van Zinderen Bakker, E.M. (1976) Palaeoecology of Africa 9: 159-202.

Wigley, T. (1977) Interim final report to NOAA. University of East Anglia, Climate Research Unit.

Wijmstra, T.A. (1978) Pages 25-45. Climatic Change, edited by J. Gribbin. Cambridge University Press.

Wilson, A.T. (1964) Nature 201: 147-149.

(1978) Pages 33-39. Glacial History and World Palaeoenvironments, edited by E.M. van Zinderen Bakker. Rotterdam: Balkema.

Winterer, E.L. (1973) Am. Assoc. Pet. Geol. Bull. 57: 265-282.

Woillard, G.M. (1975) Acta Geogr. Lovaniensia 14: 1-168.

(1978) Quatern. Res. 9: 1-21.

Yoshino, M.M. (1978) Pages 63-70. Climatic Change and Food Production, edited by K. Takahashi and M.M. Yoshino. University of Tokyo Press.